

國立交通大學

機械工程研究所

博士論文

黏著劑結合之接頭應力分析及其在取晶過程之應用

Stress Analysis of the Adhesively Bonded Joint
Applicable to the IC Chip Pick-up Process

研究生：鄭桐華

指導教授：洪景華教授、曾錦煥教授

中華民國九十五年十二月

黏著劑結合之接頭應力分析及其在取晶過程之應用

Stress Analysis of the Adhesively Bonded Joint Applicable
to the IC Chip Pick-up Process

研究生：鄭桐華

Student: Tung-Hua Cheng

指導教授：洪景華
曾錦煥

Advisor: Ching-Hua Hung
Ching-Huan Tseng

國立交通大學

機械工程研究所

博士論文

A Dissertation

Submitted to Institute of Mechanical Engineering

College of Engineering

National Chiao Tung University

in Partial Fulfillment of the Requirements

for the Degree of

Doctor of Philosophy

in

Mechanical Engineering

2006

Hsinchu, Taiwan, Republic of China

中華民國九十五年十二月

黏著劑結合之接頭應力分析及其在取晶過程之應用

研究生：鄭桐華

指導教授：洪景華教授、曾錦煥教授

國立交通大學機械工程研究所

摘 要

本文主要探討一黏著劑(adhesive)接合二個黏著物(adherends)在銷-銷(pin-pin)之邊界條件(boundary conditions)下受到集中力(concentrated force)作用，在此條件下導出其統御方程式(governing equations)為複雜之耦合方程式(coupled equations)，其解析解(analytic solutions)利用符號運算(symbolic manipulation)求得，並使用奇異值分解法(singular value decomposition, SVD)求得符合邊界條件之數值解。

文中討論黏著層(adhesive layer)的剝離應力(peel stress)及剪應力(shear stress)受到黏著物及黏著劑之材料性質、幾何形狀(厚度、長度)、接合長度、力作用點等的影響。在無因次化參數(non-dimensional parameter)的值为 $E_1=6.0$, $E_2=6.0$, $E_0=2.75$, $\tilde{P}=1$, 及參數 $d=0$ 的情形下，對於上層黏著物(upper adherend)能夠從下層黏著物(lower adherend)完全分離，必須滿足下面的條件，下層黏著物的厚度大於 10 倍的黏著層之厚度且小於 1/3 上層黏著物之厚度，並且黏著層厚度相對的薄($h_a \leq 0.01$ mm)，接合時，其長度相對的短，也就是說厚長比(thickness to length ratio)大於 0.08 ($\gamma_1 \geq 0.08$)。

接著將上述黏著接頭之分析(analysis of adhesive joint)方法結合 C++ 語言的基因演算法(genetic algorithm)運用於取晶過程之探討。當 0.1mm 厚的晶片受到 4.8N 的集中力，取晶良率(success rate)很低，且晶片不是破裂就是無法從藍膜(blue tape)分離。但當 0.34mm 厚的晶片受到 3.5N 的集中力，取晶良率很高，且晶片幾乎沒有破裂且可以完全成功的從藍膜分離。對這二實驗中，其取晶良率差異很大。本文利用基因演算法結合黏著接頭之分析方法去找尋黏著劑之材料性質。對 0.1mm 厚晶片的例子中，當黏著劑的厚度為 0.01mm 時，完全尋找不到材料性質符合之黏著劑。另外本文希望以不同的黏著劑的厚度來改善晶片厚度為 0.01mm 的取晶良率，但是結果也完全找尋不到材料性質及厚度符合之黏著劑，但是對晶片厚度為 0.34mm 的例子，當黏著劑的厚度為 0.01mm 時，就可以找尋到黏著劑的彈性係數(Young's modulus)為 2.46×10^{10} pa，而且本文希望以一般黏著劑取代實驗所使用的輻射黏著劑(radiation-cured adhesives)或稱為紫外線黏著劑(ultra-violet adhesive)時，也可找到黏著劑的彈性係數及厚度分別為 2.77×10^{10} pa 及 0.027mm。這些理論分析的結果一致於實驗的結果。

為了改善先前例子，對晶片的厚度為 0.1mm 易於破裂或無法從藍膜分離，藍膜的彈性係數必須再予增加。只要藍膜的彈性係數大於 1/10 倍的晶片之彈性係數，皆可找得到黏著劑的彈性係數及厚度值，且其畸變能應力(von Mises's stresses)皆大於 130Mpa，超過一般黏著劑的臨界應力(40-80Mpa) [51]，因此可預知當厚度 0.1mm 的晶片在取晶時，改變藍膜的材料性質，就能夠提高從藍膜成功分離之機會。

Stress Analysis of Adhesively Bonded Joints Applicable to the IC chip pick-up Process

Student: Tung-Hua Cheng

Advisor: Ching-Hua Hung

Ching-Huan Tseng

Institute of Mechanical Engineering

National Chiao Tung University

ABSTRACT

In this study, a concentrated force is applied to both adherends bonded by an adhesive under the pin-pin boundary conditions. First a mathematical model is derived with governing equations and boundary conditions. These complicated, and analytically problematic, coupled equations are solved numerically using symbolic manipulation and singular value decomposition (SVD). Also discussed are the effects of major factors, including the relative thickness of, material properties of adherends and adhesive, joint length, and the action point of the concentrated force on the peel and shear stresses in the adhesive layer. As non-dimensional parameters $E_1 = 6.0$, $E_2 = 6.0$, $E_0 = 2.75$, $\tilde{P} = 1$ and the parameter $d = 0$, this study identifies the conditions under which the upper adherend without breakage can be fully separated from the lower adherend. Particularly, it is found that the thickness of the lower adherend should be greater than ten times that of the adhesive layer but less than one-third that of the upper adherend, the adhesive layer should be relatively thin ($h_a \leq 0.01$ mm), and the adhesive joint should be relatively short (thickness to length ratio $\gamma_1 \geq 0.08$).

Subsequently, the aforementioned analysis of adhesive joint is associated with the C++ program of genetic algorithm and is applied to investigate IC chip pick-up process. As the thickness of IC chips subjected to the concentrated force 4.8 N is 0.1 mm, IC chips are easy to fail in the IC chip pick-up process while as the thickness of IC chips subjected to the concentrated force 3.5 N is 0.34 mm, IC chips are fully separated from blue tape without breakage. The two experiments have a great difference in the success rate of the IC pick-up process. The experimental results are discussed by genetic algorithm searching associated

with analysis of adhesive joint. The former case is as the thickness of the adhesive layer is 0.01mm, the solution to Young's modulus of the adhesive layer is not found. Additionally, it is expected that the success rate of the IC pick-up process can be raised by changing the adhesive's thickness. However, the searching result does not also find any solution to material properties and thickness of adhesive. The latter case is as the thickness of the adhesive layer is 0.01mm, Young's modulus of the adhesive layer is searched and the value of Young's modulus obtained is 2.46×10^{10} pa. In addition, it is expected that in the IC pick-up process, radiation-cured adhesives (ultra-violet adhesives) can be replaced by general adhesives. The searching result can also obtain Young's modulus of and the thickness of the adhesive layer which are respectively 2.77×10^{10} pa and 0.027mm. These results are in accordance with those of the experiments.

In order to reduce the easy failure of the former case regarding IC chip's thickness 0.1 mm, the Young's modulus of blue tape has to be increased. The conclusions are that only if the Young's modulus of blue tape is greater than one-tenth that of IC chips, genetic algorithm can obtain the searching results of adhesive's Young's modulus and adhesive's thickness. Thereby, only if the mechanical properties of blue tape are changed, the probability of IC chips which can be fully separated from blue tape is expected to be able to increase because the von Mises's stresses of the searching results are greater than 130Mpa exceeding the critical value (40-80Mpa) [51] of general adhesive.

ACKNOWLEDEMENTS

本人在此以最誠摯的敬意向曾錦煥博士及洪景華博士表示最大的謝意，感謝他們在我攻讀博士學位期間無私的付出與真摯的關懷，這份恩情本人永生難忘。在這期間指導教授曾錦煥博士不幸離世，更感謝洪景華老師能夠繼續給我支持、鼓勵，讓我能夠順利完成博士學位。

其次，感謝論文口試委員：清華大學賀教授陳弘、前國科會工程處處長—明新科技大學蔡教授忠杓、交通大學機械系周教授長彬、台灣大學呂教授東武、國防大學林教授聰穎，謝謝他們在百忙之中，不辭辛勞，撥冗前來擔任我的論文口試委員，並給我在論文寫作上許多寶貴的建議，同時提供相關的研究經驗，讓我的論文能夠更加完整與充實。

再者，感謝師母姚女士的幫忙及關懷，更感謝諸多朋友的幫忙，並對這些朋友致上最高的謝意。本人特別要感謝各位學長學弟的鼎力協助，讓我對這段新竹攻讀學位的日子留下不可忘懷的記憶，另外也一併感謝最佳化實驗室的師門兄弟諸多的幫助。

此外，感謝英文老師涂清欽老師及李佩倫老師，百忙之中特別撥出時間，耐心地幫忙潤飾我的論文。

我敬愛的母親—鄭林幼字女士於我大二時往生西方極樂，我敬愛的父親—鄭義立先生，在我攻讀博士期間離世，讓我悲痛萬分。想起父母親為我所做的點點滴滴，銘記在心，永生難忘。

我心中最感謝的是一路相伴我的妻子—翁淑玲女士。幾年來，她不畏艱辛，支持我、陪伴我，渡過漫長的求學生涯，協助我順利完成博士學位，同時細心地照顧我年邁的父親、兩個稚子—光庭、光祐。感謝岳父母的鼓勵及姊姊的幫助，我要以這份論文獻給我摯愛的妻子、孩子、岳父母及姊姊。

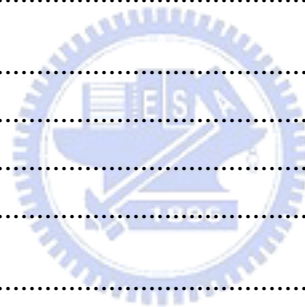
最後，在攻讀學位期間，我的父親鄭義立、老師曾錦煥往生西方極樂，我要以此論文紀念我的父親鄭義立先生、母親林幼字女士及老師曾錦煥博士，感謝他們對我的教導。

TABLE OF CONTENTS

ABSTRACT (中文摘要)	i
ABSTRACT	ii
ACKNOWLEDGEMENTS	iv
TABLE OF CONTENTS	v
LIST OF TABLES	viii
LIST OF FIGURES	ix
NOMENCLATURE	xii
CHAPTER 1 INTRODUCTION	1
1-1. Background	1
1-1-1. Adhesive	2
1-1-2. Joint Type.....	3
1-2. Objectives.....	10
1-3. Significance and Limitations.....	11
1-4. Dissertation Outlines	12
CHAPTER 2 LITERATURE REVIEW	14
2-1. Introduction	14
2-2. Adhesively Bonded Joints.....	14
2-2-1. Introduction.....	14
2-2-2. Thermal Loading.....	15
2-2-3. Anisotropic and Orthotropic Materials	16
2-2-4. Non-linear FEM and External Loading	16

2-2-5. Plastic Behavior of Adhesive Joints	17
2-2-6. Crack Analysis and Stress Singularity	17
2-2-7. Strengthening Structures	18
2-3. Genetic Algorithm and Penalty Function Method	18
2-3-1. Introduction.....	18
2-3-2. Penalty Function Method without Any Penalty Parameters.....	19
2-3-3. Adaptive Search Techniques.....	20
2-3-4. Genetic Algorithm Application to Adhesively Bonded Joints	21
2-4. Methods Applied to Solve the Issues of Adhesively Bonded Joints.....	21
2-5. Concluding Remarks	23
CHAPTER 3 ANALYSIS OF ADHESIVE JOINT	25
3-1. Introduction	25
3-2. Mathematical Model	25
3-2-1. Bending moment, Shear force, and Longitudinal Force in the Upper Adherend and Lower adherend.....	27
3-2-2. Relationship between Displacement and Stress.....	31
3-2-3. Relationships among Displacement, Longitudinal Force, and Bending Moment.....	32
3-3. Non-dimensionalization and Symbolic manipulation	34
3-4. Constraint and Boundary Conditions	40
3-5. Results and Discussion.....	42
3-5-1. Application of Closed-form Solutions	42
3-5-2. Case Studies	45
3-6. Summary	61

3-7. Concluding Remarks	62
CHAPTER 4 APPLICATION OF GENETIC ALGORITHM TO IC CHIP PICK-UP	
PROCESS	63
4-1. Introduction	63
4-2. Optimum problem	65
4-3. Results and Discussion.....	69
4-4. Concluding Remarks	72
CHAPTER 5 CONCLUSIONS AND FUTURE WORKS	75
5-1. Conclusions	75
5-2. Future works.....	78
REFERENCES	80
APPENDICES	86
Appendix A	86
Appendix B.....	94
Appendix C.....	97
Appendix D	104
VITA.....	108



LIST OF TABLES

Table 3.1 The non-dimensional terms and equations for upper adherend, adhesive layer and lower adherend.	39
Table 4.1 Mechanical properties and dimensions for IC chip and blue tape. [45],[52]	67
Table 4.2 Optimum points and values of adhesive for various Young's modulus of blue tape (E_2).....	72



LIST OF FIGURES

Fig. 1.1 Singe lap joints	5
Fig. 1.2 Butt joints	6
Fig. 1.3 Double lap joints	6
Fig. 1.4 Scarf lap joints.....	7
Fig. 1.5 Stress catalogy.....	7
Fig. 1.6 Processes in the IC manufacturing procedure. [1]	9
Fig. 1.7 Two adherends of the adhesively bonded joint bonded by an adhesive layer.	10
Fig. 3.1 The sketch showing two adherends bonded by an adhesive layer.	25
Fig. 3.2 Free-body diagram for the first segment $-L_1 \leq x \leq -c$, of lower adherend.....	27
Fig. 3.3 Free body diagram for the second segment $-c \leq x \leq -d$, of lower adherend. ...	28
Fig. 3.4 Free body diagram for the third segment $-d \leq x \leq c$, of lower adherend	28
Fig. 3.5 Free body diagram for the fourth segment of $c \leq x \leq L_2$, of lower adherend.....	28
Fig. 3.6 Free body diagram for the first segment $-c \leq x \leq -d$, of upper adherend.....	30
Fig. 3.7 Free body diagram for the second segment $-d \leq x \leq c$, of upper adherend.	31
Fig. 3.8 The sketch of the Cornell's model [29] showing cantilever beam strengthened by adhesively bonding.....	43
Fig. 3.9 Comparison of the results between the present study (top) and figure 6 of the Cornell's paper [29] (bottom).....	44
Fig. 3.10 The sketch of the Zou et al. model [30] showing a single lap joint	45
Fig. 3.11 Comparison of the results between figure 5 of the Zou et al.'s paper [30] and the present study.....	45
Fig. 3.12 Non-dimensional peel and shear stresses distributions in the adhesive layer ($\bar{x} = x/c$) for the thickness to length ratio $\gamma = \gamma_1 = \gamma_2$ with the same thickness of both adherends $\beta_1 = \beta_2 = 10$ and ($h_a = 0.01mm$)	48

Fig. 3.13 Non-dimensional peel and shear stresses versus the thickness to length ratio

$\gamma = \gamma_1 = \gamma_2$ for the same thickness of the adherends as for Case 1 ($h_a = 0.01mm$). 49

Fig. 3.14 Non-dimensional peel and shear stress distributions in the adhesive layer ($\bar{x} = x/c$)

versus the thickness to length ratio γ_1 for various thicknesses of the adherends for Case 2, ($h_a = 0.01mm$).52

Fig. 3.15 Non-dimensional peel and shear stresses versus the thickness to length ratio of the

upper adherend γ_1 for various thicknesses of the adherends for Cases 2 and 3.53

Fig. 3.16 Non-dimensional peel and shear stress distributions for the distance d from the

center of the adhesive layer to the action point of the force ($h_a = 0.01mm, \gamma = 0.01667$).
.....55

Fig. 3.17 Non-dimensional peel and shear stress distributions for different distances d from

the center of the adhesive layer to the action point of force ($h_a = 0.02mm, \gamma = 0.05$).
.....56

Fig. 3.18 Non-dimensional peel and shear stresses distributions in the adhesive layer

($\bar{x} = x/c$) for Young's modulus ratio with the same thickness of both adherends
 $\beta_1 = \beta_2 = 10$ and ($h_a = 0.01mm$)57

Fig. 3.19 Non-dimensional peel and shear stresses versus the adhesive Young's modulus ratio

with the same thickness of both adherends $\beta_1 = \beta_2 = 10$ and ($h_a = 0.01mm$).58

Fig. 3.20 Non-dimensional peel and shear stresses distributions in the adhesive layer

($\bar{x} = x/c$) for the thickness to length ratio $\gamma = \gamma_1 = \gamma_2$ with the different Young's
modulus of both adherends $E_1 = 4.5, E_2 = 6.0, E_0 = 2.75$ and with the same thickness
of both adherends $\beta_1 = \beta_2 = 10$ and ($h_a = 0.01mm$)59

Fig. 3.21 Non-dimensional peel and shear stresses versus the thickness to length ratio

$\gamma = \gamma_1 = \gamma_2$ for the same thickness of the adherends with the different Young's

modulus $E_1 = 4.5$, $E_2 = 6.0$, $E_0 = 2.75$ ($h_a = 0.01mm$). 60

Fig. 4.1 Scheme of genetic algorithm linked with Mathematics package to compute stresses of

the adhesive and adherends. 68



NOMENCLATURE

c	Half length of the joint bonded by the adhesive(i.e. $2c$ length of upper adherend)
\overline{C}	Denotation of $\cos(\alpha_{12}x)$
\overline{Ch}	Denotation of $\cosh(\alpha x)$
\overline{Ch}_1	Denotation of $\cosh(\alpha_{11}x)$
d	Distance from the action point of force to the center of the joint
E_1^*	Elastic modulus of the upper adherend
E_a	Elastic modulus of the adhesive layer
E_1	The ratio of elastic modulus of the upper adherend to shear modulus of the adhesive layer
E_0	The ratio of elastic modulus of the adhesive layer to shear modulus of the adhesive layer
E_2	The ratio of elastic modulus of the lower adherend to shear modulus of the adhesive layer
E_2^*	Elastic modulus of the lower adherend
\overline{E}_1	Elastic modulus of the upper adherend in plane stress
\overline{E}_2	Elastic modulus of the lower adherend in plane stress
F_L	Reaction force in the left-end pin boundary of the lower adherend
F_R	Reaction force in the right-end pin boundary of the lower adherend
G_a	Shear modulus of the adhesive layer
h_1	Thickness of the upper adherend
h_a	Thickness of the adhesive layer
h_b	Thickness of the adhesive layer in Cornell's paper[29]
h_2	Thickness of the lower adherend
P	The concentrated force

L_1	Distance from the center of joint to the left end of the lower adherend
L_2	Distance from the center of joint to the right end of the lower adherend
M_{ix}	Bending moment in the i segment of the lower adherend
N_{ix}	Longitudinal force in the i segment of the lower adherend
M_i	Bending moment of the upper adherend
\bar{M}_i	Non-dimensional moment of the upper adherend
\bar{M}_{ix}	Non-dimensional moment of lower adherend
N_i	Longitudinal force of the upper adherend
N_L	Longitudinal force in the left-end pin boundary of the lower adherend
N_R	Longitudinal force in the right-end pin boundary of the lower adherend
\bar{N}_i	Non-dimensional longitudinal force of the upper adherend
\bar{N}_{ix}	Non-dimensional longitudinal force of the lower adherend
Q_i	Shear force of the upper adherend
Q_{ix}	Shear force in the i segment of the lower adherend
Q_i	Shear force of the upper adherend
\bar{Q}_i	Non-dimensional shear force of the upper adherend
\bar{Q}_{ix}	Non-dimensional shear force of the lower adherend
R	Penalty parameter.
\bar{S}	Denotation of $\sin(\alpha_{12}x)$
\bar{Sh}	Denotation of $\sinh(\alpha x)$
\bar{Sh}_1	Denotation of $\sinh(\alpha_{11}x)$
u_{ix}	Longitudinal deformation in the i segment of the lower adherend

u_i	Longitudinal deformation in the i segment of the upper adherend
w_{ix}	Transverse deformation in the i segment of the lower adherend
w_i	Transverse deformation in the i segment of the upper adherend
x	x-axis coordinate
z	z-axis coordinate
$\bar{\sigma}$	Non-dimensional peel stress of the adhesive layer
$\bar{\sigma}_0$	Non-dimensional peel stress of the adhesive layer in the center
$\bar{\sigma}_1$	Non-dimensional peel stress of the adhesive layer at both ends
σ_{ai}	Peel stress in the i segment of the adhesive layer
τ_{ai}	Shear stress in the i segment of the adhesive layer
$\bar{\sigma}_{ai}$	Non-dimensional peel stress in the i segment of the adhesive layer
$\bar{\tau}_{ai}$	Non-dimensional shear stress in the i segment of the adhesive layer
$\bar{\tau}$	Non-dimensional shear stress of the adhesive layer
$\bar{\tau}_1$	Non-dimensional shear stress of the adhesive layer at both ends
$\alpha, \alpha_{11}, \alpha_{12}$	The solutions of the characteristic Eqns.
β_1	The ratio of the thickness of the upper adherend to the thickness of the adhesive layer
β_2	The ratio of the thickness of the lower adherend to the thickness of the adhesive layer
γ_1	The ratio of the thickness of the upper adherend to the length of the adhesive layer
γ_2	The ratio of the thickness of the lower adherend to the length of the adhesive layer
\bar{V}_1	Possion's ratio of the upper adherend

\bar{V}_2 Possion's ratio of the lower adherend

\bar{x} Non-dimensional coordinate (x/c)

λ The ratio of Young's modulus of the upper adherend to Young's modulus of the adhesive layer



CHAPTER 1 INTRODUCTION

1-1. Background

As technology advances, use of adhesives is becoming ever more widespread because adhesive can also help make it easier to manufacture products and be used extensively to bond metallic, ceramic, plastic and composite components in many fields where structures are subject to high levels of service. Therefore, nowadays, product designers and manufacturing engineers rely on adhesives more than ever for greater design flexibility, more efficient production, and improved performance. In addition, adhesives applied to joints have been used for many years in aircraft structures and in many other applications including particular aircraft repair, civil engineering, automotive engineering, medical field, and the electronics industry.

Adhesive bonding has many advantages over the conventional fastening techniques such as welding, riveting and bolting because its application does not require high temperatures in welding and hole in structure component like the cases of riveting and bolting. Thereby, stress concentration in the adhesive joints is less than that caused by high temperature of welding as well as hole of rivets and bolts; stress distributions of adhesive joints are more uniform. Additionally, using adhesive bonding has the substantial benefit of weight reduction that is an important advantage, especially for lightweight structures. Therefore, the use of adhesive materials as a means for assembly of structure is being accepted as an alternative means to conventional joining processes. Except weight reduction, the advantages of structural adhesive bonding over other joining techniques include cost savings (including lower labor costs), elimination of stress point concentrations by even more uniform distribution of stress over the entire bonded joint described above, bonding of dissimilar materials, and resistance to shock as well as vibration et al.. In Addition, adhesive bonding applied to composites is

being increasingly used in structural applications, which is also justified by its well-known advantages over mechanically fastened joints: fewer sources of stress concentrations, more uniform distribution of load, and better fatigue properties. Hence, the use of adhesives is more widespread than ever in technically demanding applications.

Though adhesive bonding has many aforementioned advances and great potential, it, however, results in some inconveniences. For instance, adhesive bonding is almost always irreversible; in other words, to disassemble the bonding without damaging the structural components is not easy.

1-1-1. Adhesive

As for adhesively bonded joints applied to structure component, adhesive selection is very important. The selection criteria are based upon material information, joint type and loading condition et al.. Material information involves the characteristics of adhesives and adherends as well as the bonded strength of adhesive. Understanding these characteristics is very important for selecting suitable adhesive employed in bonded joints. Because there is a great variety of adhesives over 18 different generic types of adhesives as well as numerous sub-types and hybrids of the adhesive, the selection of the most suitable adhesive for the adhesive joint probably is one of the most daunting areas in the design process.

In this research, only radiation-cured adhesives are introduced because they are often applied to the IC chip pick-up process. They become active and cured when exposed to radiation, usually ultra-violet (UV) light. The mechanism depends upon special modifications to the monomer's structure and the inclusion of light-sensitive compounds that start the reaction. Also, they are also widely used for bonding glass, ceramics and transparent plastics. However, some tapes of radiation-cured adhesives are applied to the IC pick-up process.

These adhesives make it possible to achieve a higher tack before the exposure of UV light while ensuring the easy removal of the adhesives and the reduction of bonded strength after exposure. That is to say, as exposure to UV light source breaks adhesive bond, the tack of the adhesive can be reduced. Specially, the adhesives offer worse resistance to peel force.

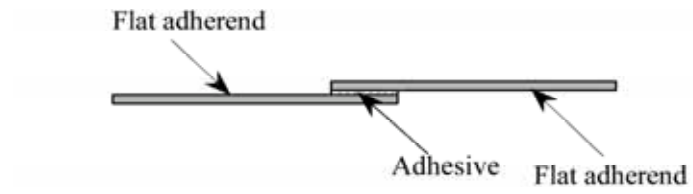
1-1-2. Joint Type

There are many sub-types of single lap joints as shown in. Generally speaking, single lap joints are the simplest joint geometry and usually used in structural joints but its shortcoming is that peel stresses still arise in this joint. Other joint geometries may be considered to reduce peel stresses; for example, butt joint, double lap joint and scarf joint as shown in Figs 1.2, 1.3 and 1.4 are better selection to reduce peel stresses. Especially, as scarf joints allow a large adhesive contact area, the joint is an ideal joint for eliminating peel stresses, but parts joined in this way must maintain a close fit; however, in practice these joints are harder to create and are not suitable for use with thin sheet adherends.

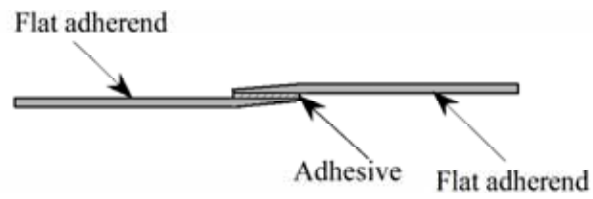
Joint design requires selection of the correct joint types depending on loading condition, geometrical shape and assembly procedures. Joint design should minimize stress concentrations by ensuring that the load is distributed over the entire bonded area. Some stresses, such as peel, cleavage, and shear stresses, should be minimized (see Fig. 1.5) because these stresses will cause the failure of adhesive joint. Most adhesives applied to structure components withstand tensile stress well, so maximizing the tensile stress and minimizing others is one of the vital targets in designing the structure components but the tensile stress is less than the critical stress of adhesives. Joint type should serve to improve bond strength. It may be important to choose the most suitable joint type of geometrical structures because this joint type minimizes the peeling or shear stresses at the edges of the

overlap in the well-bonded situation. Nevertheless, in the IC chip pick-up process, it is expected that at the edges of joint, the peeling and shear stresses can be maximized and their values also can exceed the critical stresses of adhesive; and IC chips whose stress distribution can be minimized do not fail during the process.

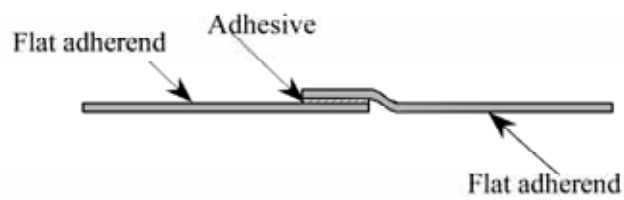




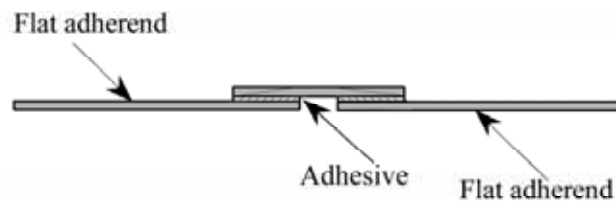
Simple single lap



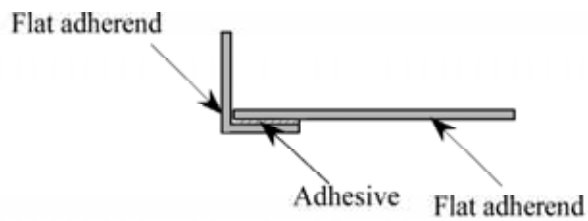
Bevel single lap



Toggle lap



Strapped lap (+Bevel option)



Corner single lap

Fig. 1.1 Single lap joints

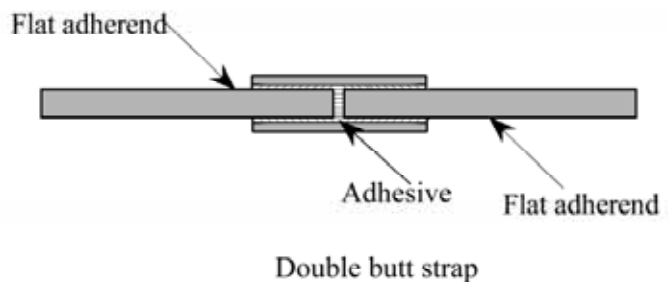
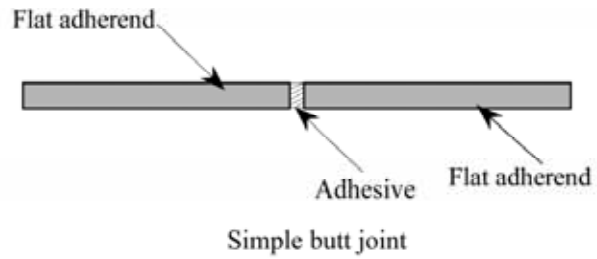


Fig. 1.2 Butt joints

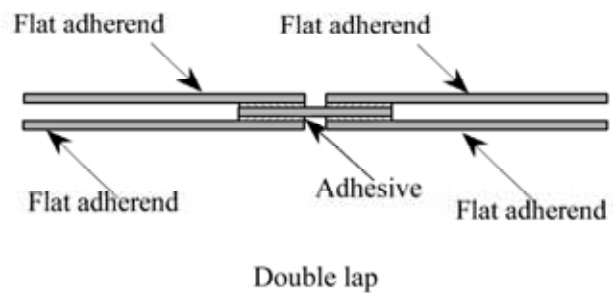
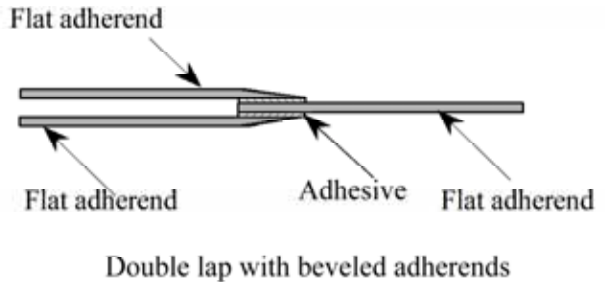
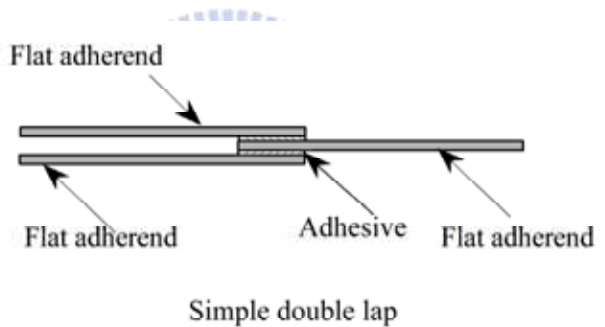


Fig. 1.3 Double lap joints

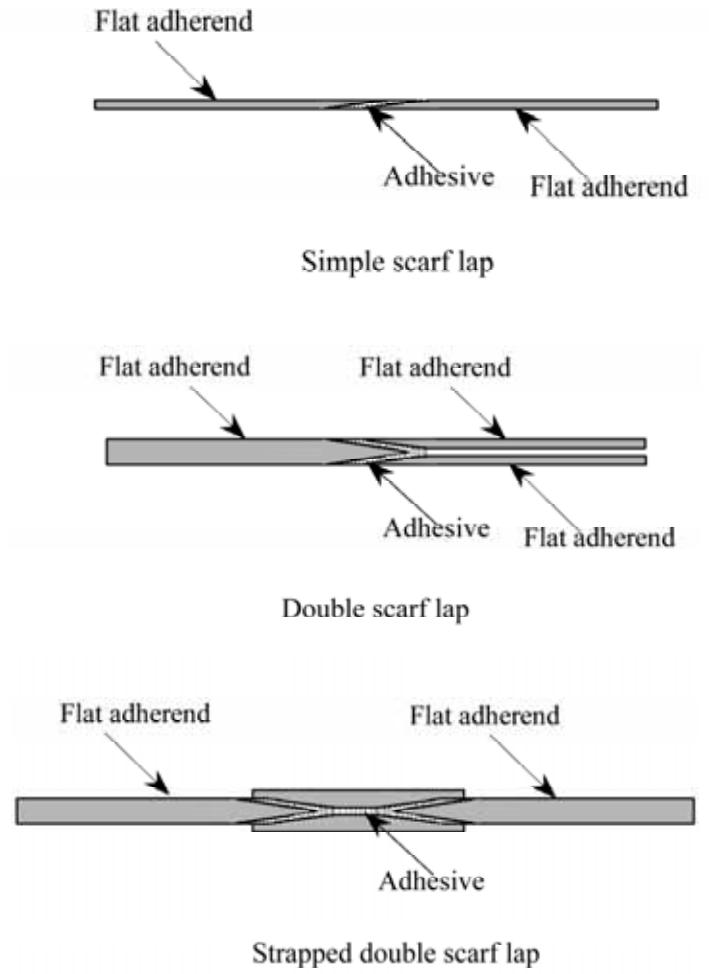


Fig. 1.4 Scarf lap joints

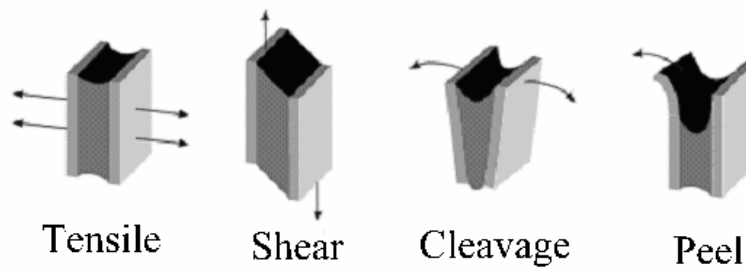


Fig. 1.5 Stress catalog

Fig. 1.6 depicts the IC manufacture procedure [1], to elucidate the causes of failure. A wafer is stuck in tape, and polished thinner and flatter. Then, it is removed from the tape and

stuck to the blue tape. The wafer can be fixed to the blue tape by radiation-cured adhesive, and cut into pieces (called IC chips) by a diamond cutter. Sequentially, in the IC chip pick-up process, the IC chips must be pierced and broken off by using the piercer, before being separated from the blue tape without any cracks. However, as IC chips are getting shorter and thinner, IC chips easily fail during IC manufacture. As shown in Fig. 1.7, adhesively bonded joint is applied to IC chip pick-up process. In the adhesively bonded joint, both adherends subjected to a concentrated force, are bonded by an adhesive under the pin-pin boundary conditions. Because its joint type is different from the aforementioned joint types but this joint is a three-laminar structure which is similar as that of a single lap joint, this dissertation mainly investigates the joint. Specially, joint's adherends are consisted of different materials.

To sum up, the use of adhesively bonded joint keeps increasing but there are still some important issues, such as stress distributions of the joints, to be explored. In this study, the stress distributions of the joints are affected by the key factors which involve the consideration of a variety of geometries, material properties of adhesive and blue tape, and loading conditions.

To perform stress analysis requires reliable and efficient closed-form solutions (analytical solutions) to obtain stress distribution of bonded joints. A large variety of models have been developed to analyze the adhesively bonded joint. Some of these techniques yield closed-form solutions, which generally involve some simplified assumptions. Many of them are limited to a certain range of geometries or loading conditions. Therefore, symbolic manipulation was employed to derive the reliable, efficient and complicated closed-form solutions which can be linked by the C++ program of genetic algorithm. Though finite element methods have provide a general tool to analyze arbitrary geometries and loading conditions, and have been extensively used with success, however, this kind of method requires much finer meshing in the issue and a large set of nodes in order to obtain reasonably accurate results. This needs a

large investment in engineering time and computer resources.

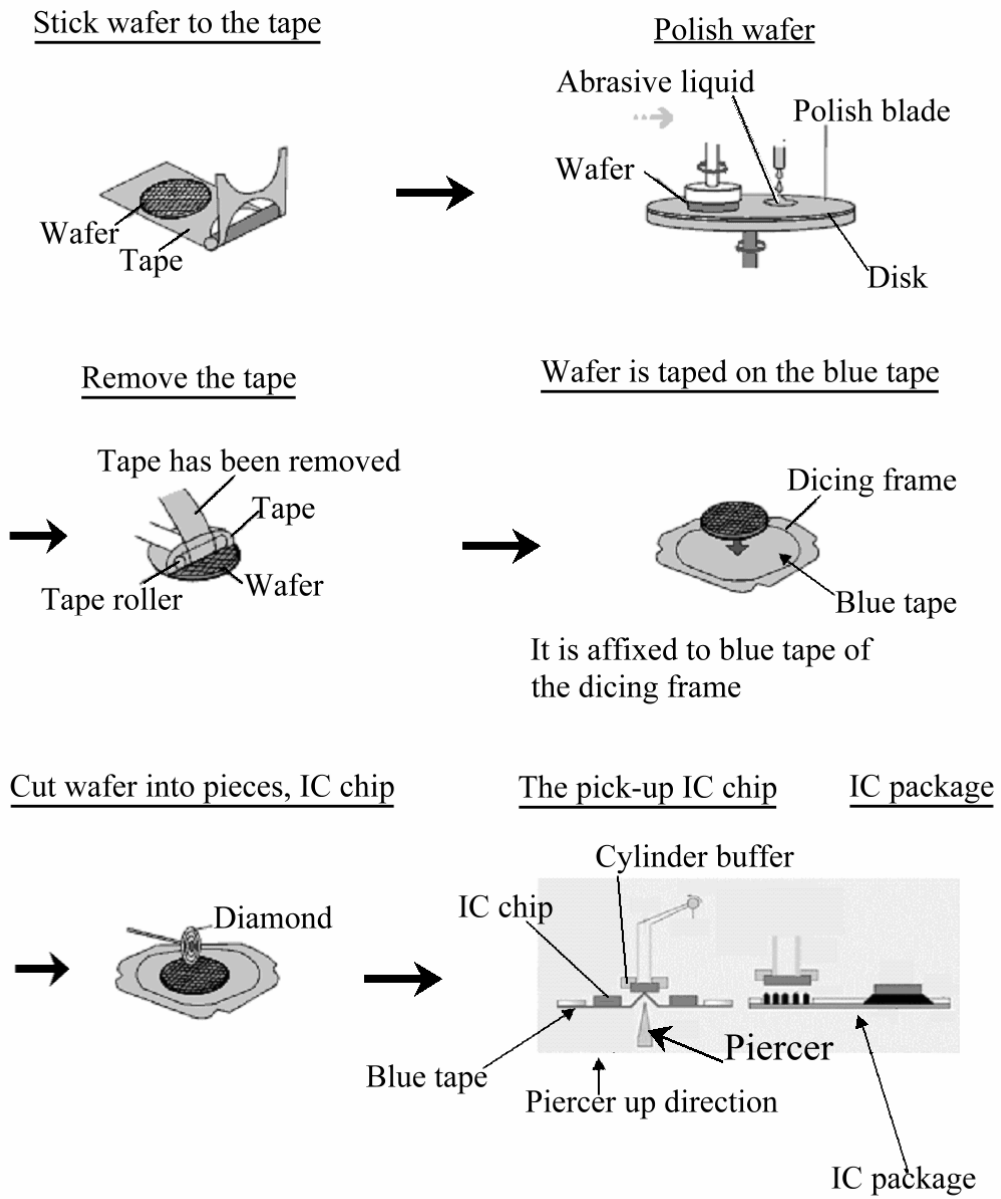


Fig. 1.6 Processes in the IC manufacturing procedure. [1]



Fig. 1.7 Two adherends of the adhesively bonded joint bonded by an adhesive layer.

1-2. Objectives

The main objective of this study is to derive closed-form solutions (analytic solutions) linked with the C++ program of genetic algorithm to predict the behavior of the adhesively bonded joint in the IC chip pick-up process. To achieve the main objective, the following objectives are indispensable:

1. To obtain closed-form solutions (analytic solutions) to peeling and shear stresses for the adhesive layer, and to normal stress due to bending moment and longitudinal force of adherends as well as to displacement and slope of adherends.
2. Close-form solutions applied to cantilever beam strengthened by adhesively bonding and a single lap joint.
3. The effect of geometric shapes, action point of concentrated force and material properties of adhesive and adherends on peeling and shear stresses.
4. Examining whether adhesive joints are in the well-bonded situation or not.
5. To apply Genetic algorithm linked with analysis of adhesive joint in the IC chip pick-up process, and to discuss the analytical results and experimental results.
6. Investigating how to improve success rate in the IC chip pick-up process.

1-3. Significance and Limitations

In this study, a concentrated force is applied to both adherends bonded by an adhesive under the pin-pin boundary conditions. The aim of the proposed research is to attain closed-form solutions that will include the most relevant factors of the adhesively bonded joint. These solutions are able to be linked with the C++ program of genetic algorithm since it is still somewhat difficult to converge and directly solve the differential equations by using the numerical method. However, Cornell [29], who claimed that obtaining complete theoretical solutions (closed-form solutions) to this problem would be very difficult, only considered a cantilever beam consisting of the same adherends. Only if the characteristic solutions of these equations have considerable values can his method produce classical solutions for the differential equations. As obtaining analytical solutions (closed-form solutions) is even more difficult here than in the work of Cornell [29], the model uses symbolic manipulation to solve the coupled differential equations in the Mathematica package, thereby enabling to find complete and complicated solutions that are not limited to solving only the characteristic solutions having large values (i.e. the characteristic solutions had to have large values [29]).

Estimating the peel and shear stresses of the adhesive between the IC chip and the blue tape is very important for the adhesive joint in the IC chip pick-up process. The results found in the experiments [45] are that as the thickness 0.1 mm of IC chips subjected to 4.8N, IC chips are easy to fail while as thickness, 0.34 mm of IC chips subjected to 3.5N, IC chips without crack can completely be separated from the blue tape. These closed-form solutions may be applied to analyze the behavior of adhesive in IC chip pick-up process. Therefore, genetic algorithm associated with these closed-form solutions aims to seek the suitable characteristic of adhesive material and blue tape to be able to reduce the failure of IC chips in the IC chip pick-up process. This research shows that conclusions drawn can increase the

success rate of IC chips which without crack, can be successfully separated from blue tape during IC chip pick-up process.

The closed-form solutions are only applied to a single lap joint. Adhesively bonded joint must be based on linear and elastic theory as well as small-deflection (Euler) beam theory under small deflection assumption.

1-4. Dissertation Outlines

In order to carry out the objective described before, the following chapters further illustrate how to accomplish the targets in more details. Here these chapters are briefly introduced in this section. Chapter 2 is devoted to discussing the related literatures regarding adhesively bonded joints and genetic algorithm. In regard to adhesively bonded joints, some published papers, basing on thermal or external load, material properties, plastic behavior, crack analysis, and strengthening structure, are introduced in order. As for genetic algorithm, here discuss some articles including penalty function, adaptive search techniques and its application to adhesively bonded joint. Next, some methods employed to solve the adhesively bonded joint are investigated.

Chapter 3 is dedicated to analysis of adhesive joint and mainly develops theoretical model of the adhesively bonded joint applied to the IC chip pick-up process. The use of symbolic manipulation is employed to solve the closed-form solutions (analytical solutions) to the adhesively bonded joint. These closed-form solutions involve the expressions of the transverse and longitudinal displacements, longitudinal and shear forces, moment in the adherends as well as peel and shear stress of the adhesive. These expressions are also shown to be correct by re-substituting them into coupled differential equations and by comparing the

results of the examples in references [29-30] with those obtained by the application of the expressions to solving those examples.

Sequentially, the IC chip pick-up problem is solved by using these closed-form solutions on which boundary and constraint conditions are imposed. Then, under some conditions, examine whether adhesively bonded joints are in the well-bonded situation or not.

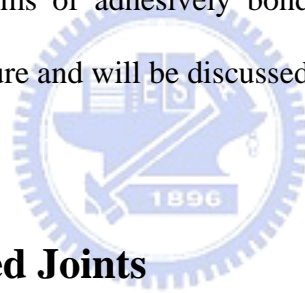
Chapter 4 focuses on comparing the results of the experiments [45] with those of the analysis of adhesive joint and drawing conclusions which can increase the success rate of IC chips in the process. In the experiments, because of the different thicknesses, 0.1mm, and 0.34mm of IC chips, the success rate of the IC chip pick-up process has a great difference. The 0.1mm IC chips nearly fail in slower speed but the 0.34mm IC chips without breakage can almost be completely separated from blue tape. These phenomena are discussed by theoretical model. However, because the characteristics of the adhesive layer are not easily found, genetic algorithm with penalty function, associates with analysis of adhesive joint method to solve the thickness and mechanical properties of the adhesive layer. The program of the genetic algorithm is written by the C++ language. Some conditions are proposed to improve the success rate in the pick-up IC process.

Chapter 5 draws conclusions and discussions about further works of this study in the future.

CHAPTER 2 LITERATURE REVIEW

2-1. Introduction

Based on some aforementioned facts, the design structure involves adhesively adhesive joints, and IC chip as well as blue tape stuck together by adhesive. Strictly speaking, in IC chip pick-up process, an adhesively bonded joint includes two adherends – the IC chip (upper adherend) and the blue tape (lower adherend) bonded by an adhesive in the IC chip pick-up process. In the published articles, many methods have been applied to solve the problems of adhesively bonded joints. Generally speaking, there are mainly several basic approaches, such as finite element method (FEM), numerical method and analytical method, which are often employed to solve the problems of adhesively bonded joints. These approaches are also applied to the following literature and will be discussed in the next sections.



2-2. Adhesively Bonded Joints

2-2-1. Introduction

Adhesively bonded single-lap joints have been widely studied since the 1950s. One of the most widely quoted papers on stresses in adhesive joints is that of Goland and Reissner [2]. Goland and Reissner have developed the cemented-lap mathematical model and found the explicit solutions (closed-form solutions) to two limiting cases. One case is that the cement layer must be so thin that its effect on the flexibility of the joint may be neglected; the other case is that the joint flexibility results mainly from that of the cement layer.

Some studies that have used and extended the Goland-Reissner theory and have compared their own results with Goland-Reissner's are described below. Oplinger [3] has released the limit of large adherend-to-adhesive layer thickness ratio to obtain the results of the Goland-

Reissner analysis. Oplinger's model should give the most accurate results for any overlap joint length because the edge moment expression was obtained by considering the large deflections of all the components of the single lap joint structure. Carpenter [4] has verified the correctness of Goland-Reissner's formulations by making comparisons between his finite element results and the results of Goland-Reissner's original equations. Ojalvo and Eidinoff [5] have used a more complete shear-strain/displacement equation to solve the single-lap adhesive joints. They explained that the shear stress is the highest value at two anti-symmetrical adherend-bound interface points of the layer; the growth of joint failures originating from these points are consistent with the results obtained from actual experiments. Carpenter [6] summarized the theories of lap joint behavior of Goland and Reissner and of Ojalvo and Eidinoff's equilibrium of a unit width differential element in the adherend-adhesive layer.



2-2-2. Thermal Loading

Stress distributions of adhesive joint affected by thermal variation are often studied. Suhir [7-9] have investigated thermal stress in an adhesive layer subjected to temperature variation for many years. First, he [7] obtained the distribution of the stresses in the interface of the thermostat bi-metal plate subjected to uniform heating or cooling. Next, in both the longitudinal and the transverse interfacial compliances of the thermostat strips subjected to thermal or external loading, he [8] found the interfacial stresses by using the elementary beam theory. Finally, he [9] developed the thermal stress analysis model in a piecewise continuous adhesive layer. These stresses are yielded by the thermal expansion (contraction) mismatch between adhesive material and the material of adherends. In addition, Rossettos [10] investigated thermal stresses of a single lap joint with identical adherends subjected to temperature changes.

2-2-3. Anisotropic and Orthotropic Materials

The effects of various materials on stress distribution of the joint are discussed in the following. Some authors have treated both the adherend and adhesive materials as anisotropic and orthotropic by using either a finite element analysis or theoretical analysis. Wah [11], who found stress distribution in a lap joint, considered the adherends to be anisotropic whereas the cement was treated as an isotropic material. Renton and Vinson [12] developed a mathematical model of composite materials and formulated methods of analysis for determining the behaviors of single-lap joints with orthotropic adherends.

2-2-4. Non-linear FEM and External Loading

Tsai and Morton [13] analyzed the single-lap joint by using a two-dimensional geometrically non-linear finite element and made comparisons between the solutions of FEM and those of the theoretical analysis. They analyzed the influence of large deflections of the overlap joint on the computation of the edge moments. They concluded that the influence of the deflections on the edge moments is negligible if the joint is short.

Subsequently, Luo and Tong [14] applied linear and higher order displacement theories to stress analysis of thick adhesive and validated their results through two-dimensional finite element analysis. In addition, Allman [15] stated that the elastic stresses are obtained in adhesive bonded lap joints subjected to bending, stretching and shearing of the adherends and that the effects of the shearing and tearing actions were accounted for on the stresses of the adhesive layer. Allman produced a model that allows linear variation of the peel stress through the adhesive thickness. The comparisons between analytical results and experimental data were displayed. Additionally, single-lap adhesive joints of dissimilar adherends have

been subjected to external bending moments and tensile loads [16-17], and a single-lap joint subjected to tension loading and moments induced by geometric eccentricity was studied using the finite element method [18].

2-2-5. Plastic Behavior of Adhesive Joints

Some studies have investigated the plastic behavior in adhesive joints using FEM and analytical methods; for example, a recent elastoplastic stress analysis of a single-lap joint subjected to bending moment was carried out using the finite element method [19]. The significant effects of adherend thickness and overlap length on the joint's strength were observed. Early on, Chen and Cheng [20] analyzed an adhesively bonded single-lap joint by minimizing the functional of the variational principle of complementary energy. Subsequently, Alexandrov and Richmond [21] addressed the approaching methods to solve three-dimensional, kinematically admissible velocity fields in a flat layer of an ideally rigid plastic material subjected to tension, while Mortensen and Thomsen [22] applied the multi-segment method of integration to solve the multiple-point boundary value problem.

2-2-6. Crack Analysis and Stress Singularity

When subjected to loading or thermal loading, debonding or failure may occur at different locations in the adhesive joint. The fracture of the adhesive joint often occurs in the interface; that is to say, debonding occurs between the adhesive and the adherent. At the scale of engineering structures, many systems are built by adhesively bonding different components, and the mechanical failure of such systems often occurs because of the failure of the bonded interfaces [23].

In fact, the stress concentrations at critical regions such as adherend-adhesive interfaces or

the fillet of an adhesive joint can be a source of damage due to interfacial shear and transverse normal stresses. Some researchers, for instance, Gleich et al. [24], Qiao and Wang [25] and Qian and Akisanya[26], have addressed cracks resulting in failure or the stress singularity in the fillet of an adhesive joint.

2-2-7. Strengthening Structures

Adhesively bonded joints are also applied to strengthen structure. Some technical studies have presented that a structure is strengthened by adhesively bonding the steel plates to the tension face of the beam [27–28]. Li et al. [27] have shown the influence of the adhesive thickness and the steel plate thickness on the behavior of strengthened concrete beam. Taljsten [28] derived the shear and peel stresses in the adhesive layer of beam bonding by a strengthening plate whose bending stiffness was neglected. That is to say, the bending moment of the plate is neglected when the shear stress of the adhesive and the strain of the plate were during derivation. Nevertheless, the plate really had the bending moment when the peel stress of the adhesive was formulated. He simplified this issue and made it easy to be solved. However, Cornell [29], who claimed that obtaining complete theoretical solutions to this problem would be very difficult, only considered a cantilever beam consisting of the same adherends. Only if the characteristic solutions of these equations have appropriately large values can his method produce classical solutions for the differential equations.

2-3. Genetic Algorithm and Penalty Function Method

2-3-1. Introduction

Genetic algorithms are used in search and optimization, such as finding the maximum (minimum) of a function over some domain space. Genetic algorithms are less susceptible to

getting 'stuck' at local optima than gradient search methods. But they tend to be computationally expensive. Genetic algorithm with penalty function is adopted by this study because the geometrical dimensions and material properties of adhesive and adherends deeply affect stress distributions of the adhesively bonded joint in IC chip pick-up process (see Figs. 3.10 and 3.16); and choosing the most suitable adhesive among numerous types of adhesive is difficult.

2-3-2. Penalty Function Method without Any Penalty Parameters

Some authors employed genetic algorithms (GAs) and the penalty function method which does not require any penalty parameter to solve real-world search and optimization problems involving inequality and/or equality constraints.

Deb [32], for example, devised a penalty function approach by using the approach of making pair-wise comparison in a tournament selection operator. Lin and Wu [33-34] proposed a selforganizing adaptive penalty function strategy (SOAPS) without penalty parameters, and provided a robust and efficient means for constrained genetic searches but its performance occasionally fails to reach the expectation on some highly constrained problems. Also, SOAPS also often failed to attain the optimum when the optimization problems involve equality constraints. Subsequently, They developed a new generation of the self-organizing adaptive penalty function strategy (SOAPSII) that can be effectively applied to diverse problems with inequality and equality constraints genetic algorithms. Nanakorn and Meesomklin [35] developed a new penalty scheme that is free from the disadvantages. Those disadvantages of most penalty schemes have included that (1) some coefficients of penalty function had to be specified at the beginning of the calculation, (2) the coefficients usually had no clear physical meanings, and (3) furthermore, appropriate values of the coefficients were estimated even by experience. Nevertheless, their penalty function was able to adjust

itself during the evolution so that the desired degree of penalty was always obtained. The coefficient of their penalty scheme had a clear physical meaning.

2-3-3. Adaptive Search Techniques

Some penalty schemes and adaptive search techniques are proposed to improve the efficiency of genetic algorithm. Barbosa and Lemonge [36] proposed a parameter-less adaptive penalty scheme for genetic algorithms applied to constrained optimization problems. They examined the performance of this scheme by using test problems from the related literature and constrained optimization problems of structural engineering. Coit and Smith [37] presented a penalty guided genetic algorithm which identified a final, feasible optimal, or near optimal solution in effective and efficient search of promising feasible and infeasible regions of reliability optimization with the highly constrained nature. Their proposed penalty function was adaptive and responds to the search history. Bullock et al. [38] presented that increasingly efficient and cost effective hybrid approaches incorporate an adaptive search and knowledge-based techniques of genetic algorithm, and outlined design sensitivity. Hasancebi and Erbatur [39] have obtained a better efficiency of GAs by developing two new crossover techniques. Comparative results are fully discussed between the proposed and the common crossover techniques.

The other technique methods improving genetic algorithm were also listed some literatures here. Kwon et al. [40] proposed a successive zooming genetic algorithm (SZGA) for identifying global solutions by using continuous zooming factors. The algorithm was that the search space was zoomed around the design point with the best fitness per 100 generations and compared with a simple genetic algorithm and a micro-genetic algorithm for their ability to minimize multi-modal continuous functions and simple continuous functions. The results showed that the SZGA significantly improved the ability of a GA to identify a precise global

minimum and identified a more exact optimum value than the conventional GAs. Wu and Chow [41] applied genetic algorithms to a constrained nonlinear optimization problem with a mix of discrete sizing and continuous configuration variables. The discrete sizing variable was formed by mapping relationships between binary digit strings and discrete values by the medium or unsigned decimal integers.

2-3-4. Genetic Algorithm Application to Adhesively Bonded Joints

Genetic algorithm was applied to the subjects related to the studies of adhesively bonded joints. Govindaraj and Ramasamy [42] applied Genetic Algorithms to optimize the design of reinforced concrete continuous beams, which satisfied the strength, serviceability, ductility, durability and other constraints. Their optimum design considered the cross-sectional dimensions of the beam alone as the design variables and design results are compared with those in the available and related literature. Cho and Rhee [43] optimized the maximum interlaminar stresses of laminated composites with free edges under extension, bending, and twisting loads by using genetic algorithm (GA) in which a repair strategy was adopted to satisfy given constraints. Moreover, uncertainties were taken into account in lightweight design of laminated composite structures.

2-4. Methods Applied to Solve the Issues of Adhesively Bonded Joints

Three basic approaches presented by the aforementioned literatures including direct numerical method, finite element method (FEM) and analytical method are often employed to solve the issues of adhesively bonded joint. These approaches are discussed as follows.

In the first approach, solutions of differential equations with boundary conditions are

obtained by iteration methods or finite difference methods. Nevertheless, the use of numerical methods in real applications is under many limitations because these methods are based on a very limited number of geometries. Furthermore, it is easily divergent to solve the coupled differential equations by using direct numerical method.

The second approach employs finite element method which is widely used in many scientific and engineering fields including fluid flow, heat conduction, and structural analysis. The finite element method is often applied to the determination of stresses in adhesively bonded joint structures. The continuum model is firstly discretized and represented by a discrete model. (i.e. a discretization procedure is to divide the structure into small parts and to formulate the model of each one of these parts and then to re-assemble those small parts to model the whole structure.) Subsequently, a system of algebraic equations is derived, commonly from energy functionals. Consequently, no general expressions are obtained for the solution and, therefore, stresses are given at specific points, such as Gauss points. The rapid development of computers has made the use of numerical techniques more appealing and feasible. Finite element methods can be used to analyze models with arbitrary geometries and loading conditions. They are suitable for the analysis of structures comprised of different materials. However, if one dimension value in the geometrical model is much greater than the others (i.e. dimension values have the great differences in the geometrical shape), numerical solutions (such as values of peel and shear stresses) become much more difficult to be accurately achieved by FEM because of the mesh problem. In other words, it is a little bit difficult to generate the finer mesh of adhesive and adherends if either the ratio of adhesive's thickness to joint length or the ratio of adherend's thickness to joint length is very large. Additionally, because the stresses of this joint are obtained more accurate solutions of FEM, the much finer mesh is required. However, if this joint with the much finer mesh is accurately solved, much more CPU run time of the computer is required and taken.

In the last approach, a set of differential equations and boundary conditions is formulated. The solutions of these equations are analytical expressions which give values of stresses at any point of the joint. Analytical solutions (closed-form solutions), such as those presented here for single lap joint, provide a good insight into the behavior of adhesively bonded joints. They are also useful for analysis and planning of tests and for parametric analysis which can lead to the establishment of design criteria. However, the use of the method in real applications is very much limited because they are based on restrictive assumptions and a very limited number of geometries. In addition, the closed-form solutions are difficult to be found. Especially, as the governing equations are coupled differential equations, the closed-form solutions are still more difficult to be obtained.

2-5. Concluding Remarks

In this present study both adhesively bonded adherends are subjected to a concentrated force and the peel and shear stress distributions in the adhesive layer joining the two adherends are examined. Such stress distributions are affected by geometric conditions, including the thicknesses of adherends and the length and thickness of the adhesive layer, as well as by the action point of the concentrated force.

These preceding advantages are the reasons why the close-formed solutions are adopted in this research while the aforementioned disadvantages of coupled differential equations die out by the application of symbolic manipulation. Additionally, FEM is not suitable to solve this issue because of the mesh problem described before. That is to say, if the ratio of adhesive's thickness to joint length is large and if the stresses of the joint are accurately solved, the joint must have much finer mesh and much more CPU run time of the computer is required and taken.

Under some limited conditions, close-formed solutions may be derived by some literatures described before. For examples, two adherends have to have the same material properties. Furthermore, many literatures only investigate the relations of force (or moment) to stresses. However, in this present study, the relations of the displacements to force (or moment) have to be derived because of boundary and constraint conditions.

Cornell [29] claimed that obtaining complete theoretical solutions to this problem would be very difficult. As obtaining analytical solutions is even more difficult here than in the work of Cornell, the model uses symbolic manipulation to solve the coupled differential equations in the Mathematica package, thereby enabling to find complete and complicated solutions that are not limited to solving only the characteristic solutions with large values (i.e. the characteristic solutions had to have large values [29]). In this analysis, 31 constraint and boundary conditions are imposed on the analytical solutions. Thus, the numerical solutions can be found by singular value decomposition (SVD) [31] employed as the basis for finding the inverse matrix of a matrix in which the magnitude of the matrix elements varies much. Nevertheless, it is still somewhat difficult to converge and directly solve the coupled differential equations by using the numerical method.

This theoretical model can be easily linked with genetic algorithm with penalty function and be applied to solve the IC chip pick-up problem. This method also can decrease the CPU run time of this problem.

CHAPTER 3 ANALYSIS OF ADHESIVE JOINT

3-1. Introduction

Basing on the preceding descriptions, the theoretical model is developed and the closed-form solutions also are found. In this present study both adhesively bonded adherends are subjected to a concentrated force and the peel and shear stress distributions in the adhesive layer joining the two adherends are examined as shown in Fig. 3.1. Such stress distributions are affected by geometric conditions, including the thicknesses and Young's modulus adherends and the length, thickness, and Young's modulus of the adhesive layer, as well as by the action point of the concentrated force. These stress distributions are investigated and the closed-form solutions are obtained by symbolic manipulation in the following sections.

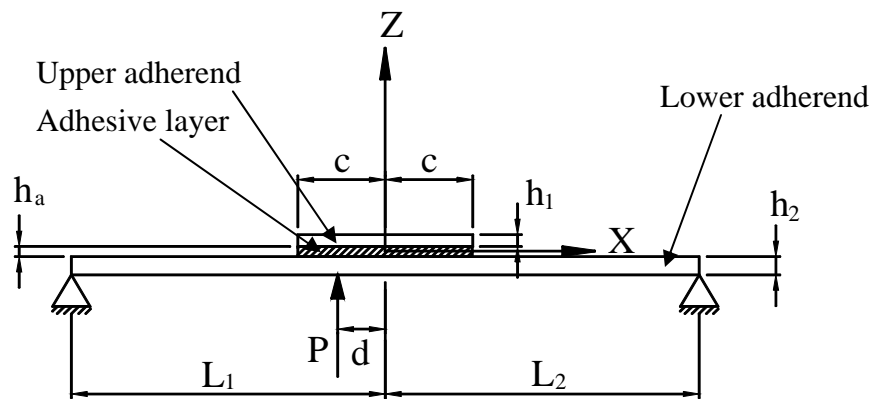


Fig. 3.1 The sketch showing two adherends bonded by an adhesive layer.

3-2. Mathematical Model

In this model the two adherends – the upper adherend and lower adherend – are bonded by an adhesive layer with the center coinciding with the origin of the coordinate system. (see Fig. 3.1). The thicknesses of the upper adherend, lower adherend, and adhesive layer are denoted

by h_1 , h_2 , and h_a , respectively. Their lengths are represented, respectively, by $2c$, (L_1+L_2) , and $2c$. The lower adherend is subjected to a concentrated force P under the pin-pin boundary conditions.

The governing equations for this study are based on the following assumptions:

- (a) The transverse displacements of both the upper adherend and of the lower adherend subjected to the concentrated force P are much smaller than their dimensions, and their transverse displacements are presumed to be linear and small.
- (b) The upper adherend and the lower adherend deform under a plane-stress condition; in other words, the plane section remains plane and the deformation of the cross sections is correspondingly normal to the neutral surfaces.
- (c) The variations in both longitudinal and transverse displacements are linear in the adhesive layer.
- (d) In the adhesive layer, the stress resulting from the longitudinal force is ignored when compared with stresses in the upper adherend and lower adherend. [14].

Based on the preceding assumptions, the governing equations are derived as follows. First, the lower adherend is divided into four segments whose ranges are $-L_1 \leq x \leq -c$, $-c \leq x \leq -d$, $-d \leq x \leq c$, and $c \leq x \leq L_2$, respectively on the x-axis. Next, the upper adherend is divided into two segments whose ranges are $-c \leq x \leq -d$ and $-d \leq x \leq c$ on the x-axis. Finally, the adhesive layer is also divided into two segments, each of which has the same range as the corresponding segment in the upper adherend.

3-2-1. Bending moment, Shear force, and Longitudinal Force in the Upper Adherend and Lower adherend

The free-body diagram for the first segment ($-L_1 \leq x \leq -c$) is shown in Fig. 3.2– where N_L , and F_L represent the longitudinal force and reaction force, respectively, of the left-end support – and the bending moment, shear force, and longitudinal force of the first segment’s right-hand section are denoted by M_{1x} , Q_{1x} , and N_{1x} , in which the 1x subscript refers to the first segment of the lower adherend. According to force and moment equilibrium equations, the bending moment M_{1x} , the shear force Q_{1x} , and the longitudinal force N_{1x} can be derived in terms of N_L , and F_L as:

$$M_{1x} = -F_L(L_1 + x), \tag{3.1}$$

$$Q_{1x} = F_L. \tag{3.2}$$

and

$$N_{1x} = N_L, \tag{3.3}$$

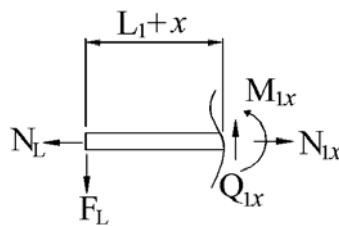


Fig. 3.2 Free-body diagram for the first segment $-L_1 \leq x \leq -c$, of lower adherend.

Similarly, in the free-body diagrams for the second, third, and fourth segments (displayed in Figs. 3.3, 3.4 and 3.5, respectively), the bending moment, shear force, and longitudinal

force of the section for the i th ($i = 2 \sim 4$) segment, denoted by M_{ix} , Q_{ix} , and N_{ix} , respectively, can be written as shown below.

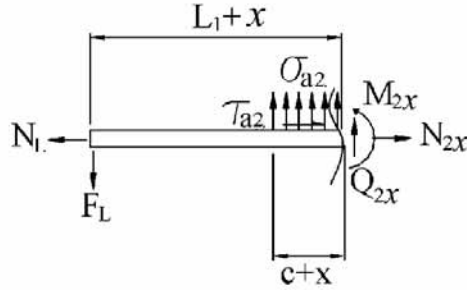


Fig. 3.3 Free body diagram for the second segment $-c \leq x \leq -d$, of lower adherend.

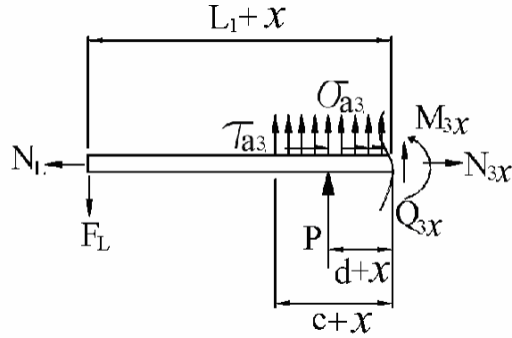


Fig. 3.4 Free body diagram for the third segment $-d \leq x \leq c$, of lower adherend

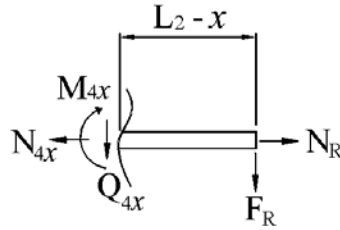


Fig. 3.5 Free body diagram for the fourth segment of $c \leq x \leq L_2$, of lower adherend.

Specifically, the bending moment, shear force, and longitudinal force of the second segment's right-hand section ($-c \leq x \leq -d$) are as follows:

$$M_{2x} = -F_L(L_1 + x) + \int_{-c}^x x \sigma_{a2} dx + \frac{h_2}{2} \int_{-c}^x \tau_{a2} dx, \quad (3.4)$$

$$Q_{2x} = F_L - \int_{-c}^x \sigma_{a2} dx, \quad (3.5)$$

and

$$N_{2x} = N_L - \int_{-c}^x \tau_{a2} dx, \quad (3.6)$$

where σ_{a2} and τ_{a2} are the peel stress and shear stress for the first segment of the adhesive layer.

Similarly, the bending moment, shear force, and longitudinal force of the third segment's right-hand section ($-d \leq x \leq c$) are

$$M_{3x} = -F_L(L_1 + x) + \int_{-c}^x x \sigma_{a3} dx + \frac{h_2}{2} \int_{-c}^x \tau_{a3} dx + P(d + x), \quad (3.7)$$

$$Q_{3x} = F_L - \int_{-c}^x \sigma_{a3} dx - P, \quad (3.8)$$

and

$$N_{3x} = N_L - \int_{-c}^x \tau_{a3} dx, \quad (3.9)$$



where σ_{a3} and τ_{a3} are the peel stress and shear stress for the second segment of the adhesive layer.

Lastly, the bending moment, shear force, and longitudinal force of the fourth segment's left-hand section ($c \leq x \leq L_2$) are

$$M_{4x} = -F_R(L_2 - x) = (F_L - P)(L_2 - x), \quad (3.10)$$

$$Q_{4x} = -F_R = (F_L - P). \quad (3.11)$$

and

$$N_{4x} = N_R = N_L, \quad (3.12)$$

The upper adherend, whose range is $-c \leq x \leq c$ on the x-axis, must be divided into two segments whose ranges are $-c \leq x \leq -d$ and $-d \leq x \leq c$, respectively. Free-body diagrams of these two segments are presented in Figs. 3.6 and 3.7. The bending moment, shear force, and longitudinal force of the right section of the i th segment of the upper adherend, denoted as M_i , Q_i , and N_i , respectively, are as follows:

$$M_i = \int_{-c}^x x \sigma_{ai} dx + \frac{h_1}{2} \int_{-c}^x \tau_{ai} dx \quad i=2 \text{ or } 3, \quad (3.13)$$

$$Q_i = \int_{-c}^x \sigma_{ai} dx \quad i=2 \text{ or } 3, \quad (3.14)$$

$$N_i = \int_{-c}^x \tau_{ai} dx \quad i=2 \text{ or } 3. \quad (3.15)$$

When $i = 2$, the range of the upper adherend is $-c \leq x \leq -d$ (i.e. the first segment of the upper adherend). However, when $i = 3$, the range of the upper adherend is $-d \leq x \leq c$ (i.e. the second segment of the upper adherend).

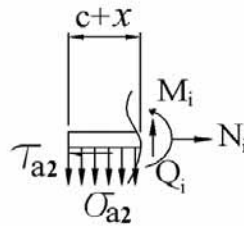


Fig. 3.6 Free body diagram for the first segment $-c \leq x \leq -d$, of upper adherend.

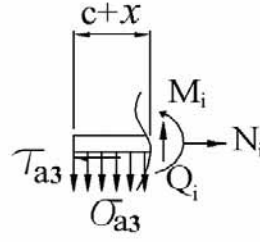


Fig. 3.7 Free body diagram for the second segment $-d \leq x \leq c$, of upper adherend.

3-2-2. Relationship between Displacement and Stress

When the range of the adhesive layer for bonding the upper adherend to the lower adherend is $-c \leq x \leq c$, the equations adopted from Ref. [5] are simplified by the small strain (i.e. the slope of the beam = 0) and are expressed as follows:

$$\sigma_{ai} = E_a \frac{(w_i - w_{ix})}{h_a} \quad i=2 \text{ or } 3, \quad (3.16)$$

$$\tau_{ai} = \frac{G_a (u_i(\frac{h_a}{2}) - u_{ix}(-\frac{h_a}{2}))}{h_a} \quad i=2 \text{ or } 3, \quad (3.17)$$

where u_i and w_i represent longitudinal and transverse displacements when $i = 2$ represents the first segment ($-c \leq x \leq -d$) of the upper adherend and $i = 3$ represents its second segment ($-d \leq x \leq c$). In equations (3.16) – (3.17), when $i = 2$, transverse and longitudinal displacements for the second segment of the lower adherend are denoted by w_{2x} , u_{2x} , and when $i = 3$, those for the third segment of the lower adherend are denoted by w_{3x} , u_{3x} . These variables, which are either functions of both x and z or only a function of x , are expressed as $u_i = u_i(x, z)$, $u_{ix} = u_{ix}(x, z)$, $w_i = w_i(x)$, and $w_{ix} = w_{ix}(x)$ ($i = 2$ or 3). The longitudinal displacement $u_i(\frac{h_a}{2})$ of the upper adherend and the longitudinal displacement

$u_{ix}(-\frac{h_a}{2})$ of the lower adherend are then represented as a function of x and are expressed as either $z = \frac{h_a}{2}$ or $z = -\frac{h_a}{2}$. The symbols G_a , E_a , and h_a , respectively, denote the shear modulus, Young's modulus, and the thickness of the adhesive layer.

The stresses of the upper adhered and lower adherend are expressed as follows:

$$\sigma_i = \frac{du_i}{dx} \quad i = 2 \text{ or } 3, \quad (3.18)$$

when $i = 2$ represents the first segment ($-c \leq x \leq -d$) of the upper adherend and $i = 3$ represents its second segment ($-d \leq x \leq c$)

The stresses of the lower adherend are expressed in

$$\sigma_{ix} = \frac{du_{ix}}{dx} \quad i = 1, 2, 3, \text{ or } 4, \quad (3.19)$$

when $i = 1, 2, 3$ or 4 represents the first, second, third, or fourth segments of the lower adherend.



3-2-3. Relationships among Displacement, Longitudinal Force, and Bending Moment

Following the beam theory, the transverse displacements w_i of the upper adherend and w_{ix} of the lower adherend are written as shown below:

$$\frac{d^2 w_{ix}}{dx^2} = \frac{12M_{ix}}{E_2^* h_2^3} \quad i = 1 \text{ or } 4, \quad (3.20)$$

$$\frac{d^2 w_i}{dx^2} = \frac{12M_i}{E_1^* h_1^3} \quad i = 2 \text{ or } 3, \quad (3.21)$$

where $E_2^* = \bar{E}_2$, $E_1^* = \bar{E}_1$ represent Young's modulus of the upper adherend and of the lower adherend in plane stress.

The longitudinal displacements u_i of the upper adherend , and u_{ix} of the lower adherend can then be written as follows:

$$\frac{du_{ix}}{dx} = \frac{1}{E_2^*} \left(\frac{N_{ix}}{h_2} + \frac{12M_{ix}z''}{h_2^3} \right) \quad i = 1 \text{ or } 4, \quad (3.22)$$

$$\frac{du_i}{dx} = \frac{1}{E_1^*} \left(\frac{N_i}{h_1} + \frac{12M_i z'}{h_1^3} \right) \quad i = 2 \text{ or } 3, \quad (3.23)$$

where $z'' = z + \frac{h_2 + h_a}{2}$ and $z' = z - \frac{h_1 + h_a}{2}$.

To obtain the longitudinal displacements, transverse displacements, and slopes of the first and fourth segments in the lower adherend, Eqs. (3.1) – (3.3) and (3.10) – (3.12) are substituted into Eqs. (3.20) and (3.22) which are integrated over x to produce the following expressions:

$$\frac{dw_{1x}}{dx} = -\frac{6F_L(2L_1x + x^2)}{E_2^*h_2^3} + c_{11}, \quad -L_1 \leq x \leq -c, \quad (3.24)$$

$$w_{1x} = -\frac{2F_L(3L_1x^2 + x^3)}{E_2^*h_2^3} + c_{11}x + c_{12}, \quad -L_1 \leq x \leq -c, \quad (3.25)$$

$$u_{1x} = \frac{1}{E_2^*} \left(\frac{N_L}{h_2} x - \frac{6F_L(2L_1x + x^2)z''}{h_2^3} \right) + c_{13}, \quad -L_1 \leq x \leq -c, \quad (3.26)$$

$$\frac{dw_{4x}}{dx} = -\frac{6(P - F_L)(2L_2x - x^2)}{E_2^*h_2^3} + c_{41}, \quad c \leq x \leq L_2, \quad (3.27)$$

$$w_{4x} = -\frac{2(P - F_L)(3L_2x^2 - x^3)}{E_2^*h_2^3} + c_{41}x + c_{42}, \quad c \leq x \leq L_2, \quad (3.28)$$

$$u_{4x} = \frac{1}{E_2^*} \left(\frac{N_L}{h_2} x - \frac{6(P - F_L)(2L_2x - x^2)z''}{h_2^3} \right) + c_{43}, \quad c \leq x \leq L_2, \quad (3.29)$$

where c_{ik} are constants. The subscripts i and k of c_{ik} represent the i th segment of the lower adherend and the index of the constants.

Substituting M_{ix} and N_{ix} from Eqs. (3.20 – 3.23) into Eqs. (3.4), (3.6), (3.7), and (3.9), where σ_{a2} , τ_{a2} , σ_{a3} , and τ_{a3} are replaced by Eqs. (3.16) – (3.17), gives the following equations for the second and third segments of the lower adherend:

$$\frac{d^4 w_{ix}}{dx^4} = \frac{12}{E_2^* h_2^3} \left\{ \frac{E_a}{h_a} (w_i - w_{ix}) + \frac{E_2^* h_2^2}{2} \left(-z'' \frac{d^4 w_{ix}}{dx^4} - \frac{d^3 u_{ix}}{dx^3} \right) \right\} \quad i = 2 \text{ or } 3, \quad (3.30)$$

$$\frac{d^2 u_{ix}}{dx^2} = \frac{12}{E_2^* h_2} \left[-\frac{G_a}{h_a} \left(u_i \left(\frac{h_a}{2} \right) - u_{ix} \left(-\frac{h_a}{2} \right) \right) \right] - z'' \frac{d^3 w_{ix}}{dx^3} \quad i = 2 \text{ or } 3. \quad (3.31)$$

Using the previous procedure, the formulas for the first and second segments of the upper adherend can be obtained as follows:

$$\frac{d^4 w_i}{dx^4} = \frac{12}{E_1^* h_1^3} \left\{ \frac{E_a}{h_a} (w_i - w_{ix}) + \frac{E_1^* h_1^2}{2} \left(z' \frac{d^4 w_i}{dx^4} + \frac{d^3 u_i}{dx^3} \right) \right\} \quad i = 2 \text{ or } 3, \quad (3.32)$$

$$\frac{d^2 u_i}{dx^2} = \frac{12}{E_1^* h_1} \left[-\frac{G_a}{h_a} \left(u_i \left(\frac{h_a}{2} \right) - u_{ix} \left(-\frac{h_a}{2} \right) \right) \right] - z' \frac{d^3 w_i}{dx^3} \quad i = 2 \text{ or } 3. \quad (3.33)$$

3-3. Non-dimensionalization and Symbolic manipulation

To regulate the magnitude of some parameters and illustrate clearly the detailed relationships among them, the parameters are non-dimensionalized and are listed in Table 1. For the first and fourth segments of the lower adherend, Eqs. (3.24) – (3.29) may be non-dimensionalized and rearranged as follows:

$$\frac{dw_{1x}}{dx} = -\frac{6\tilde{F}_L (2L_1 x + x^2)}{E_2 h_2^3} + c_{11}, \quad -L_1 \leq x \leq -c, \quad (3.34)$$

$$w_{1x} = -\frac{2\tilde{F}_L(3L_1x^2 + x^3)}{E_2h_2^3} + c_{11}x + c_{12}, \quad -L_1 \leq x \leq -c, \quad (3.35)$$

$$u_{1x} = \frac{1}{E_2} \left(\frac{\tilde{N}_L}{h_2} x - \frac{6\tilde{F}_L(2L_1x + x^2)z''}{h_2^3} \right) + c_{13}, \quad -L_1 \leq x \leq -c, \quad (3.36)$$

$$\frac{dw_{4x}}{dx} = -\frac{6(\tilde{P} - \tilde{F}_L)(2L_2x - x^2)}{E_2h_2^3} + c_{41}, \quad c \leq x \leq L_2, \quad (3.37)$$

$$w_{4x} = -\frac{2(\tilde{P} - \tilde{F}_L)(3L_2x^2 - x^3)}{E_2h_2^3} + c_{41}x + c_{42}, \quad c \leq x \leq L_2, \quad (3.38)$$

$$u_{4x} = \frac{1}{E_2} \left(\frac{\tilde{N}_L}{h_2} x - \frac{6(\tilde{P} - \tilde{F}_L)(2L_2x - x^2)z''}{h_2^3} \right) + c_{43}, \quad c \leq x \leq L_2, \quad (3.39)$$

where $E_1 = \frac{E_1^*}{G_a}$, $E_0 = \frac{E_a}{G_a}$, $E_2 = \frac{E_2^*}{G_a}$, $\tilde{N}_L = \frac{N_L}{G_a}$, $\tilde{F}_L = \frac{F_L}{G_a}$, and $\tilde{P} = \frac{P}{G_a}$.

Eqs. (3.30) – (3.33) can then be rewritten in the matrix form as:

$$\begin{bmatrix} D^2 - \frac{1}{E_1\beta_1h_a^2} & \frac{1}{E_1\beta_1h_a^2} & -\frac{\beta_1h_a}{2}D^3 - \frac{1}{E_1\beta_1h_a}D & 0 \\ \frac{1}{E_2\beta_2h_a^2} & D^2 - \frac{1}{E_2\beta_2h_a^2} & 0 & \frac{\beta_2h_a}{2}D^3 + \frac{1}{E_2\beta_2h_a}D \\ \frac{6}{\beta_1h_a}D^3 & 0 & -4D^4 - \frac{1}{h_ad_1} & \frac{1}{h_ad_1} \\ 0 & \frac{-6}{\beta_2h_a}D^3 & \frac{1}{h_ad_2} & -4D^4 - \frac{1}{h_ad_2} \end{bmatrix} \begin{bmatrix} \tilde{u}_i \\ \tilde{u}_{ix} \\ w_i \\ w_{ix} \end{bmatrix} \quad (3.40)$$

$$=[\mathbf{A}_D][u]=0,$$

where $\tilde{u}_i = u_i(\frac{h_a}{2})$, $\tilde{u}_{ix} = u_{ix}(-\frac{h_a}{2})$ and $D = \frac{d}{dx}$, i may be either 2 or 3, the non-dimensional

terms are $\beta_1 = \frac{h_1}{h_a}$ and $\beta_2 = \frac{h_2}{h_a}$, and other parameters are $d_1 = \frac{h_1^3 E_1^*}{12E_a}$, $d_2 = \frac{h_2^3 E_2^*}{12E_a}$.

The characteristic equation, $\det|\mathbf{A}_D|=0$, of coupled differential equations (40) can then be derived as follows:

$$[D^{12} - (\frac{4}{\beta_1 E_1 h_a^2} + \frac{4}{\beta_2 E_2 h_a^2})D^{10} + (\frac{1}{d_1 h_a} \frac{1}{d_2 h_a})D^8 - (\frac{1}{\beta_1 d_1 E_1 h_a^3} + \frac{4}{\beta_1 d_2 E_1 h_a^3} + \frac{3\beta_2}{\beta_1^2 d_2 E_1 h_a^3} + \frac{3\beta_1}{\beta_2^2 d_1 E_2 h_a^3} + \frac{4}{\beta_2 d_1 E_2 h_a^3} + \frac{1}{\beta_2 d_2 E_2 h_a^3})D^6] \{\tilde{u}_i, w_i, \tilde{u}_{ix}, w_{ix}\} = 0, \quad i = 2 \text{ or } 3, \quad (3.41)$$

Assuming that α , and $\pm \alpha_{11} \pm i\alpha_{12}$ are the roots of the characteristic Eq. (3.41), the transverse displacements w_i of the upper adherend are written in the following form:

$$w_i = c_{i0} + c_{i1}x + c_{i2}x^2 + c_{i3}x^3 + c_{i4}x^4 + c_{i5}x^5 + c_{i6}\overline{Ch} + c_{i7}\overline{Sh} + \overline{Ch}_1(c_{i8}\overline{C} + c_{i9}\overline{S}) + \overline{Sh}_1(c_{i10}\overline{C} + c_{i11}\overline{S}), \quad i = 2 \text{ or } 3, \quad (3.42)$$

where $\overline{Ch} = \cosh(\alpha x)$, $\overline{Sh} = \sinh(\alpha x)$, $\overline{Ch}_1 = \cosh(\alpha_{11}x)$, $\overline{Sh}_1 = \sinh(\alpha_{11}x)$, and the unknown constants are c_{ij} , $i = 2 \text{ or } 3$, $j = 0 \sim 11$, $\overline{C} = \cos(\alpha_{12}x)$, and $\overline{S} = \sin(\alpha_{12}x)$.

As the complete solutions of the model are extremely complex, this study employed Mathematica's symbolic manipulation to solve \tilde{u}_i , \tilde{u}_{ix} , w_{ix} , $\frac{dw_{ix}}{dx}$, and $\frac{dw_i}{dx}$ in terms of c_{ij} , \overline{S} , \overline{C} , \overline{Ch} , \overline{Sh} , \overline{Ch}_1 , and \overline{Sh}_1 . Because these detailed analytical solutions are complicated and easily keyed in error, they taken from the output results of Mathematica package are pasted in Appendix A. To prove these analytical solutions are correct, they are once again substituted into the system differential equation (3.41), which shows c_{i4} and c_{i5} to be equal to zero.

The analytical solutions \tilde{u}_i , \tilde{u}_{ix} , w_i , and w_{ix} (from Appendix: Eqs. A.1, A.2, A.15 and Eq. 3.40), which are substituted into Eqs. (3.16 – 3.17), and the adhesive layer's non-dimensional peel and shear stresses $\overline{\sigma}_{ai} = \frac{2c\sigma_{ai}}{P}$ and $\overline{\tau}_{ai} = \frac{2c\tau_{ai}}{P}$ (listed in Table 3.1) are then formulated in terms of c_{ij} , \overline{S} , \overline{C} , \overline{Ch} , \overline{Sh} , \overline{Ch}_1 , and \overline{Sh}_1 (i.e. analytical stress solutions, $\overline{\sigma}_{ai}$ and $\overline{\tau}_{ai}$ are revealed in Appendix B).

The analytical stress solutions, $\bar{\sigma}_{ai}$ and $\bar{\tau}_{ai}$, (from Appendix: Eqs. B1, B2) are substituted into Eqs. (3.4 – 3.9, 3.13 – 3.15). The shear force $\bar{Q}_i = \frac{Q_i}{P}$, the bending moment $\bar{M}_i = \frac{M_i}{2Pc}$, and the longitudinal force $\bar{N}_i = \frac{N_i}{P}$ for the upper adherend, as well as the shear force $\bar{Q}_{ix} = \frac{Q_{ix}}{P}$, the bending moment $\bar{M}_{ix} = \frac{M_{ix}}{2Pc}$, and the longitudinal force $\bar{N}_{ix} = \frac{N_{ix}}{P}$ for the lower adherend (all listed in Table 3.1 are also expressed in terms of c_{ij} , \bar{S} , \bar{C} , \bar{Ch} , \bar{Sh} , \bar{Ch}_1 , and \bar{Sh}_1). These equations are shown in Appendix C.

The preceding bending moments M_i , M_{ix} and longitudinal forces N_i , N_{ix} are substituted into Eqs (3.18)-(3.19). The non-dimensional stresses, $\bar{\sigma}_i = \frac{2c\sigma_i}{P}$, and $\bar{\sigma}_{ix} = \frac{2c\sigma_{ix}}{P}$ of upper and lower adherends can be found in terms of the coefficients of bending moments M_i , M_{ix} and of longitudinal forces N_i , N_{ix} .

For the first and fourth segments, Eqs. (3.1 – 3.3, 3.10 – 3.12) are rewritten and non-dimensionalized. The resulting non-dimensional bending moment, shear force, and longitudinal force (\bar{M}_{1x} , \bar{Q}_{1x} , \bar{N}_{1x} , \bar{M}_{4x} , \bar{Q}_{4x} , and \bar{N}_{4x}), are formulated as shown below:

$$\bar{M}_{1x} = \frac{M_{1x}}{2Pc} = -\frac{F_L}{2Pc}(L_1 + x) = -\frac{\tilde{F}_L}{2\tilde{P}c}(L_1 + x), \quad (3.43)$$

$$\bar{Q}_{1x} = \frac{Q_{1x}}{P} = \frac{F_L}{P} = \frac{\tilde{F}_L}{\tilde{P}}, \quad (3.44)$$

$$\bar{N}_{1x} = \frac{N_{1x}}{P} = \frac{N_L}{P} = \frac{\tilde{N}_L}{\tilde{P}}, \quad (3.45)$$

$$\bar{M}_{4x} = \frac{M_{4x}}{2Pc} = -\frac{F_R}{2Pc}(L_2 - x) = \frac{(F_L - P)}{2Pc}(L_2 - x) = \frac{(\tilde{F}_L - \tilde{P})}{2\tilde{P}c}(L_2 - x), \quad (3.46)$$

$$\bar{Q}_{4x} = \frac{Q_{4x}}{P} = -\frac{F_R}{P} = \frac{F_L - P}{P} = \frac{\tilde{F}_L - \tilde{P}}{\tilde{P}}, \quad (3.47)$$

$$\bar{N}_{4x} = \frac{N_{4x}}{P} = \frac{N_R}{P} = \frac{N_L}{P} = \frac{\tilde{N}_L}{\tilde{P}}. \quad (3.48)$$



Table 3.1 The non-dimensional terms and equations for upper adherend, adhesive layer and lower adherend.

Non-dimensional terms for upper adherend	Equation	Non-dimensional terms for lower adherend	Equation
Thickness ratio	$\beta_1 = \frac{h_1}{h_a}$	Thickness ratio	$\beta_2 = \frac{h_2}{h_a}$
Thickness to length ratio	$\gamma_1 = \frac{h_1}{2c}$	Thickness to length ratio	$\gamma_2 = \frac{h_2}{2c}$
Elastic modulus	$E_1 = \frac{E_1^*}{G_a}$	Elastic modulus	$E_2 = \frac{E_2^*}{G_a}$
Shear force	$\bar{Q}_i = \frac{Q_i}{P}$	Shear force	$\bar{Q}_{ix} = \frac{Q_{ix}}{P}$
Moment	$\bar{M}_i = \frac{M_i}{2Pc}$	Moment	$\bar{M}_{ix} = \frac{M_{ix}}{2Pc}$
Longitudinal force	$\bar{N}_i = \frac{N_i}{P}$	Longitudinal force	$\bar{N}_{ix} = \frac{N_{ix}}{P}$
Normal stress	$\bar{\sigma}_i = \frac{2c\sigma_i}{P}$	Normal stress	$\bar{\sigma}_{ix} = \frac{2c\sigma_{ix}}{P}$
Non-dimensional terms for adhesive layer	Equation		
Peel stress	$\bar{\sigma}_{ai} = \frac{2c\sigma_{ai}}{P}$		
Shear stress	$\bar{\tau}_{ai} = \frac{2c\tau_{ai}}{P}$		
Elastic modulus	$E_0 = \frac{E_a}{G_a}$		
x axis	$\bar{x} = \frac{x}{c}$		

3-4. Constraint and Boundary Conditions

The constraint and boundary conditions for this study, shown in Fig. 3.1, can be identified and described in the following manner.

At the left-end pin support ($x = -L_1$) of the lower adherend, there are two boundary conditions, i.e. zero transverse displacement and zero longitudinal displacement of the lower adherend. At $x = -c$, there are eight constraint conditions, six of which are continuity conditions for the lower adherend. That is, at junction point ($x = -c$) between the first and second segments of the lower adherend, both segments must have the same values of transverse displacement, slope, bending moment, shear force, longitudinal force, and longitudinal displacement. The other two conditions at $x = -c$ are that both the bending moment and longitudinal force of the upper adherend must be equal to zero.

At junction point ($x = -d$) between the second and third segments, there are eleven conditions, eight of which are continuity conditions. First, in both upper and lower adherends, both segments must again have the same values of transverse displacement, slope, bending moment, and longitudinal displacement. Three other conditions are written as follows: (i) the total shear force in the left neighborhood of the junction point ($x = -d^-$) is \tilde{F}_L / \tilde{P} , (ii) the total shear force in the right neighborhood of the junction point ($x = -d^+$) is $(\tilde{F}_L - \tilde{P}) / \tilde{P}$, and (iii) the total longitudinal force has the same value at junction point ($x = -d$) for both second and third segments.

The model also is subjected to eight constraint conditions at $x = c$. At the junction point ($x = c$) between the third and fourth segments of the lower adherend, both segments must have the same values of transverse displacement, slope, bending moment, shear force, longitudinal force, and longitudinal displacement. In addition, the bending moment and longitudinal force of the upper adherend must be equal to zero.

At the right-end pin support ($x = L_2$) of the lower adherend, there are again two boundary conditions, i.e. the transverse displacement and longitudinal displacement for the lower adherend must be zero.

Overall, the number of boundary and constraint conditions totals 31, equal to the number of unknown constants. The unknown constants include c_{ij} , c_{ai1} , c_{ai2} , c_{1k} , c_{4k} , and N_L – where subscript i is equal to 2 or 3, k ranges from 1 to 3, and j ranges from 1 to 12 – but c_{i4} and c_{i5} (found in the preceding descriptions) equal zero. c_{ai1} and c_{ai2} are the unknown constants of the longitudinal displacements and result from substituting the analytical solutions \tilde{u}_i , \tilde{u}_{ix} , w_i and w_{ix} (from Appendix: Eqs. A.1, A.2, A.15 and Eq. 3.46) into the integrated Eqs. (3.29) and (3.31).

Imposing 31 constraint and boundary equations on the analytical solutions through symbolic manipulation produces 31 system equations expressed in the following matrix form.

$$[\mathbf{A}][\mathbf{C}]=[\mathbf{B}] \tag{3.49}$$

where matrix $[\mathbf{A}]$ has 31 rows and 31 columns, denoted by $[\mathbf{A}]_{31 \times 31}$, and matrices $[\mathbf{B}]$ and $[\mathbf{C}]$ have 31 rows and 1 column, denoted by $[\mathbf{B}]_{31 \times 1}$ and $[\mathbf{C}]_{31 \times 1}$, respectively. The elements in matrix $[\mathbf{C}]_{31 \times 1}$ consist of 31 unknown constants, c_{ij} , c_{ai1} , c_{ai2} , c_{1k} , c_{4k} , and N_L . $[\mathbf{A}]_{31 \times 31}$, $[\mathbf{B}]_{31 \times 1}$ and $[\mathbf{C}]_{31 \times 1}$ are shown in the Appendix D

The matrix $[\mathbf{C}]_{31 \times 1}$ is solved using Mathematica's SVD algorithm because matrix $[\mathbf{A}]$ has a greater variation in the magnitude of the matrix elements. If one eigenvalue in the characteristic equation (3.39) is large, some elements of matrix $[\mathbf{A}]$ that involve \overline{Sh} , \overline{Ch} , \overline{Sh}_1 , and \overline{Ch}_1 become much larger. However, the magnitude of those elements in matrix $[\mathbf{A}]$ that do not involve \overline{Sh} , \overline{Ch} , \overline{Sh}_1 and \overline{Ch}_1 is much smaller. Thus, there is a discrepancy in the magnitude of matrix $[\mathbf{A}]$ elements exceeding the exponential order of 10s.

In addition, because of computer truncation errors, the inverse of matrix $[A]$ cannot be obtained by the adjoint method. Therefore, matrix $[C]_{31 \times 1}$ is solved by SVD algorithm and the non-dimensional peel stress and shear stress in the adhesive layer can be obtained by substituting matrix $[C]_{31 \times 1}$ into the expressions $\bar{\sigma}_{ai}$ and $\bar{\tau}_{ai}$.

3-5. Results and Discussion

3-5-1. Application of Closed-form Solutions

It is depicted below in more details that the preceding close-formed solutions are applied to cantilever beam strengthened by adhesively bonding [29] and a single lap joint [30].

Cornell [29] proposed the model of a cantilever beam strengthened by adhesively bonding. The sketch of Cornell's model is shown in Fig. 3.8 and the symbols h_1 , h_2 , and h_a are denoted as the thicknesses of the two adherends and the thickness of the adhesive. Fig. 3.9 shows the analytical solutions of this model employed to solve the problem proposed by Cornell, using the following values: (i) $h_1 = 0.04$ in (1.016mm), $h_2 = 0.25$ in (6.35mm), and $h_a = 0.1$ in (2.54mm), 0.01 in (0.254mm), and 0.001 in (0.0254mm), (ii) Young's modulus of two adherends and adhesive are respectively 30×10^6 psi, 30×10^6 psi, and 15×10^6 psi, and (iii) shear modulus of adhesive layer is 5×10^6 psi. Because Cornell's Fig. 6 shown in the bottom diagram of Fig. 3.9 has used inch (in) as length units, Fig. 3.9 also uses inch as length units. All figures except Fig. 3.9 use mm as length units. It should be noted that the symbol h_a in this study is synonymous with Cornell's h_b and the profiles of Fig. 3.9 are nearly consistent with those of Cornell's Fig. 6. Single lap joint shown in Fig. 3.10 is one of Zou et al.'s examples [30] and the sketch of Zou et al.'s example shows the dimensions of the single lap joint. The Aluminum adherends bonded by adhesive are subjected to bending moment

100N.m in the Zou et al.'s example. Zou et al.'s example uses the following values: (i) Young's modulus of Aluminum adherends and adhesive are 75GPa and 2.5GPa, and (ii) shear modulus of Aluminum adherends and adhesive are 28.846GPa and 1.0GPa. The numerical results obtained by employing the analytical solutions to solve the problem in Zou et al. are shown in Fig. 3.11. These data are almost consistent with those of Fig. 5 in the Zou et al.'s paper, except that for this study, the maximum shear stress is 4.38, while in Zou et al. it is 4.30 (MPa).

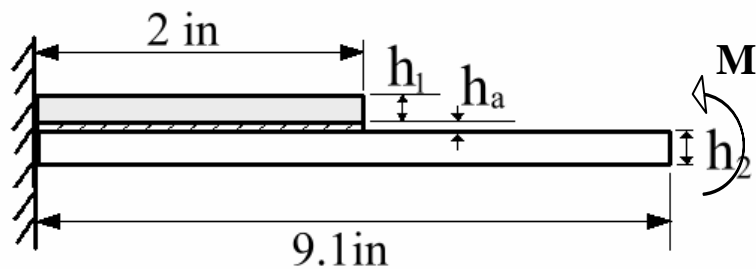


Fig. 3.8 The sketch of the Cornell's model [29] showing cantilever beam strengthened by adhesively bonding

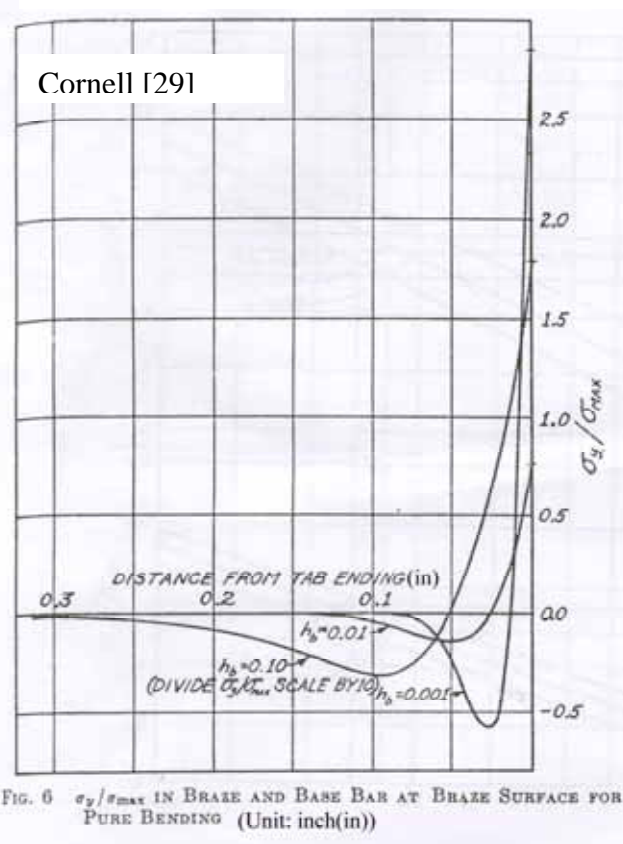
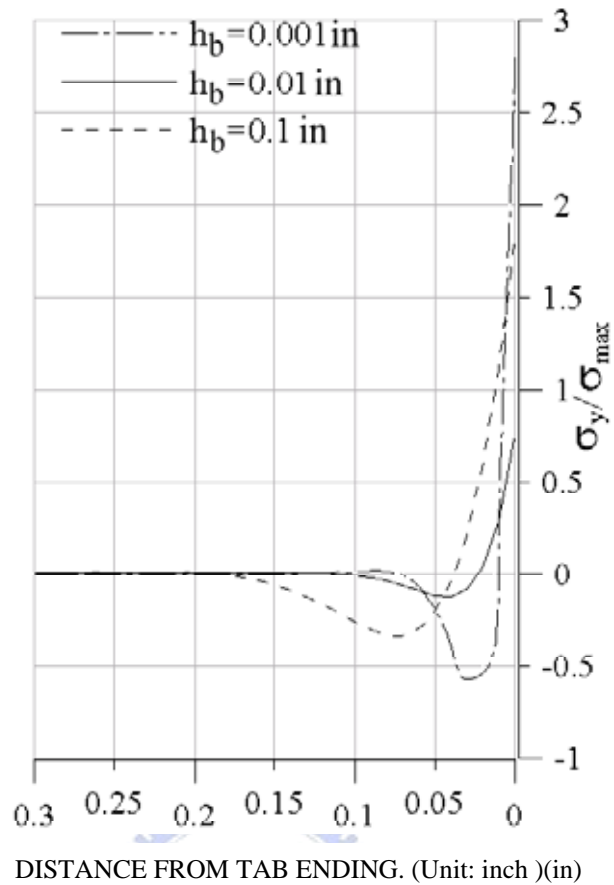


Fig. 3.9 Comparison of the results between the present study (top) and figure 6 of the Cornell's paper [29] (bottom).

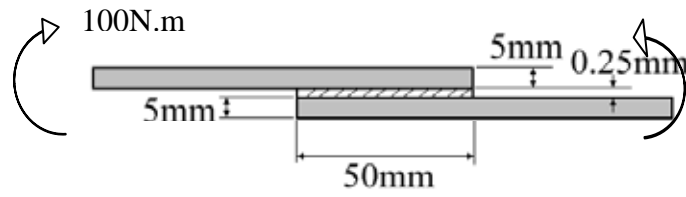


Fig. 3.10 The sketch of the Zou et al. model [30] showing a single lap joint

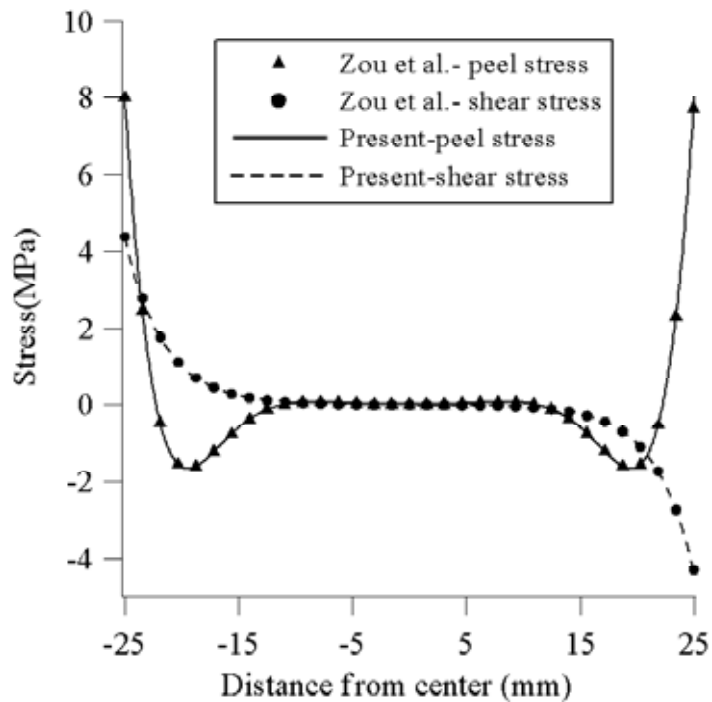


Fig. 3.11 Comparison of the results between figure 5 of the Zou et al.'s paper [30] and the present study.

3-5-2. Case Studies

The values $E_1 = 6.0$, $E_2 = 6.0$, $E_0 = 2.75$, $\tilde{P} = 1$, and $d = 0$ are used as the following case 1-4. The symbols E_1 , E_2 , and E_0 (listed in Table 3.1) represent the ratios of the elastic modulus of the upper adherend, lower adherend, and adhesive layer, respectively, to the shear

modulus of the adhesive layer. The symbol d represents the distance from the center of the adhesive layer to the action point of the force.

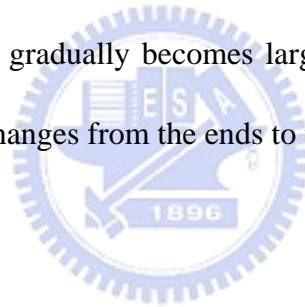
Case 1: Upper adherend (h_1) and lower adherend (h_2) with the same thickness

Fig. 3.12 shows distributions of the non-dimensional peel stress and shear stress in the adhesive layer, whose thickness is $h_a = 0.01mm$. The thickness ratios $\beta_1 = \frac{h_1}{h_a} = 10$ and $\beta_2 = \frac{h_2}{h_a} = 10$ are defined as the thickness of the upper adherend and lower adherend respectively relative to the adhesive layer's thickness. $\bar{x} = \frac{x}{c}$ is both the normalized axis and the non-dimensional term of the adhesive layer, where $-1 \leq \bar{x} \leq 1$. The thickness to length ratio $\gamma = \gamma_1 = \gamma_2 = \frac{h}{2c}$ is the ratio of the thickness $h = h_1 = h_2$ of the upper adherend to the length ($2c$) of the adhesive layer: $\gamma = 0.01667$ and $\gamma = 0.06667$ are used in this case. Moreover, when $\gamma = 0.01667$, the length of the adhesive layer is four times that when $\gamma = 0.06667$. Thus, the non-dimensional peel and shear stress distributions for an adhesive layer when $\gamma = 0.01667$ are different from those when $\gamma = 0.06667$. As the thickness to length ratio decreases – $\gamma = 0.06667$ to $\gamma = 0.01667$ – the non-dimensional peel and shear stresses in the adhesive layer become slightly less than 0.1.

Fig. 3.12 also illustrates that the non-dimensional maximum peel and shear stresses may occur either in the center or at the ends of the adhesive layer. Therefore, the values and positions of the non-dimensional maximum peel and shear stresses are the focus of the following paragraphs.

For the adhesive layer, as shown in Fig. 3.13, the non-dimensional peel stress occurs either in the center ($\bar{x} = 0$) or at the ends ($\bar{x} = \pm 1$), and the non-dimensional shear stress

occurs at the ends versus the thickness to length ratio γ . As γ becomes larger – i.e. the length (2c) of the adhesive layer becomes smaller in the same thickness ratios $\beta = \beta_1 = \beta_2$ – the peel stress in the center ($\bar{x} = 0$) is at first positive and smaller (i.e. tensile stress) but then becomes larger and then negative and even larger (i.e. compressive stress). As also shown in Fig. 3.13, the different thickness ratios $\beta = \frac{h}{h_a}$ produce the same results – $\beta = \beta_1 = \beta_2 = 10, 20, \text{ or } 30$ – meaning that the thickness of the upper adherend as well as of the lower adherend can be 10, 20, or 30 times that of the adhesive layer. Thus, if both the upper adherend and lower adherend become thinner (i.e. β decreases from 30 to 10), the peel stress in the center becomes even larger as the thickness to length ratio γ increases. Moreover, since the maximum peel stress is always located either in the center ($\bar{x} = 0$) or at the ends ($\bar{x} = 1$), as the thickness to length ratio γ gradually becomes larger, the location of the maximum peel stresses in the adhesive layer changes from the ends to the center (see Fig. 3.13).



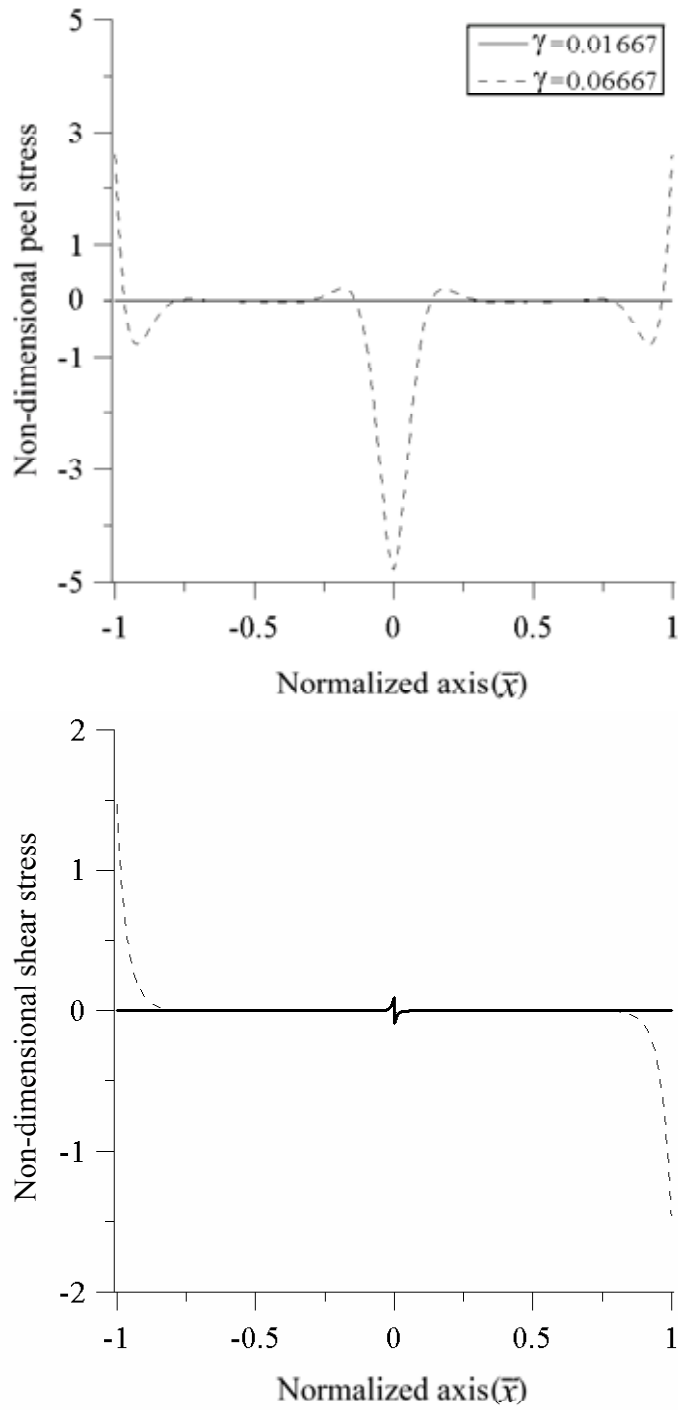


Fig. 3.12 Non-dimensional peel and shear stresses distributions in the adhesive layer ($\bar{x} = x/c$) for the thickness to length ratio $\gamma = \gamma_1 = \gamma_2$ with the same thickness of both adherends $\beta_1 = \beta_2 = 10$ and ($h_a = 0.01mm$)

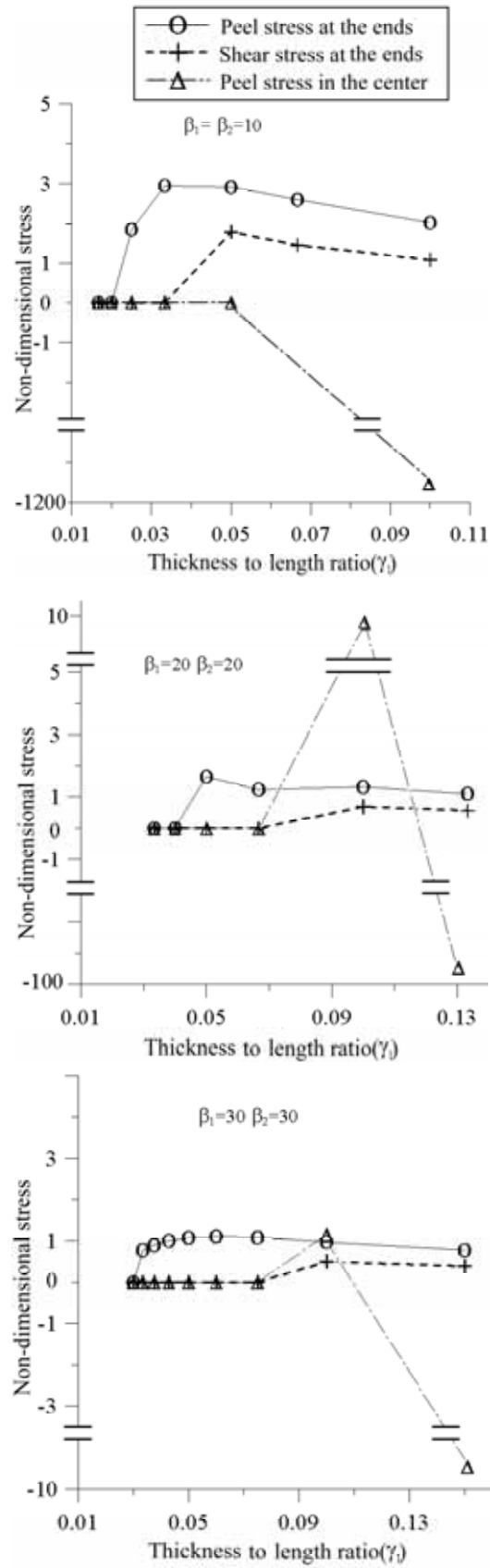


Fig. 3.13 Non-dimensional peel and shear stresses versus the thickness to length ratio $\gamma = \gamma_1 = \gamma_2$ for the same thickness of the adherends as for Case 1 ($h_a = 0.01mm$).

Case 2: Upper adherend (h_1) and lower adherend (h_2) with different thicknesses

As Fig. 3.14(a) shows, in this case, the thickness of the upper adherend is three times that of the lower adherend, meaning that the thickness of the upper adherend in Fig. 3.14(a) is three times that in Fig. 3.12 even though the two figures have the same conditions otherwise. . For $\gamma_1 = 0.05$ and $\gamma_2 = \frac{1}{3}\gamma_1 = 0.01667$ in Fig. 3.14(a), the non-dimensional peel stress and shear stress distributions are very similar to those in Fig. 3.12 ($\gamma = 0.01667$). However, for $\gamma_1 = 0.2$ and $\gamma_2 = 0.06667$, the non-dimensional peel stress in Fig. 3.14(a), in total contrast to the larger compressive peel stress in the center in Fig. 3.12 ($\gamma = 0.06667$), vanishes in the center of the adhesive layer. In Fig. 3.14(a), the maximum peel stress at the ends is about one-and-a-quarter times that in Fig. 3.12, while the maximum shear stress at the ends in Fig. 3.14(a) is about 1.5 which is close to that in Fig. 3.12.

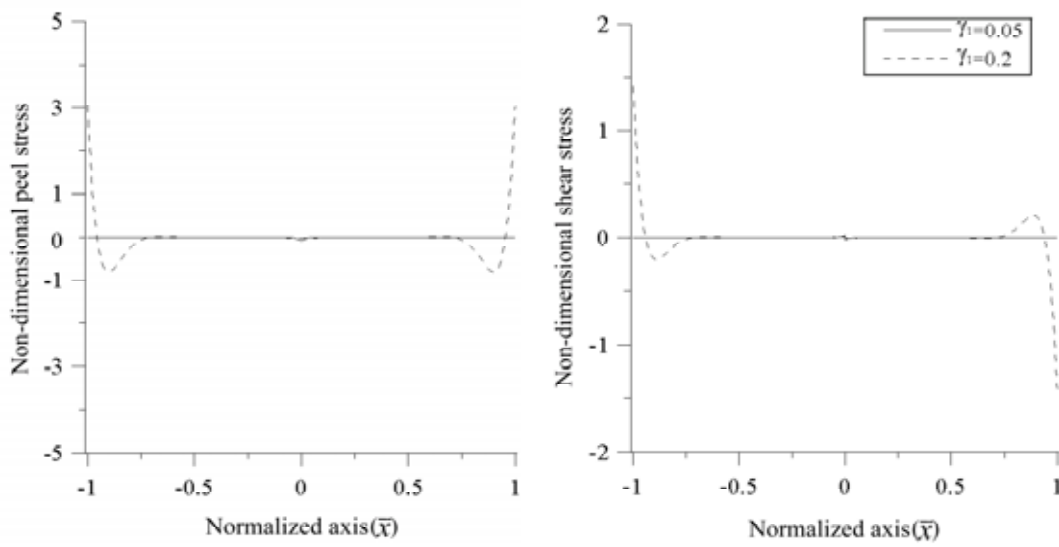
As Fig. 3.14(b) indicates, the thickness of the lower adherend is three times that of the lower adherend in Fig. 3.12, even though otherwise the two figures have the same conditions. However, whether $\gamma_1 = 0.06667$ or $\gamma_1 = 0.01667$, the non-dimensional peel stress vanishes in the center of the adhesive layer. Moreover, the maximum peel stress at the ends of the adhesive layer in Fig. 3.14(b) is about one-seventh of that in Fig. 3.14(a), while the maximum shear stress at the ends in Fig. 3.14(b) is about one-fifth of that in Fig. 3.14(a).

Fig. 3.15 shows the relationships among non-dimensional peel and shear stresses (at the ends and in the center), as different condition between Fig. 3.15(a) and the top diagram of Fig. 3.13 is that the thickness of the upper adherend in the former is three times that in the latter. However, in Fig. 3.15(a), in contrast to Fig. 3.13, the compressive peel stress in the center does not occur for γ_1 . Consequently, in Fig. 3.15(b) the peel stress in the center again vanishes for γ_1 and the maximum peel and shear stresses occur only at the ends. Moreover,

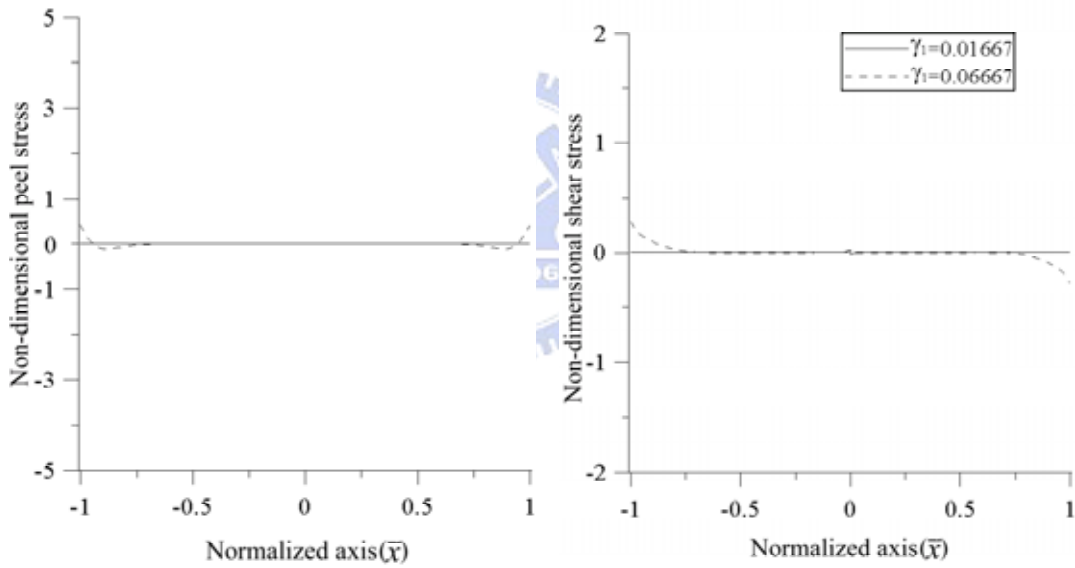
whether $\gamma_1 = 3\gamma_2$ or $\gamma_1 = \frac{1}{3}\gamma_2$, the maximum peel and shear stresses for the various lengths of the adhesive layer always occur at the ends. Nevertheless, the maximum peel and shear stresses in Fig. 3.15(a) are larger than those in Fig. 3.15(b). well as the thickness to length ratio γ_1 for the upper adherend: γ_1 is equal to $3\gamma_2$ for Fig. 3.15(a) and to $\frac{1}{3}\gamma_2$ for Fig. 3.15(b). The only

Case 3: Adhesive layer with different thickness (h_a)

Comparisons between Fig. 3.15(c) and 3.15(d) with the $h_a = 0.05$ mm thickness of the adhesive layer and between Fig. 3.15(a) and 3.15(b) with $h_a = 0.01$ mm adhesive layer thickness are made and described as follows. The only difference between the two sets of figures is the different thickness and the other conditions are the same. Again, the peel stress almost vanishes in the center for Fig. 3.15(a-d), and whether $\gamma_1 = 3\gamma_2$ or $\gamma_1 = \frac{1}{3}\gamma_2$, the maximum peel and shear stresses occur at the ends. The thicknesses $h_a = 0.05$ mm and $h_a = 0.01$ mm of the adhesive layer are compared in Fig. 3.15(a)(b) and 3.15(c)(d). The maximum peel and shear stresses occur at the ends in Fig. 3.15(a-d), but their maximum values in Fig. 3.15(a)(b) ($h_a = 0.01$ mm) are larger than those in Fig. 3.15(c)(d) ($h_a = 0.05$ mm). In Fig. 3.15(a) (b) (c), and (d), γ_1 values of 0.08, 0.025, 0.05, and 0.015, respectively, begin to bring about the maximum peel and shear stresses at the ends. However, when the adhesive layer is relatively thicker (i.e. $h_a = 0.05$ mm), the thickness to length ratios ($\gamma_1 = 0.05, 0.015$) that begin to bring about the maximum peel and shear stresses at the ends is smaller. That is, the adhesive layer with $h_a = 0.05$ mm thickness may be longer than that with $h_a = 0.01$ mm thickness, but its maximum peel and shear stresses may still occur at the ends.

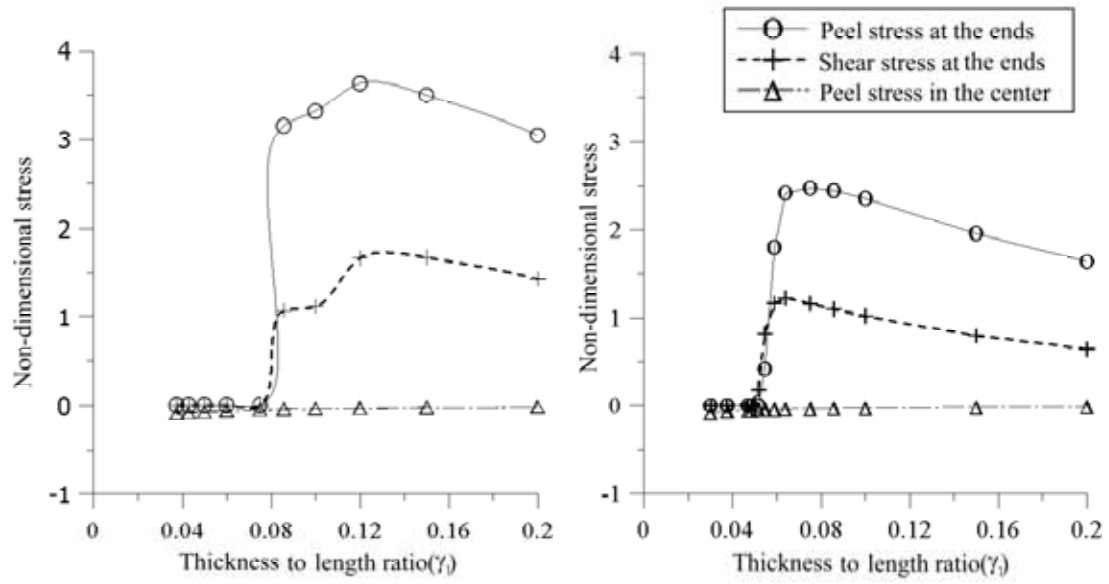


(a) Thickness ratio $\beta_1 = 30$, $\beta_2 = 10$ ($\gamma_1 = 3\gamma_2$)

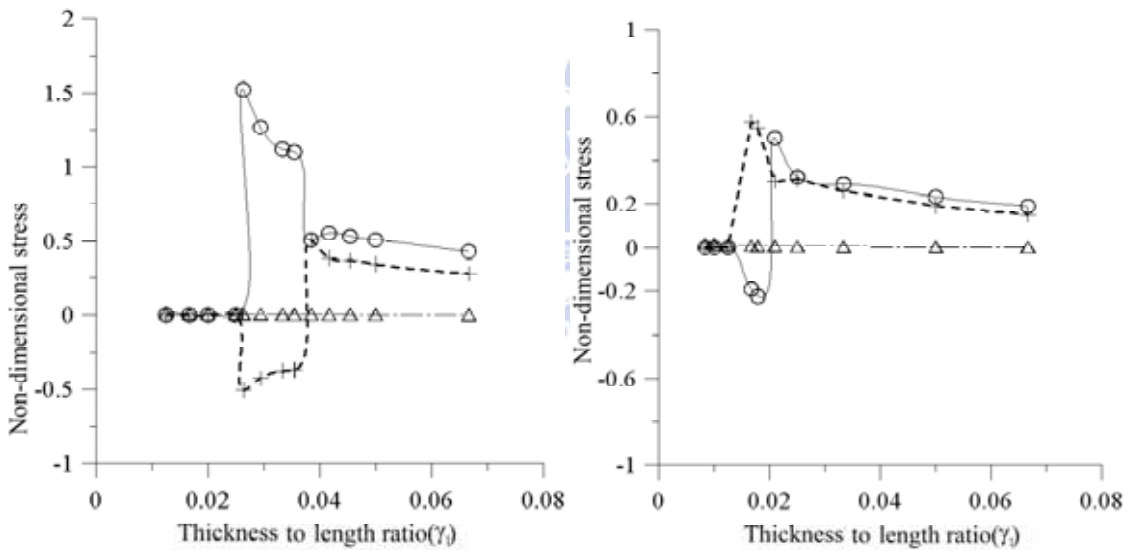


(b) Thickness ratio $\beta_1 = 10$, $\beta_2 = 30$ ($\gamma_1 = \frac{1}{3}\gamma_2$)

Fig. 3.14 Non-dimensional peel and shear stress distributions in the adhesive layer ($\bar{x} = x/c$) versus the thickness to length ratio γ_1 for various thicknesses of the adherends for Case 2, ($h_a = 0.01mm$).



(a) $\beta_1 = 30, \beta_2 = 10 (\gamma_1 = 3\gamma_2), h_a = 0.01mm$ (c) $\beta_1 = 6, \beta_2 = 2 (\gamma_1 = 3\gamma_2), h_a = 0.05mm$



(b) $\beta_1 = 10, \beta_2 = 30 \left(\gamma_1 = \frac{1}{3}\gamma_2 \right), h_a = 0.01mm$ (d) $\beta_1 = 2, \beta_2 = 6 \left(\gamma_1 = \frac{1}{3}\gamma_2 \right), h_a = 0.05mm$

Fig. 3.15 Non-dimensional peel and shear stresses versus the thickness to length ratio of the upper adherend γ_1 for various thicknesses of the adherends for Cases 2 and 3.

Case 4: Force P action point

As Fig. 3.16 shows, when $\beta = 10, h_a = 0.01 \text{ mm}$, and $\gamma = \gamma_1 = \gamma_2 = 0.01667$, the distributions of the non-dimensional peel and shear stresses are relative to the distance d from

the center of the adhesive layer to the action point of force P. Most particularly, the non-dimensional peel and shear stress distributions have a great effect on the distance d for an adhesive layer with a thickness of 0.01mm. However, as Fig. 3.17 illustrates, when $\beta = 10$, $h_a = 0.02$ mm, and $\gamma = \gamma_1 = \gamma_2 = 0.05$, the non-dimensional peel stress distribution has only little effect on the distance d for an adhesive layer with a thickness of 0.02 mm. In Fig. 3.17, not only does the distribution of the peel stress lead to change in only a small region of the action point, but also it causes virtually no change at the ends. The non-dimensional shear stress at the right end does not change because it is located far from the action point of the force. At the same time, the change in shear stress is due to the action point of the force near the left end.

Case 5: Young's modulus of adherends and adhesive layer

Fig. 3.18 shows non-dimensional stress distributions relative to Young's modulus ratio. Then, Young modulus ratio is defined as Young's modulus of the upper adherend divided by that of the lower adherend. The data values of the dashed line in Fig. 3.18 are the same as those in Fig. 3.12 with the same Young's modulus of adherends. As Young's modulus ratio is equal to 10.0, except that the Young's modulus of the upper adherend is ten times that of the dashed line, the other parameters' values are the same as those of the dotted line. Young's modulus ratio 10.0 at both ends has nearly the same peel and shear stresses' value as Young's modulus ratio 1.0 but its peel stress in the center is about zero. Similarly, As Young's modulus ratio is equal to 0.1, only one condition is changed i.e. the Young's modulus of the lower adherend is changed into 0.1 times of that of the dashed line. Then, its peel and shear stresses at both ends are about one-third and one-fourth of those of the dashed line. However, its peel stress in the center is about zero. Hence, the stress distributions of this model should be affected by the change of the adherend's mechanical properties.

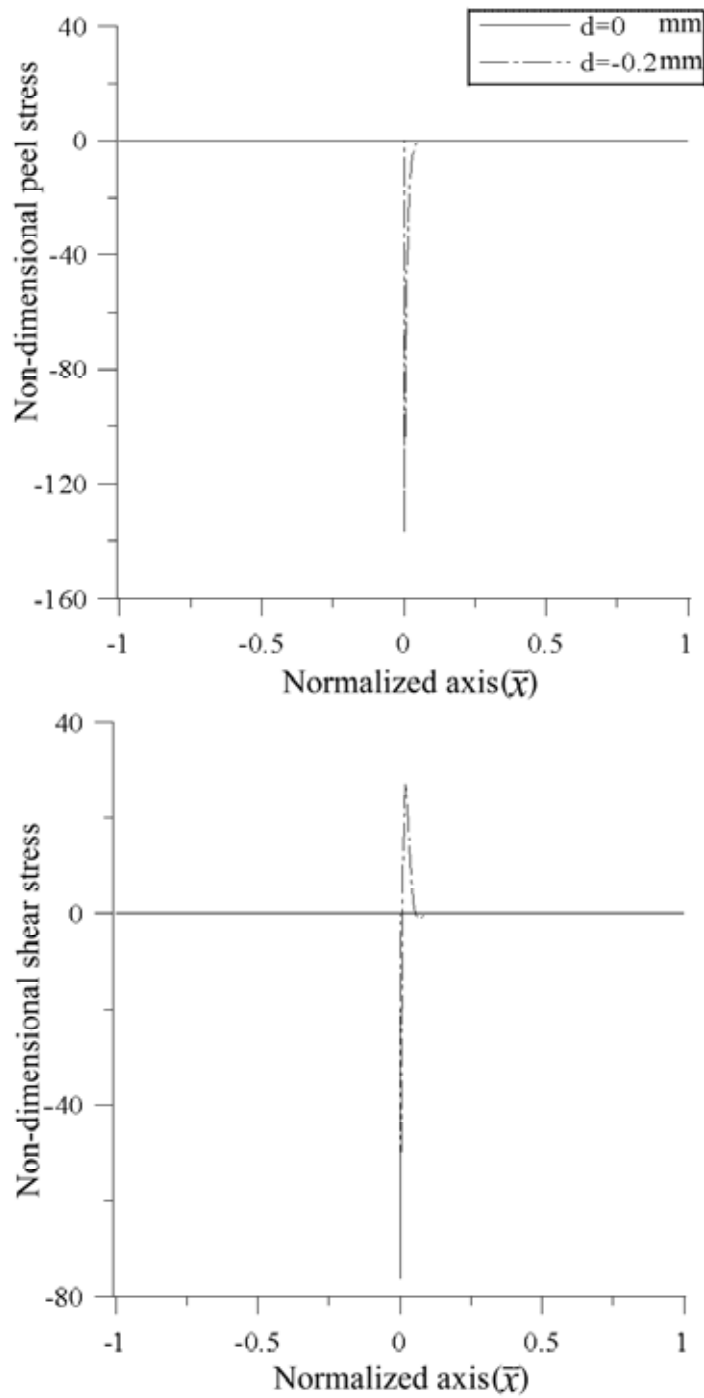


Fig. 3.16 Non-dimensional peel and shear stress distributions for the distance d from the center of the adhesive layer to the action point of the force ($h_a = 0.01\text{mm}$, $\gamma = 0.01667$).

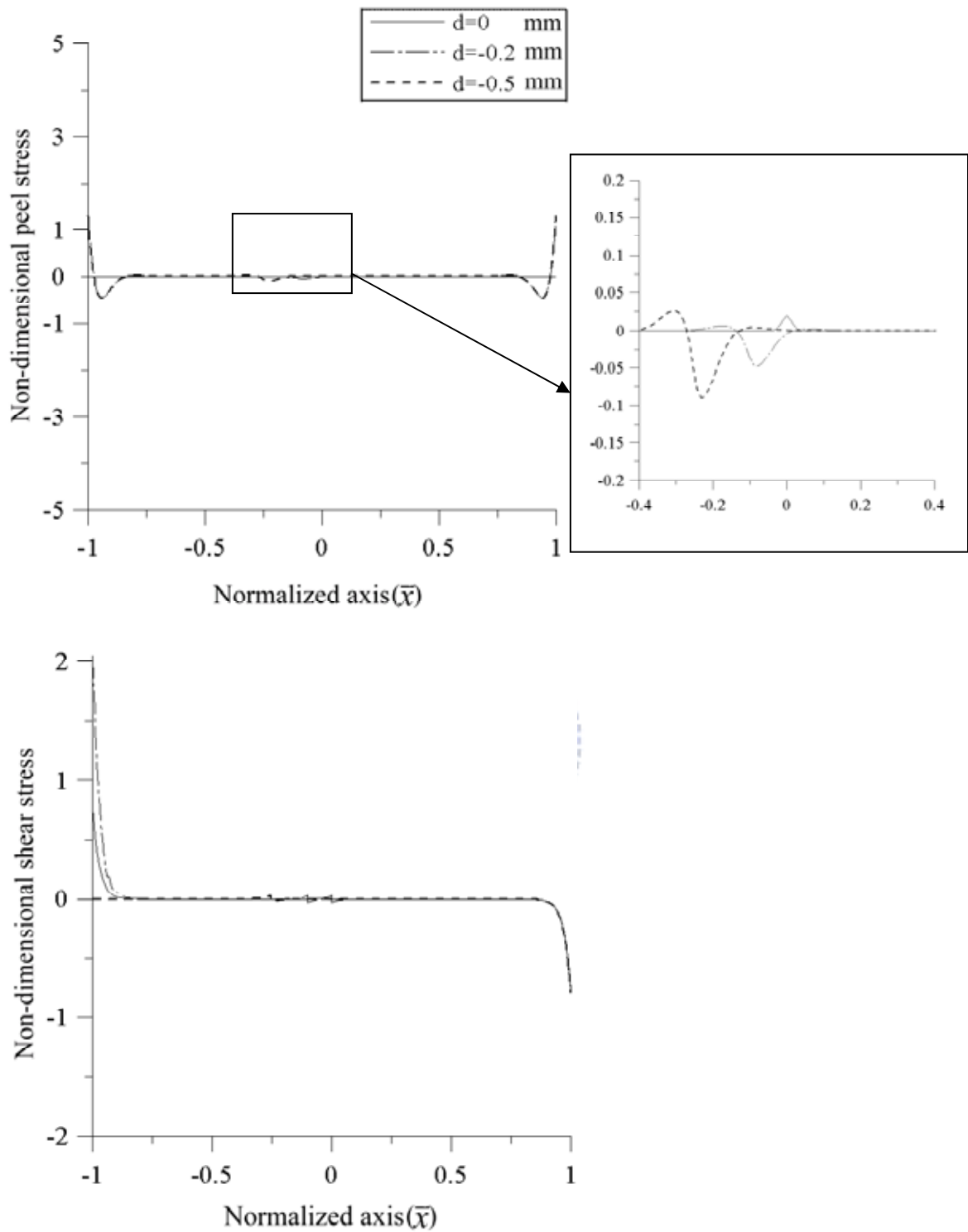


Fig. 3.17 Non-dimensional peel and shear stress distributions for different distances d from the center of the adhesive layer to the action point of force ($h_a = 0.02\text{mm}$, $\gamma = 0.05$).

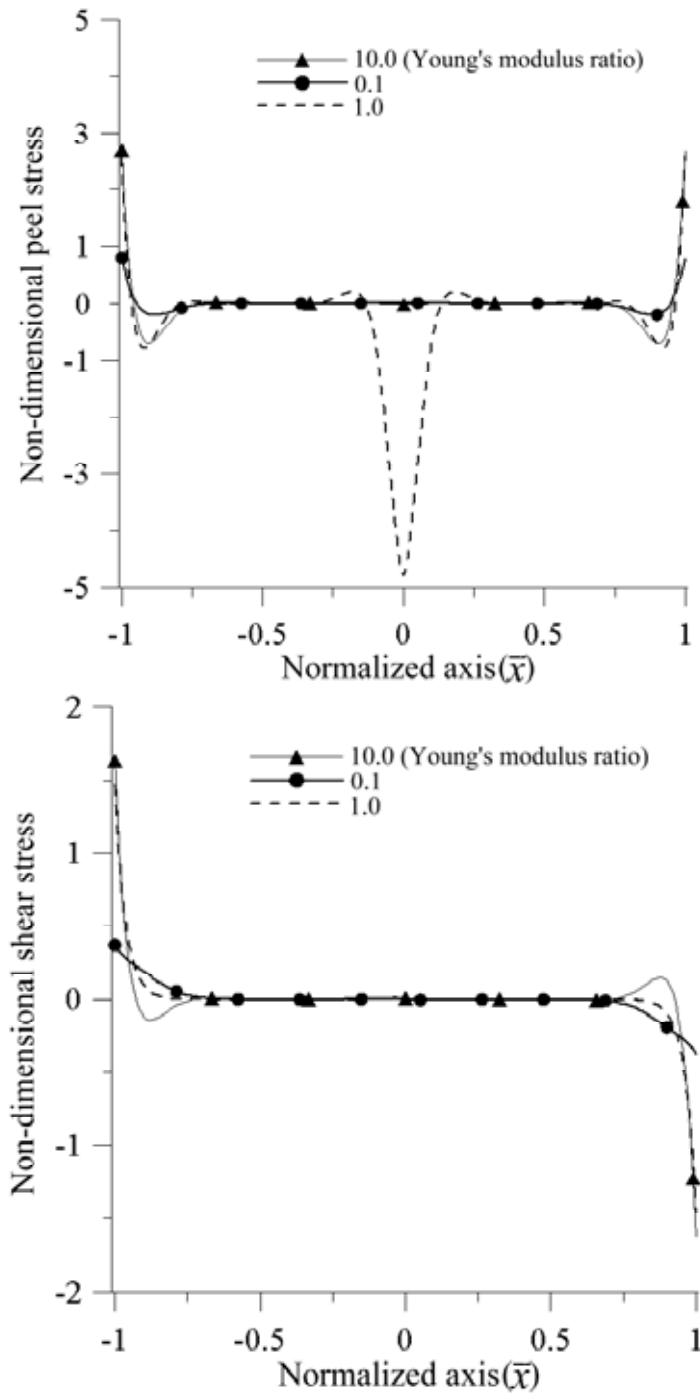


Fig. 3.18 Non-dimensional peel and shear stresses distributions in the adhesive layer ($\bar{x} = x/c$) for Young's modulus ratio with the same thickness of both adherends $\beta_1 = \beta_2 = 10$ and ($h_a = 0.01mm$)

Fig. 3.19 shows non-dimensional stresses versus adhesive Young's modulus ratio. Adhesive Young's modulus ratio is defined as the ratio of adhesive Young's modulus to adhesive Young's modulus of the dashed line in Fig. 3.12. Young's modulus of the adhesive layer in the Fig. 3.19 only is relatively changed for Young's modulus of the dashed line in Fig. 3.12. The peel and shear stresses at both ends do not have obvious variance relative to adhesive Young's modulus ratio but the peel stress in the center varies from compressive stress to tensile stress and then become once again compressive stress. Thus, the effects of adhesive mechanical properties on the stress distributions of this model are significant and apparent.

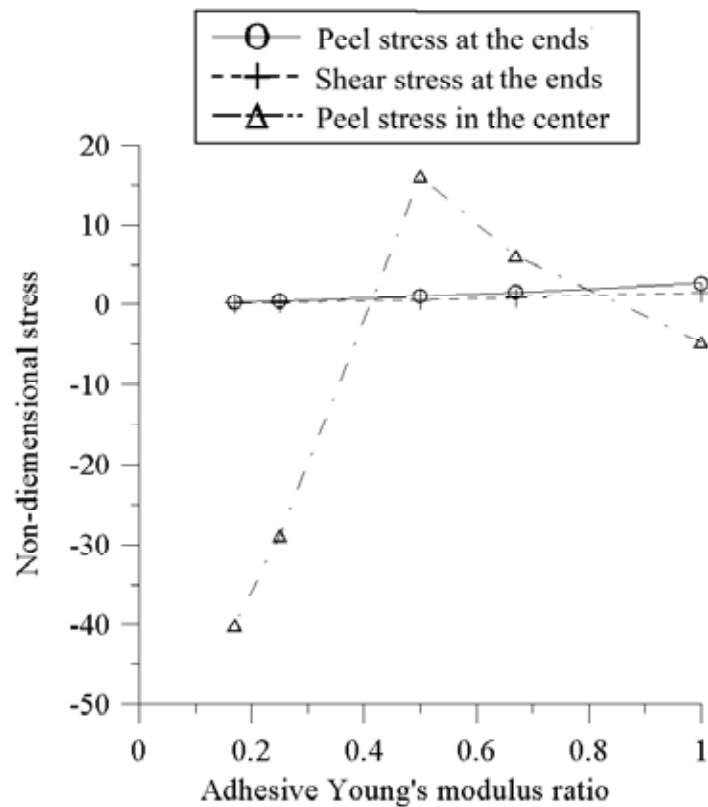


Fig. 3.19 Non-dimensional peel and shear stresses versus the adhesive Young's modulus ratio with the same thickness of both adherends $\beta_1 = \beta_2 = 10$ and ($h_a = 0.01mm$)

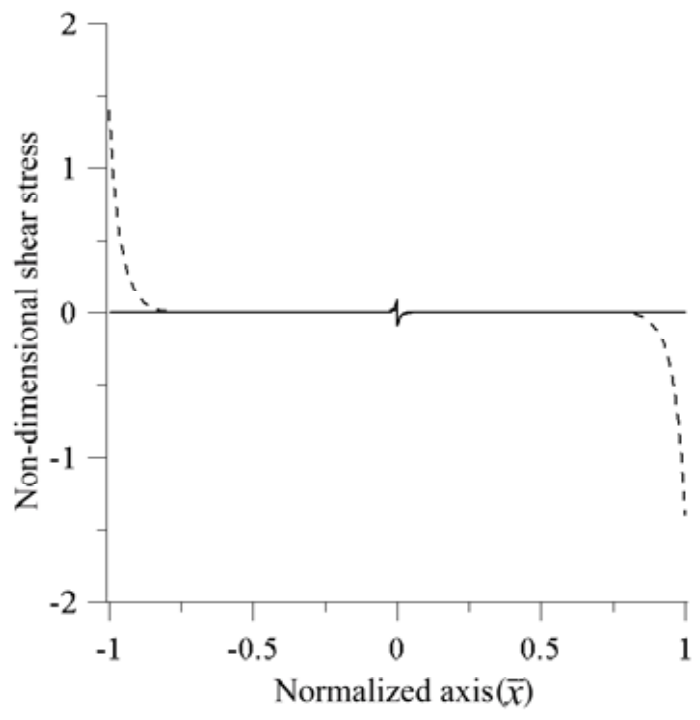
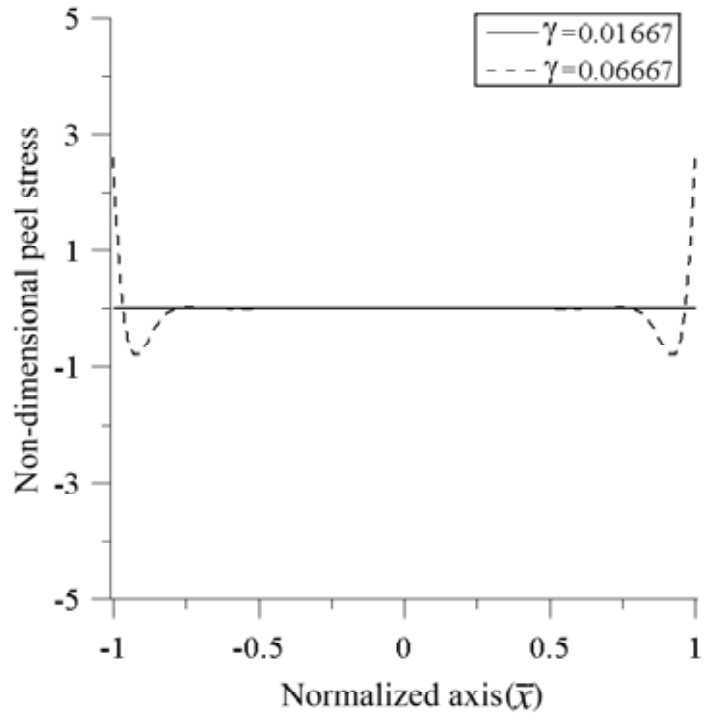


Fig. 3.20 Non-dimensional peel and shear stresses distributions in the adhesive layer ($\bar{x} = x/c$) for the thickness to length ratio $\gamma = \gamma_1 = \gamma_2$ with the different Young's modulus of both adherends $E_1 = 4.5$, $E_2 = 6.0$, $E_0 = 2.75$ and with the same thickness of both adherends $\beta_1 = \beta_2 = 10$ and ($h_a = 0.01mm$)

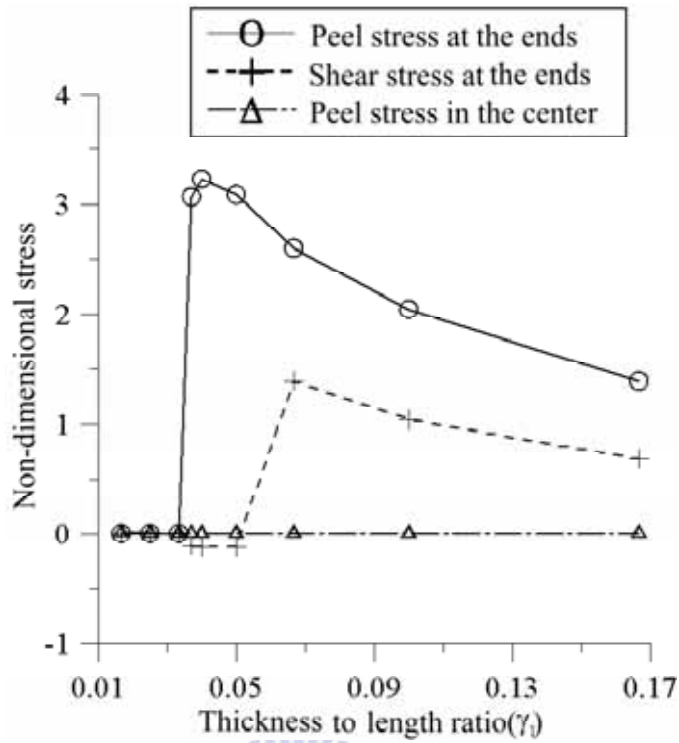


Fig. 3.21 Non-dimensional peel and shear stresses versus the thickness to length ratio $\gamma = \gamma_1 = \gamma_2$ for the same thickness of the adherends with the different Young's modulus $E_1 = 4.5$, $E_2 = 6.0$, $E_0 = 2.75$ ($h_a = 0.01mm$).

The values $E_1 = 4.5$, $E_2 = 6.0$, $E_0 = 2.75$, $\tilde{P} = 1$, and $d = 0$ are used as Figs. 3.20 and 3.21.

The upper and lower adherends of these figures have the different Young's modulus and the same thickness $\beta_1 = \beta_2 = 10$. Fig. 3.20 shows distributions of the non-dimensional peel stress and shear stress in the adhesive layer, whose thickness is $h_a = 0.01mm$. Comparisons between the dashed line of Fig. 3.12 and of Fig. 3.20 are made and described as follows. The only difference between Fig. 3.12 with $E_1 = 6.0$ and Fig. 3.20 with $E_1 = 4.5$ is the different Young's modulus of the upper adherends. The peel stress almost vanishes in the center for Fig. 3.20 and the maximum peel and shear stresses occur at the ends for Fig. 3.20 while the maximum peel stress occurs in the center for Fig. 3.12.

Fig. 3.21 shows the relationships among non-dimensional peel and shear stresses (at the ends and in the center), as well as the thickness to length ratio γ_1 for the upper adherend. The Young's modulus of the upper adherend is compared in Fig. 3.13 and Fig. 3.21. Except that the only difference between the top figure of Fig. 3.13 with $E_1 = 6.0$ and Fig. 3.21 with $E_1 = 4.5$ is the different Young's modulus of the upper adherends, these figures have the same conditions. The peel stress almost vanishes in the center for Fig. 3.21 and the maximum peel and shear stresses occur at the ends for Fig. 3.21 while the maximum peel stress occurs in the center for the top figure of Fig. 3.13.

3-6. Summary

When the maximum peel stress occurring in the center of the adhesive layer is much larger than the peel and shear stresses at the ends, the upper adherend (an IC chip) can easily break. Moreover, according to the preceding results, when both the upper and lower adherends have the same thickness, the thinner adhesive layer $h_a = 0.01$ mm, the thicker adherends, and the shorter joint (i.e. thickness to length ratio $\gamma = \gamma_1 = \gamma_2$ is larger), the adhesively bonded upper adherend (the IC chip) easily breaks.

Additionally, when the ends and the center of the adhesive layer have small peel and shear stresses, lower adherend subjected to the concentrated force will also be well joined with the upper adherend. Such joint should be possible under the following conditions: the thickness of the lower adherend is different from that of the upper adherend, and the adhesive layer is thicker and longer. For example, the thicker adhesive layer is 0.05 mm and its length is longer, while the upper and lower adherends are twice and six times thicker than the adhesive layer.

Conversely, the upper adherend (an IC chip) without breakage can be completely separated from the lower adherend subjected to the concentrated force when the maximum

peel and shear stresses in the adhesive layer at the ends are greater than adhesive criteria stresses. Additionally, when the maximum peel and shear stresses occurring at the ends of the joint are large and the compressive stress in the center of the joint is small, the probability of the upper adherend (an IC chip) being easily separated from the lower adherend increases [44]. Thus, the following conditions can satisfy the IC chip pick-up process. The thickness of the lower adherend should be greater than ten times that of the adhesive layer and less than one-third that of the upper adherend; and a thin adhesive layer $h_a \leq 0.01$ mm and a short joint ($\gamma_1 \geq 0.08$) should be used.

3-7. Concluding Remarks

For two adhesively bonded adherends, the peel and shear stresses in the adhesive layer are affected by the layer's thickness Young's modulus and length, as well as by the thicknesses and Young's modulus of the adherends and the action point of the concentrated force. The complicated coupled equations for this problem were numerically solved using SVD and symbolic manipulation which finds closed- form solutions. The maximum peel and shear stresses occurring at the ends of the adhesive layer were analyzed because they dictate whether or not the upper adherend (an IC chip) without breakage can be fully separated from the lower adherend (blue tape). The results indicate that the upper adherend can be completely, easily, and fully separated from the lower adherend under the following conditions: (i) the thickness of the lower adherend should be greater than ten times that of the adhesive layer but less than one-third that of the upper adherend and (ii) the adhesive layer should be relatively thin ($h_a \leq 0.01$ mm) and the adhesive joint relatively short (i.e. γ_1 should be greater than 0.08). These results can be applied to the IC chip pick-up process.

CHAPTER 4 APPLICATION OF GENETIC ALGORITHM TO IC CHIP PICK-UP PROCESS

4-1. Introduction

As mentioned above, the closed-form solutions and some conclusions of the adhesive joint are employed to investigate stress distribution during pick-up IC process. Particularly, as IC chips became thinner, IC chips were easy to fail in the IC chip pick-up process. When the thickness of IC chips is 0.1mm, IC chips most likely fail during the IC chip pick-up process. However, when IC chip's thickness is 0.34 mm, success rate is nearly 100% for the same adhesive and blue tape. These data and results were obtained from the experiments [45]. The experiments have been done in IC chip pick-up machine, MIRI CP602, produced by the Industrial Technology Research Institute (ITRI). Especially, as the thickness of IC chips is 0.1mm, IC chips are easy to fail. In order to improve success rate of 0.1mm IC chips in pick-up IC process, the preceding analysis of adhesive joint associated with optimum search method is applied in IC chip pick-up process.

As the preceding chapters discussed, many factors can affect stresses distribution of the adhesive layer. Although the geometrical shape and properties of IC chips (upper adherend) have already been determined in the IC chip pick-up process, the factors including the mechanical properties and the thickness of the adhesive, and the mechanical properties of blue tape (lower adherend) are discussed to analyze peel and shear stresses of the adhesive layer and stresses of adherends (IC chips and blue tape). This work mainly investigates these factors to improve success rate of the 0.1 mm IC chips in IC chip pick-up process, and the different results regarding the IC chip's thickness 0.1mm and 0.34mm during the IC chip pick-up process. As mentioned above, it is difficult to select the most suitable adhesive among

numerous types of adhesive; consequently, two-variable optimum search method is employed to investigate the characteristics of the adhesive and the effect of various Young's modulus on blue tape. As for optimum search method [46-48], genetic algorithm with penalty function and Multifunctional Optimization System Tool (MOST) software designed by Tseng [50] are adopted in this research. The genetic algorithm sources modified from GALib A C++ Library of Genetic Algorithm Components of M. I. T. [49] incorporates penalty function and links the Mathematics package which mainly analyzes peel and shear stresses of the adhesive and stresses of the adherends in pick-up IC process by using the analysis of adhesive joint (i.e. the preceding chapter has discussed). Simultaneously, the genetic algorithm results are examined and identified by MOST which was employed, generally speaking, sometimes not to easily find optimum solutions of such a problem sensitively affected by initial design values, side constraints and design variables.

In this work, the optimum problem is mainly used to search the appropriate value of Young's modulus and thickness of the adhesive layer. Therefore, Elastic ratio λ and thickness ratio β_1 are design variables of the optimum problem and are applicable to analysis of adhesive joint. Elastic ratio and thickness ratio are defined as the ratio of the Young's modulus and thickness (E_1 and h_1) of the upper adherend (IC chips) to the Young's modulus and the thickness (E_a and h_a) of the adhesive layer, respectively. Because the Poisson's ratio of plastic materials is mostly about 0.35~0.4 and the middle value, 0.375 of these materials is adopted.

4-2. Optimum problem

This section outlines some of the basics of genetic algorithms [47-48]. The three important aspects of using genetic algorithms are: (1) definition of the objective (cost) function, (2) constraint conditions, and (3) crossover probability, mute probability, population size and generations given.

Because in experimental study [45], mechanical properties and thickness of adhesive are assumed for two unknown variables, optimum problem includes two design variables - Elastic ratio λ and thickness ratio β_1 . The cost function and constrained conditions of optimum problem are described in the following equations.

Cost function minimizes von Mises's stress of the adhesive layer at both ends of the upper adherend (IC chips) and is written down below.

$$f = -\sqrt{\sigma_{ai}^2 + 3\tau_{ai}^2} \quad i=2, 3 \quad (4.1)$$

Constraint conditions are described and shown in the expression as follows:

1. The largest value of the upper adherend's stress is not greater than the allowance stress of the IC chips.
2. The largest value of the lower adherend's is not greater than allowance stress of blue tape.
3. The peel stress is the positive value in the adhesive; i.e. the tension stress.

$$\left| \bar{\sigma}_i \right| - \frac{\bar{\sigma}_{ul}}{F_S} \leq 0 \quad i=2, 3 \quad (4.2)$$

$$\left| \bar{\sigma}_{ix} \right| - \frac{\bar{\sigma}_{ypx}}{F_S} \leq 0 \quad i=2, 3 \quad (4.3)$$

$$-\bar{\sigma}_{ai} < 0 \quad i=2, 3 \quad (4.4)$$

Then, similarly the non-dimensional yielding stresses of the upper adherend (IC chips) and lower adherend (blue tape) are expressed in $\bar{\sigma}_{ul} = \frac{2c\sigma_{ul}}{P}$ and $\bar{\sigma}_{ypx} = \frac{2c\sigma_{ypx}}{P}$. σ_{ul} and σ_{ypx} are depicted in the critical stresses of the IC chips and the yielding stresses of blue tape.

Expressions (4.2-4.4) are rewritten in equations (4.5-4.7)

$$g_1(\beta_1, \lambda) = \frac{|\bar{\sigma}_i|Fs}{\sigma_{ul}} - 1 \leq 0 \quad (4.5)$$

$$g_2(\beta_1, \lambda) = \frac{|\bar{\sigma}_{ix}|Fs}{\sigma_{ypx}} - 1 \leq 0 \quad (4.6)$$

$$g_3(\beta_1, \lambda) = -\bar{\sigma}_{ai} < 0 \quad (4.7)$$

The values of material constants and of the parameters listed in Table 4.1 are used in the numerical solution. Based on the cost values of this issue with sensitively violent variance in the margin of the upper adherend (IC chips), the genetic algorithm is employed in search for the optimum problem. The C++ program of the genetic algorithm modifying from the C++ source of MIT [49], incorporates penalty function and links Mathematics package. The program of genetic algorithm is applied to solve these stresses including normal stresses of the upper and lower adherends as well as peel and shear stresses of the adhesive layer. The penalty function is expressed in

$$P(R, \beta_1, \lambda) = \sum_1^3 R|g_i(\beta_1, \lambda)| \text{ if } g_i(\beta_1, \lambda) > 0. \quad (4.8)$$

where R is penalty parameter. As genetic algorithm incorporates constraint equations, original minimization of the cost function f (von Mises's stress of the adhesive layer) is modified into minimizing

$$F = f + P \quad (4.9)$$

Table 4.1 Mechanical properties and dimensions for IC chip and blue tape. [45],[52]

Material	Young's Modulus (Pa)	Poisson's Ratio	Thickness (mm)	Critical stress (Yielding stress)	Dimension (mm)
IC chip (Silicon)	1.29×10^{11}	0.28	0.1 or 0.34	130Mpa	5×5 3×3
Blue tape UE-1085GX	3×10^9	0.38	0.07	30Mpa	r=15
Adhesive (radiation-cured)	---	0.375	0.01	5.9Mpa (before UV) 1.45Mpa (after UV)	----

----- Unknown

The genetic algorithm of this problem using roulette wheel scheme and encoding the values of design variables into 16 binary is written in C++ language. Flow char of its calculation process, shown in Fig. 4.1 is described in more detail and illustrated as follows.

First, generate randomly populations whose values are assigned to the thickness and elastic ratios (β_1, λ) which are employed to calculate normal stresses of the upper and lower adherends as well as von Mises stress of the adhesive layer in Mathematics package. Next, the genetic program reads the values of these stresses to computer cost function F (with penalty function) whose values are used to determine fitness of gene and to test convergence criteria. If the results satisfy convergence criteria, the program is perfectly ended. If the satisfying result is not achieved, the better phenotype left will be selected to generate new populations to go backward to the second step again by using crossover and mute techniques. Additionally, some parameters of genetic algorithm include penalty parameter= 10^{11} ; crossover probability=0.6 or 0.8; mute probability=0.01; population size=50 and 100 generations [40]. However, when the program runs in Duo-Core T2300 PC computer with 512Mbyte ram and 1.6 GMz CPU, it spends about 16~30 hours. This program is, in fact, quite time-consuming.

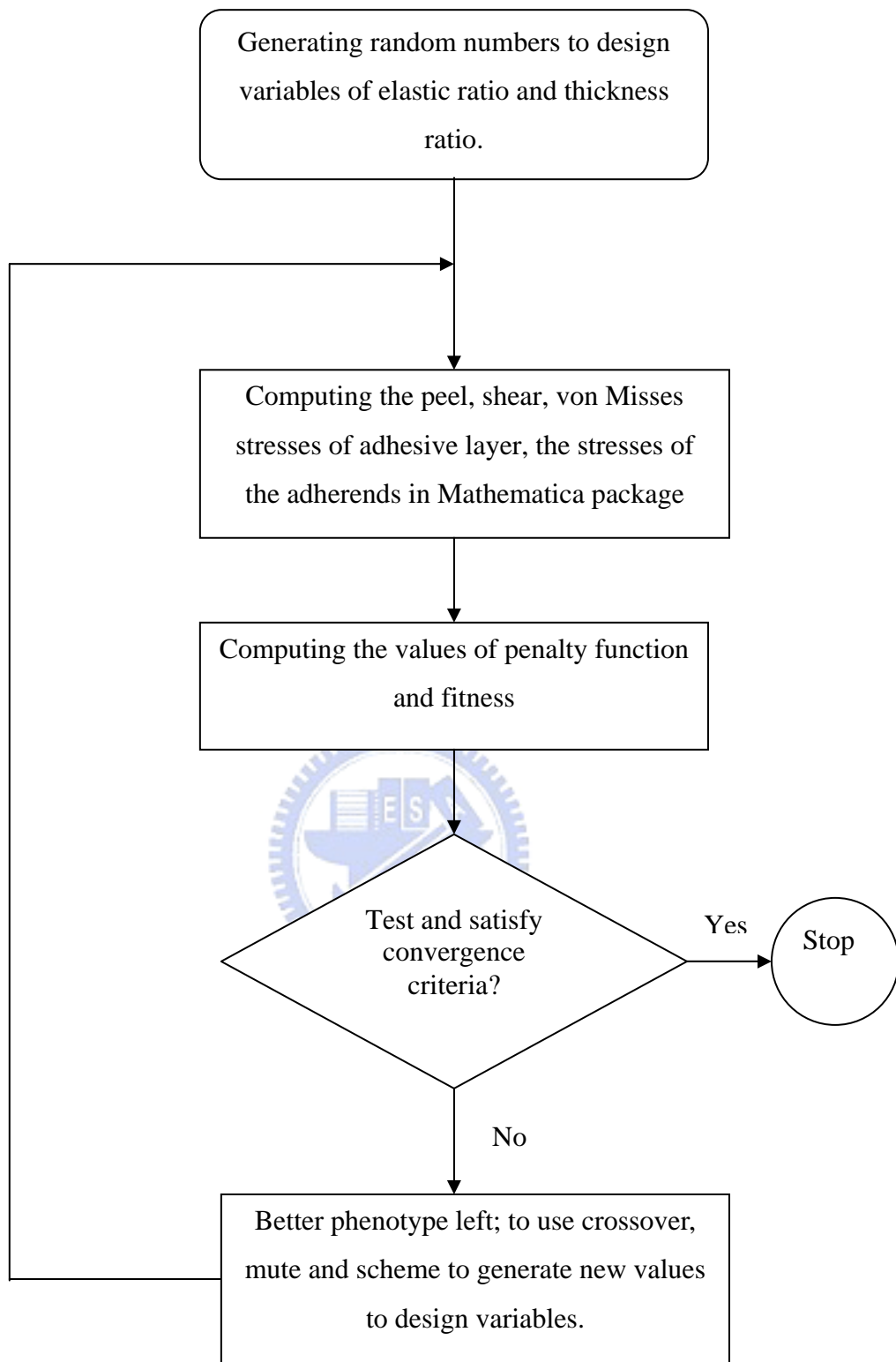


Fig. 4.1 Scheme of genetic algorithm linked with Mathematica package to compute stresses of the adhesive and adherends.

4-3. Results and Discussion

Three cases discussed are listed below. Case A analyzes and discusses the failure regarding the thickness, 0.1mm, and length, 5mm, of IC chips in IC chip pick-up process [45]. Case B investigates the situation of IC chips with regard to the thickness, 0.34 mm and length 5mm of IC chips in IC chip pick-up process. Case C discusses the way to improve the success rate of Case A.

Case A: Analysis of IC chip's thickness 0.1mm and length 5mm

Analysis of the failure regarding IC chip's thickness as 0.1mm and length as 5mm adopted from the reference [45] is made and some mechanical properties and geometrical shape are listed in Table 4.1. According to the reference [45], the critical stresses of IC chip, blue tape and adhesive are 130Mpa, 30 Mpa and 1.45 Mpa (after exposure of UV light), respectively and the thickness of the adhesive layer is 0.01mm. Additionally, the concentrated force is 4.8 N and Safety factor is 1.1. The Young's modulus of the adhesive layer is searched and ranges from hundred to one-fiftieth times that of IC chip (That is, side constraints: $0.01 \leq \lambda \leq 50$ or the Young's modulus of the adhesive layer varies form 1.29×10^{13} pa to 2.58×10^9 pa). As the thickness of the adhesive layer is 0.01mm, the employment of genetic algorithm aims only to search for the Young's modulus of the adhesive layer, no solution to Young's modulus of the adhesive layer and to satisfying constraint conditions is obtained.

Subsequently, it is expected that the success rate of the IC pick-up process can be raised through the change of adhesives' thickness. Therefore, the employment of genetic algorithm aims to search for two variables including Young's modulus of and thickness of the adhesive layer. The Young's modulus of the adhesive layer is searched and still ranges from hundred to one-fiftieth times that of IC chip. The thickness of the adhesive layer is also searched and ranges from one to one-fiftieth times that of IC chips. (That is, $1 \leq \beta_1 \leq 50$ or the thickness of

the adhesive layer varies from 0.1mm to 0.002 mm.) The employment of genetic algorithm aims to search for the side-constraint ranges; however, no solutions to Young's modulus and thickness of the adhesive layer and to satisfying constraint conditions is found after running the program about more than 10 times. Therefore, in such a situation, it is very difficult and nearly impossible that IC chips without breakage, can be fully separated from blue tape.

Case B: Analysis of IC chip's thickness 0.34 mm and length 5 mm

Similarly, except IC chip's thickness as 0.34mm and the concentrated force as 3.5N adopted from the reference [45], these parameter's value and mechanical properties are the same as those of case A. As the thickness of the adhesive layer is 0.01mm, the employment of genetic algorithm aims only to search for the Young's modulus of the adhesive layer. The ranges of adhesive's Young's modulus are searched from 1.29×10^{11} pa to 2.58×10^9 pa (That is, side constraints: $1 \leq \lambda \leq 50$). The searching result of von Mises stress 4.05 Mpa is obtained over the critical stress 1.45 Mpa (after exposure of UV light) of radiation-cured adhesive listed in Table 4.1. The solution to Young's modulus of the adhesive layer and to satisfying constraint conditions is 2.46×10^{10} .

Subsequently, it is expected that general adhesives can be used in the IC pick-up process. The employment of genetic algorithm aims to search for Young's modulus of and thickness of the adhesive layer. Furthermore, the ranges of adhesive's Young's modulus and thickness are searched from 1.29×10^{11} pa to 2.58×10^9 pa and from 0.1mm to 0.002mm (That is, side constraints: $1 \leq \lambda \leq 50$ $1 \leq \beta_1 \leq 50$). The results show that Young's modulus and the thickness of the adhesive layer are, respectively 2.77×10^{10} pa and 0.027mm. Moreover, those results also reveal that the optimum value of von Mises's stress of the adhesive layer is 352Mpa exceeding a lot more than the critical value of general adhesive (40-80Mpa) [51]. Thus, under

constraint conditions and the von Mises's stress, it is extremely possible that IC chips without failure can be successfully and entirely separated from blue tape.

Case C: Effects of various elastic modulus of blue tape and various adhesive layers on stresses of IC chips (thickness 0.1 mm and length 5 mm)

Based on Case A, the failure of IC chips easily occurs in IC chip pick-up process. In order to improve the success rate of Case A in the process, various mechanical properties of the adhesive layer and of blue tape need to be considered. In Case A, as adhesive's Young's modulus ranges from 2.58×10^9 Mpa to 1.29×10^{13} Mpa and adhesive's thickness ranges from 0.1mm to 0.002mm. (That is, $0.01 \leq \lambda \leq 50$ $1 \leq \beta_1 \leq 50$), the solutions to Young's modulus and thickness in the adhesive layer are not found. Sequentially, Young's modulus of blue tape is increased to one-twentieth, one-tenth, one-fifth, one, five times, ten times, twenty times, and forty-three times that of IC chips; and adhesive's Young's modulus is changed and ranges from 2.58×10^{10} Mpa to 1.29×10^{13} Mpa (That is, $0.01 \leq \lambda \leq 5$, from one-fifth to a hundred times that of IC chips). On the other hand, the search range of adhesive's thickness from 0.1mm to 0.002mm is not changed. The optimum values of von Mises stresses, the values of adhesive Young's modulus and of thickness are listed in Table 3. As the Young's modulus of blue tape is 3.0×10^9 pa and 6.45×10^9 pa (i.e. the ratio, 1/43.3 and 1/20 of Young's modulus of blue tape to Young's modulus of IC chip), the ranges of Young's modulus and thickness of adhesive have been searched about ten times but no answers can be obtained to satisfy such constraint conditions mentioned above. Nevertheless, as Young's modulus of blue tape is increased to greater than 8.6×10^9 pa (i.e. the ratio is greater than 1/15), the Young's modulus and thickness of adhesive can be found by genetic algorithm under the constraint conditions. As Young's modulus of blue tape is only 8.6×10^9 pa, the value 44.45Mpa of von Mises stress is less than 100 Mpa and the other values is greater than 130 Mpa. Then, the range of

Young's modulus of adhesive is from 9×10^{13} to 10^{11} . Therefore, as Young's modulus of blue tape is greater than one-tenth that of IC chips, the probability of IC chips being fully separated from blue tape can be raised because the von Mises's values is greater than 130Mpa.

Table 4.2 Optimum points and values of adhesive for various Young's modulus of blue tape (E_2)

Young's modulus of Blue tape(E_2)	Ratio of E_2 to E_1	Young's modulus of adhesive	Thickness of adhesive	Optimum value (von Mises's stress)
$3.0 \times 10^9 \text{ pa}$	1/43.3	-----	-----	-----
$6.45 \times 10^9 \text{ pa}$	1/20	-----	-----	-----
$8.6 \times 10^9 \text{ pa}$	1/15	$6.47 \times 10^{11} \text{ pa}$	0.097mm	44.45Mpa
$1.29 \times 10^{10} \text{ pa}$	1/10	$2.51 \times 10^{12} \text{ pa}$	0.007mm	138.18Mpa
$2.58 \times 10^{10} \text{ pa}$	1/5	$1.08 \times 10^{12} \text{ pa}$	0.01mm	157.84Mpa
$1.29 \times 10^{11} \text{ pa}$	1	$2.06 \times 10^{11} \text{ pa}$	0.011mm	218.46Mpa
$6.45 \times 10^{11} \text{ pa}$	5	$1.17 \times 10^{13} \text{ pa}$	0.095mm	334.37Mpa
$1.29 \times 10^{12} \text{ pa}$	10	$1.20 \times 10^{13} \text{ pa}$	0.093mm	329.68Mpa
$1.935 \times 10^{12} \text{ pa}$	15	$1.27 \times 10^{13} \text{ pa}$	0.081mm	474.25Mpa
$2.58 \times 10^{12} \text{ pa}$	20	$2.13 \times 10^{12} \text{ pa}$	0.005mm	464.56Mpa
$5.55 \times 10^{12} \text{ pa}$	43.3	$1.01 \times 10^{11} \text{ pa}$	0.003mm	334.08Mpa

Young's modulus of IC chips ($E_1 = 1.29 \times 10^{11} \text{ pa}$)

Searching domain:

$2.58 \times 10^{10} \text{ pa} \leq \text{Young's modulus of adhesive} \leq 1.29 \times 10^{13} \text{ pa}$,

$0.002 \text{ mm} \leq \text{thickness of adhesive} \leq 0.1 \text{ mm}$

* ----- No solution

4-4. Concluding Remarks

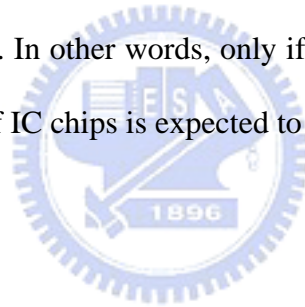
The results of the experiments and the dimensions of IC chips used in the experiments are described as follows. The experiments reveal that as the thickness and length of IC chips are respectively 0.1mm and 5mm, these chips nearly fail in the IC pick-up process if the IC chips are subjected to the force, 4.8N. As the size of IC chips is used in this model, the stress

distributions of adhesive and adherends is investigated by genetic algorithm associated with the analysis of adhesive joint. As the thickness of the adhesive layer is 0.01mm, Young's modulus of adhesive are searched in the range from 1.29×10^{11} pa to 2.58×10^9 pa. No solution to Young's modulus of the adhesive layer and to satisfying constraint conditions is obtained. Subsequently, it is expected that the success rate of the IC pick-up process can be raised through the change of adhesives' thickness. The Young's modulus and thickness of adhesive are searched in the range from 1.29×10^{11} pa to 2.58×10^9 pa and from 0.1mm to 0.002 mm, respectively. No solutions to Young's modulus and the thickness of the adhesive layer are found under the constraint conditions described above. These results are in accordance with those of the experiments.

As the thickness of IC chips is changed to 0.34mm and IC chips are subjected to the force, 3.5N, the results from the experiments show that all IC chips can be successful to be separated from blue tape (i.e. the probability of success rate is nearly 100 percent). Similarly, this model is also applied to such a case: the remaining conditions are the same as the preceding IC chip's thickness as 0.1 mm case except the force as 3.5N and IC chips' thickness as 0.34mm. As the thickness of the adhesive layer is 0.01mm, the solution to Young's modulus of the adhesive layer and to satisfying constraint conditions is 2.46×10^{10} pa. von Mises stress 4.05 Mpa is also obtained over the critical stress 1.45 Mpa (after exposure of UV light) of radiation-cured adhesive. Subsequently, it is expected that general adhesives can replace the radiation-cured adhesive and can be used in the IC pick-up process. The research results are that as Young's modulus and the thickness of the adhesive layer are 2.77×10^{10} pa and 0.027mm, respectively, the optimum value of von Mises's stress of the adhesive layer is 352Mpa exceeding a lot more than the critical value of general adhesive. Under such constraint conditions and the von Mises's stress, it is extremely possible and obvious that IC

chips without failure can be successfully and fully separated from blue tape. The results are totally different from the case of IC chip's thickness as 0.1mm.

Since it is apparent that when the IC chip is subjected to 4.8N force, and its thickness is 0.1 mm, the IC chip is very easy to fail, thus, the result of this study is expected to improve the success rate of IC chips in IC chip pick-up process. The conclusions are drawn that as Young's modulus of blue tape is greater than one-fiftieth that of IC chips, the success rate of IC chips increases in IC chip pick-up process. The values of Young's modulus, thickness of and the von Mises stresses of the adhesive layer attained by genetic algorithm are listed in Table 4.2. Because the von Mises stresses of the adhesive layer are greater than 130Mpa exceeding the critical value (40-80 Mpa) [51] of the general adhesive, the probability of IC chips without any crack, being fully separated from blue tape in the pick-up IC process is expected to be able to increase. In other words, only if the mechanical properties of blue tape are changed, the success rate of IC chips is expected to increase.



CHAPTER 5 CONCLUSIONS AND FUTURE WORKS

5-1. Conclusions

Two adhesively bonded adherends subjected to a concentrated force are applied to the IC chip pick-up process. Based some assumptions described before, some conclusions drawn in this work are depicted in the followings:

1. Stress distributions of the adhesive layer are deeply affected by geometric conditions and material properties including the thicknesses and Young's modulus of adherends and the length, thickness, and Young's modulus of the adhesive, as well as by the action point of the concentrated force.
2. Complete and complicated closed-form solutions (analytical solutions) may be formulated with the aforementioned relevant factors of the adhesively bonded joint and are obtained by using symbolic manipulation to solve the coupled differential equations in the Mathematica package. These solutions are not limited to solving only the characteristic solutions having large values and the same adherends. The solutions, in fact, include analytical solutions to peeling and shear stresses for the adhesive layer as well as to bending moment, shear force and longitudinal force for upper and lower adherends. Moreover, these solutions also include analytical solutions to displacement and slope of upper and lower adherends. These analytical solutions are applicable to analyzing single lap joints and the strengthening beam. These closed-formed solutions incorporating boundary and constraint conditions are applied to numerically solve peel and shear stresses of the adhesive joints by SVD. That is applicable to analyzing stress distributions of IC chip pick-up process.
3. It is also under discussion that whether the adhesively bonded joint is in the well-bonded situation or not. When both the upper and lower adherends have the same thickness, the

thinner adhesive layer $h_a = 0.01$ mm, the thicker adherends, and the shorter joint (i.e. thickness to length ratio $\gamma = \gamma_1 = \gamma_2$ is larger), the adhesively bonded upper adherend (the IC chip) breaks easily. In another condition, the lower adherend is well joined with the upper adherend. The thickness of the lower adherend is different from that of the upper adherend, and the adhesive layer is thicker and longer. (The thicker adhesive layer is 0.05 mm and its length is longer, while the upper and lower adherends are twice and six times thicker than the adhesive layer.) In still another conditions, as the maximum peel and shear stresses occur at the ends of the adhesive layer, they dictate the upper adherend (IC chips) without breakage can be separated from the lower adherend (blue tape). This result is generated by satisfying the following conditions: (i) the thickness of the lower adherend should be greater than ten times that of the adhesive layer but less than one-third that of the upper adherend and (ii) the adhesive layer should be relatively thin ($h_a \leq 0.01$ mm) and the adhesive joint relatively short (i.e. γ_1 should be greater than 0.08). Thus, the numerical results of this study outline the characteristics of the adhesive layer relative to the adherends, which can be used to develop adhesive joints in the IC chip pick-up process.

4. The experiments present two cases: one case is that as the IC chips are subjected to the force 4.8N, with 0.1mm thickness and 5mm length, these chips are much likely to fail in the IC chip pick-up process. The other case is that as the IC chips with 0.34 mm thickness and 5 mm length are subjected to the force 3.5N, the chips without any breakage can be entirely separated from blue tape. Subsequently, the genetic algorithm associated with the analysis of adhesive joint is applied to analyze stress distributions of the adhesive layer for two cases in the experiments. As the thickness of the adhesive layer is 0.01mm, for the former case, no solutions to Young's modulus of the adhesive layer can be obtained; for the latter case, the solution to Young's modulus of the adhesive layer and to satisfying

constraint conditions is 2.46×10^{10} . Additionally, the Young's modulus and thickness of adhesive are searched in the range from 1.29×10^{11} pa to 2.58×10^9 pa and from 0.1mm to 0.002 mm, respectively. For the former case, as it is expected that the success rate of the IC pick-up process can be raised through the change of adhesives' thickness, no solutions to Young's modulus and the thickness of the adhesive layer can be obtained. However, for the latter case, as it is expected that general adhesives can be used in the IC pick-up process, the searching result is found and described as follows. As Young's modulus and the thickness of the adhesive layer are 2.77×10^{10} pa and 0.027mm respectively, the optimum value of von Mises's stress of the adhesive layer is 352Mpa exceeding a lot more than the critical value of general adhesive (40-80Mpa) [51]. Hence, under constraint conditions and the von Mises's stress, it is extremely possible that IC chips without failure can be successfully and completely separated from blue tape.

5. On account of the former case, IC chips are easy to fail in the IC chip pick-up process. To improve the failure occurring while IC chips' thickness is 0.1 mm, Young's modulus of blue tape needs to be adjusted. Adhesive's Young's modulus is searched in the range from 2.58×10^9 Mpa to 1.29×10^{13} Mpa and adhesive's thickness is searched in the range of from 0.1mm to 0.002mm. As the Young's modulus of blue tape is 3.0×10^9 pa or 6.45×10^9 pa and that is to say, the ratio of Young's modulus of blue tape to Young's modulus of IC chip is 1/43.3 or 1/20, no solution to Young's modulus and the thickness of the adhesive layer can be obtained to satisfy such constraint conditions mentioned above. However, as the Young's modulus of blue tape is increased to greater than 8.6×10^9 pa (i.e. the ratio is greater than 1/15 of Young's modulus of IC chips), the Young's modulus and thickness of adhesive can be attained by genetic algorithm search under the constraint conditions. When the von Mises stress of the adhesive layer is greater than 130Mpa exceeding a lot more than the critical value (40-80 Mpa) [51] of general adhesive (i.e. the

ratio is greater than 1/10 of Young's modulus of IC chips), the probability of IC chips without crack, fully separated from blue tape in the IC chip pick-up process can be expected to increase. That is to say, only if the mechanical properties of blue tape are changed, IC chips without any breakage can be completely separated from blue tape; moreover, the success rate of IC chips is expected to increase.

On the whole, the numerical results of this study outline the characteristics of the adhesive layer relative to the adherends, which can be used to develop adhesive joints in the IC chip pick-up process.

5-2. Future works

The effects of many key factors on stress distributions of the adhesively bonded joint in the IC chip pick-up process are still investigated because of this complicated issue. The full description and analysis of the IC chip pick-up process actually pose severely practical and computational difficulties. This study only is a static beam model to consider the IC chip pick-up process in lower speed. Therefore, there are many issues for further study about the IC chip pick-up problem.

In the future, this study can be extended to the topics described as follows

1. This model does not take thermal effects on stress distribution of the adhesive layer into consideration. As the bonded strength of the adhesively bonded joint varies much with temperature, the adhesively bonded joint is deeply affected by thermal loading. Especially, thermal loading significantly influences the adhesive application to IC package. Moreover, thermal variation has a lot of effects on the characteristic of adhesive. If thermal factor can furthermore be considered in this model, the model can be applicable to IC package.

2. If the small deformation assumption is omitted in the study, the application of the model can still be widely used in the adhesively bonded joint. That is, as the adhesive layer is thicker, large deformation of adhesive is concerned but this study is not appropriately employed in this condition.
3. Use plate theory instead of beam theory because of a two-dimension problem in the IC chip pick-up process
4. The IC chip pick-up process is a dynamical system. This study can be extended to consider the dynamical effect of the pick-up process. The results of this study can approach to the practical problem more deeply.
5. Considering the facture of the fillet in this problem can approach to the practical problem of adhesive bonded joints because defects may exist in the curing process of adhesive.



REFERENCES

- [1] Takatori Corporation, Semiconductor Machinery Division/Introduction to the manufacturing process, http://www.takatori-g.co.jp/e_top.html. 2003.
- [2] M. Goland and E. Reissner, "The stresses in cemented joints", ASME Journal Applied Mechanics, Vol. 11, pp. A17-A27, March 1944.
- [3] D. W. Oplinger, "Effects of adherend deflections in single lap Joints", International Journal Solids Structures, Vol. 31, No. 18, pp. 2565-2587, 1994.
- [4] W. C. Carpenter, "Goland and Reissner were correct" Journal Strain Analysis, Vol. 24, No. 3, pp. 185-187, 1989.
- [5] I. U. Ojalvo and H. L. Eidinoff, "Bound thickness effects upon stresses in single-lap adhesive joints", AIAA Journal, Vol. 16, No. 3, pp. 204-211, 1978.
- [6] W. C. Carpenter, "A comment on two current adhesive lap joint theories", AIAA Journal, Vol. 18, No. 3, pp. 250-352, 1980.
- [7] E. Suhir, "Stresses in bi-metal thermostats", ASME Journal Applied Mechanics, Vol. 53, pp. 657-660, 1986.
- [8] E. Suhir, "Interfacial stresses in bimetal thermostats", ASME Journal Applied Mechanics, Vol. 56, pp. 595-600, 1989.
- [9] E. Suhir, "Adhesively bonded assemblies with identical nondeformable adherends and 'piecewise continuous' adhesive layer: predicted thermal stresses in the adhesive", International Journal Solids Structures, Vol. 37, pp. 2229-2252, 2000.
- [10] J.N. Rossettos, "Thermal peel, warpage and interfacial shear stresses in adhesive joints", Journal Adhesion Science and Technology, Vol. 17, pp. 115-128, 2003.
- [11] T. Wah, "Stress distribution in a bounded anisotropic lap joint", ASME Journal Applied Mechanics, Vol. 40, pp. 174-181, July 1973.

- [12] W. J. Renton and J. R. Vinson, "Analysis of adhesively bonded joints between panels of composite materials", ASME Journal Applied Mechanics, Vol. 44, pp. 101-106, March 1977.
- [13] M. Y. Tsai and J. Morton, "An evaluation of analytical and numerical solutions to the single-lap joint", International Journal Solids Structures, Vol. 31, No. 18, pp. 2537-2563, 1994.
- [14] Q. Luo and L. Tong, "Linear and higher order displacement theories for adhesively bonded lap joints", International Journal Solids Structures, Vol. 41, pp. 6351-6381, 2004.
- [15] D. J. Allman, "A theory for elastic stresses in adhesive bonded lap joints", Quarterly Journal Mechanics and Mathematics, Vol. 30, pp. 414-436, 1977.
- [16] T. Sawa, J. Liu, K. Nakano and J. Tanaka, "A two-dimensional stress analysis of single-lap adhesive joints of dissimilar adherends subjected to tensile loads", Journal Adhesion Science and Technology, Vol. 14, No. 1, pp. 43-66 (2000).
- [17] J. Liu and T. Sawa, "Stress analysis and strength evaluation of single-lap band adhesive joints of dissimilar adherends subjected to external bending moments", Journal Adhesion Science and Technology, Vol. 14, No. 1, pp. 67-92, 2000.
- [18] J. Lee and H. Kim, "Stress Analysis of Generally Asymmetric Single Lap Adhesively Bonded Joints", Journal Adhesion Vol. 81, No. 5, pp. 443-472, 2005.
- [19] A. Özel, M. Aydin and S. Temiz, "The effects of overlap length and adherend thickness on the strength of adhesively bonded joints subjected to bending moment", Journal Adhesion Science and Technology, Vol. 18, No. 3, pp. 313-325, 2004.
- [20] D. Chen and S. Cheng, "An analysis of adhesive-bonded single-lap joints", ASME Journal Applied Mechanics, Vol. 50, pp. 109-115, 1983.

- [21] S. Alexandrov and O. Richmond, "On estimating the tensile strength of an adhesive plastic layer of arbitrary simply connected contour", *International Journal Solids Structures*, Vol. 37, pp. 669-686, 2000.
- [22] F. Mortensen and O. T. Thomsen, "Analysis of adhesive bonded joints: a unified approach", *Composites Science and Technology*, Vol. 62, pp. 1011-1031, 2002.
- [23] C. Su, Y.J. Wei, and L. Anand, "An elastic-plastic interface constitutive model: application to adhesive joints", *International Journal of Plasticity*, Vol. 20, pp. 2063-2081, 2004.
- [24] D. M. Gleich, M. J. L. Van Tooren and A. Beukers, "A stress singularity approach to failure initiation in a bonded joint with varying bondline thickness", *Journal Adhesion Science and Technology*, Vol. 15, pp. 1247-1259, 2001.
- [25] P. Qiao and J. Wang, "Mechanics and fracture of crack tip deformable bi-material interface", *International Journal Solids Structures*, Vol. 41, pp. 7423-7444, 2004.
- [26] Z.Q. Qian and A.R. Akisanya, "An investigation of the stress singularity near the free edge of scarf joints", *European Journal Mechanics A/Solids*, Vol. 18, pp. 443-463, 1999.
- [27] A. Li, T Assih and Y. Delmas, "Influence of the adhesive thickness and steel plate thickness on the behaviour of strengthened concrete beams", *Journal Adhesion Science and Technology*, Vol. 14, No. 13, pp. 1639-1656, 2000.
- [28] B. Taljsten, "Strengthening of beams by plate bonding", *Journal of Materials in Civil Engineering*, Vol. 9, No. 4, pp. 206-212, 1977.
- [29] R. W. Cornell, "Determination of stresses in cemented lap joints", *ASME Journal Applied Mechanics*, Vol. 20, pp. 355-364, September 1953.
- [30] G.P. Zou, K. Shahin and F. Taheri, "An analytical solution for the analysis of symmetric composite adhesively bonded joints", *Composite Structures*, Vol. 65, pp. 499-510, 2004.

- [31] W. H. Press, S. A. Teukolsky, W. T. Vetterling, and P. F. Brian, Numerical Recipes in C, second edition, pp 59-70:Cambridge University Press, Cambridge, 1992.
- [32] K. Deb, “An efficient constraint handling method for genetic algorithms”, *Computer Methods in Applied Mechanics and Engineering*. Vol. 186, pp. 311-338, 2000.
- [33] Chyi-Yeu Lin and Wen-Hong Wu, “Self-organizing adaptive penalty strategy in constrained genetic search.”, *Structural Multidiscip Optimization*, Vol. 26, No. 6, pp. 417-28, 2004.
- [34] Wen-Hong Wu and Chyi-Yeu Lin, “The second generation of self-organizing adaptive penalty strategy for constrained genetic search”, *Advances in Engineering Software*, Vol. 35, pp. 815-825, 2004.
- [35] P. Nanakorn and K. Meesomklin, “An adaptive penalty function in genetic algorithms for structural design optimization”, *Computers and structures*, Vol. 79, pp. 2527-2539, 2001.
- [36] H. J.C. Barbosa and A. C.C. Lemonge, “A new adaptive penalty scheme for genetic algorithms”, *Information Sciences*, Vol. 156, pp. 215-251, 2003.
- [37] D. W. Coit and A. E. Smith, “Penalty guide genetic search for reliability design optimization”, *Computers & Industrial Engineering*, Vol. 30, No. 4, pp. 895-904, 1996.
- [38] G. N. Bullock, M. J. Denham, I. C. Parmee, and J. G. Wade, “Developments in the use of genetic algorithm in engineering design”, *Design studies*, Vol. 16, No. 4, pp. 507-524, October 1995.
- [39] O. Hasancebi and F. Erbatur, “Evaluation of crossover techniques in genetic algorithm based optimum structural design”, *Computers and Structures*, Vol. 78, pp. 435-448, 2000.
- [40] Young-Doo Kwon, Soon-Bum Kwon, Seung-Bo Jin, and Jae-Yong Kim, “Convergence enhanced genetic algorithm with successive zooming method for solving continuous optimization problems”, *Computers and Structures* Vol. 81, No. 17, pp. 1715-1725, 2003.

- [41] Shyue-Jian Wu and Pei-Tse Chow, "Integrated discrete and configuration optimization of trusses using genetic algorithms", *Computers & Structures*, Vol. 55, No. 4, pp. 695-702, 1995.
- [42] V. Govindaraj and J.V. Ramasamy, "Optimum detailed design of reinforced concrete continuous beams using Genetic Algorithms.", *Computers and Structures*, Vol. 84, No. 1-2, pp. 34-48, 2005.
- [43] M. Cho and S. Y. Rhee, "Optimization of laminates with free edges under bounded uncertainty subject to extension, bending and twisting", *International Journal of Solids and Structures*, Vol. 41, pp. 227-245, 2004.
- [44] L. Tong and G. P. Steven, *Analysis and Design of Structural Bonded Joints*, Kluwer Academic Publishers, 1999.
- [45] Tung-Hua Cheng, Chen-Chung Du, and Ching-Huan Tseng," Study in IC chip failure during pick-up process by using experimental and finite element methods", *Journal of Materials Processing Technology*, Vol. 172, No. 3, pp. 407-416, March 2006.
- [46] J. S. Arora, *Introduction to optimum design*, McGraw-Hill, 1989.
- [47] D. E. Goldberg, *Genetic algorithms in search, Optimization, and machine learning*, Addison-Wesley, 1989.
- [48] R. L. Haupt and S. E. Haupt, *Practical genetic algorithms*, 2nd, John Wiley & Sons Inc., 2004.
- [49] *GALib A C++ Library of Genetic Algorithm Components in M. I. T.*, <ftp://lancet.mit.edu/pub/ga/>, <http://lancet.mit.edu/ga/dist/>, 2002.
- [50] C. H. Tseng, MOST 1.1 Manual, Technical Report No. AODL-96-01, Department of Mechanical Engineering, National Chiao Tung University, Taiwan, ROC, 1996.

[51] Matweb, a division of Automation Creations, Inc. (ACI) of Blacksburg, Virginia.

<http://www.matweb.com/search/SpecificMaterial.asp?bassnum=PREINT642>, 2005

[52] NITTO DENKO Corporation, 2-5-25, Umeda, Kita-ku,Osaka 530-0001, Japan,

<http://www.nitto.co.jp/index.html>, 2005



APPENDICES

Some equations for the adherends joined by the adhesive layer are complex and difficultly expressed. These equations and their coefficients are written in the Appendices.

Appendix A

The equations and their coefficients of longitudinal displacements, transverse displacement and slope for the upper adherend and for the lower adherend are shown as follows.

Longitudinal displacements

The equations of longitudinal displacements ($z = h_a / 2$) for the upper adherend and ($z = -h_a / 2$) for the lower adherend are formulated in the followings.

$$\begin{aligned} \tilde{u}_i = & c_{u0} + c_{u3}x + c_{i3}(3c_{u1} + \frac{3}{2}c_{u4}x^2) + c_{u8}(c_{i6}\overline{Sh} + c_{i7}\overline{Ch}) + \\ & c_{i8}(-c_{u10}\overline{Ch_1}\overline{S} + c_{u9}\overline{Sh_1}\overline{C}) + c_{i9}(c_{u10}\overline{Ch_1}\overline{C} + c_{u9}\overline{Sh_1}\overline{S}) + \\ & c_{i10}(c_{u9}\overline{Ch_1}\overline{C} - c_{u10}\overline{Sh_1}\overline{S}) + c_{i11}(c_{u9}\overline{Ch_1}\overline{S} + c_{u10}\overline{Sh_1}\overline{C}), \end{aligned} \quad (A.1)$$

$$\begin{aligned} \tilde{u}_{ix} = & c_{bi0} + c_{bi3}x + c_{i3}(3c_{b1} + \frac{3}{2}c_{b4}x^2) + c_{b8}(c_{i6}\overline{Sh} + c_{i7}\overline{Ch}) + \\ & c_{i8}(-c_{b10}\overline{Ch_1}\overline{S} + c_{b9}\overline{Sh_1}\overline{C}) + c_{i9}(c_{b10}\overline{Ch_1}\overline{C} + c_{b9}\overline{Sh_1}\overline{S}) + \\ & c_{i10}(c_{b9}\overline{Ch_1}\overline{C} - c_{b10}\overline{Sh_1}\overline{S}) + c_{i11}(c_{b9}\overline{Ch_1}\overline{S} + c_{b10}\overline{Sh_1}\overline{C}), \end{aligned} \quad (A.2)$$

where

$$\overline{Ch} = \cosh(\alpha x), \quad \overline{Sh} = \sinh(\alpha x), \quad \overline{Ch_1} = \cosh(\alpha_{11}x), \quad \overline{Sh_1} = \sinh(\alpha_{11}x),$$

$$\overline{C} = \cos(\alpha_{12}x) \text{ and } \overline{S} = \sin(\alpha_{12}x).$$

Their coefficients of longitudinal displacements ($z = h_a / 2$) for the upper adherend and ($z = -h_a / 2$) for the lower adherend are


$$c_{ui0} = -\frac{c_{ai1}}{a_0}, \quad (\text{A.3})$$

$$c_{bi0} = -\frac{c_{aai1}}{a_0}, \quad (\text{A.4})$$

$$c_{ui1} = c_{bi1} = \frac{\beta_1^2 E_1 - \beta_2^2 E_2}{\beta_1 \beta_2 a_0^2 E_1 E_2 h_a} \quad (\text{A.5})$$

$$c_{ui3} = c_{bi3} = -\frac{c_{ai2}}{a_0}, \quad (\text{A.6})$$

$$c_{u4} = c_{b4} = \frac{\beta_1^2 E_1 - \beta_2^2 E_2}{\beta_1 \beta_2 a_0 E_1 E_2 h_a}, \quad (\text{A.7})$$



$$c_{u8} = \frac{\beta_1 \alpha (\beta_1^2 E_1 (-1 + \beta_2 E_2 h_a^2 \alpha^2) + \beta_2^2 E_2 (1 + 4 d_1 h_a \alpha^4))}{2 \beta_2 E_2 (3 \beta_2 d_1 \alpha^4 + \beta_1^2 E_1 h_a (-a_0 + \alpha^2))};$$

$$c_{u9} = (\beta_1 (-3 \beta_1^2 \beta_2 d_1 E_1 (\alpha_{11}^2 + \alpha_{12}^2) (\alpha_{11}^3 - 3 \alpha_{11} \alpha_{12}^2) + 3 \beta_2^3 d_1 E_2 \alpha_{11} (\alpha_{11}^2 + \alpha_{12}^2) (\alpha_{11}^2 + 4 d_1 h_a \alpha_{11}^6 - 3 \alpha_{12}^2 + 12 d_1 h_a \alpha_{11}^4 \alpha_{12}^2 + 12 d_1 h_a \alpha_{11}^2 \alpha_{12}^4 + 4 d_1 h_a \alpha_{12}^6) + \beta_1^4 E_1^2 h_a \alpha_{11} (a_0 (1 - \beta_2 E_2 h_a^2 (\alpha_{11}^2 - 3 \alpha_{12}^2)) + (\alpha_{11}^2 + \alpha_{12}^2) (-1 + \beta_2 E_2 h_a^2 (\alpha_{11}^2 + \alpha_{12}^2))) + \beta_1^2 \beta_2^2 E_1 E_2 h_a \alpha_{11} ((\alpha_{11}^2 + \alpha_{12}^2) (1 + d_1 h_a (7 \alpha_{11}^4 - 2 \alpha_{11}^2 \alpha_{12}^2 - 9 \alpha_{12}^4)) - a_0 (1 + 4 d_1 h_a (\alpha_{11}^4 - 10.0 \alpha_{11}^2 \alpha_{12}^2 + 5 \alpha_{12}^4)))) / (2 \beta_2 E_2 (9 \beta_2^2 d_1^2 (\alpha_{11}^2 + \alpha_{12}^2)^4 + \beta_1^4 E_1^2 h_a^2 (a_0^2 - 2 a_0 (\alpha_{11}^2 - \alpha_{12}^2) + (\alpha_{11}^2 + \alpha_{12}^2)^2) - 6 \beta_1^2 \beta_2 d_1 E_1 h_a (- (\alpha_{11}^2 - \alpha_{12}^2) (\alpha_{11}^2 + \alpha_{12}^2)^2 + a_0 (\alpha_{11}^4 - 6 \alpha_{11}^2 \alpha_{12}^2 + \alpha_{12}^4)))));$$

$$c_{u10} = (\beta_1 (-3 \beta_1^2 \beta_2 d_1 E_1 \alpha_{12} (-3 \alpha_{11}^2 + \alpha_{12}^2) (\alpha_{11}^2 + \alpha_{12}^2) + 3 \beta_2^3 d_1 E_2 \alpha_{12} (\alpha_{11}^2 + \alpha_{12}^2) (4 d_1 h_a \alpha_{11}^6 + \alpha_{12}^2 + 12 d_1 h_a \alpha_{11}^4 \alpha_{12}^2 + 4 d_1 h_a \alpha_{12}^6 + 3 \alpha_{11}^2 (-1 + 4 d_1 h_a \alpha_{12}^4)) + \beta_1^4 E_1^2 h_a \alpha_{12} (a_0 (1 + \beta_2 E_2 h_a^2 (-3 \alpha_{11}^2 + \alpha_{12}^2)) + (\alpha_{11}^2 + \alpha_{12}^2) (1 + \beta_2 E_2 h_a^2 (\alpha_{11}^2 + \alpha_{12}^2))) - \beta_1^2 \beta_2^2 E_1 E_2 h_a \alpha_{12} (- (\alpha_{11}^2 + \alpha_{12}^2) (-1 + d_1 h_a (9 \alpha_{11}^4 + 2 \alpha_{11}^2 \alpha_{12}^2 - 7 \alpha_{12}^4)) + a_0 (1 + 4 d_1 h_a (5 \alpha_{11}^4 - 10.0 \alpha_{11}^2 \alpha_{12}^2 + \alpha_{12}^4)))) / (2 \beta_2 E_2 (9 \beta_2^2 d_1^2 (\alpha_{11}^2 + \alpha_{12}^2)^4 + \beta_1^4 E_1^2 h_a^2 (a_0^2 - 2 a_0 (\alpha_{11}^2 - \alpha_{12}^2) + (\alpha_{11}^2 + \alpha_{12}^2)^2) - 6 \beta_1^2 \beta_2 d_1 E_1 h_a (- (\alpha_{11}^2 - \alpha_{12}^2) (\alpha_{11}^2 + \alpha_{12}^2)^2 + a_0 (\alpha_{11}^4 - 6 \alpha_{11}^2 \alpha_{12}^2 + \alpha_{12}^4))))); \quad (\text{A.8})$$

$$\begin{aligned}
c_{b8} &= -(\beta_1 \alpha (\beta_1^2 E_1 (-a_0 + \alpha^2) + \beta_2^2 E_2 (a_0 + 4 a_0 d_1 h_a \alpha^4 - \alpha^2 (1 + d_1 h_a \alpha^4)) + \\
&\quad \beta_1 \beta_2 E_1 h_a \alpha^2 (3 d_1 \alpha^4 + \beta_2 E_2 h_a (-a_0 + \alpha^2 - 4 a_0 d_1 h_a \alpha^4 + d_1 h_a \alpha^6))) / \\
&\quad (2 \beta_2 E_2 (-a_0 + \alpha^2) (3 \beta_2 d_1 \alpha^4 + \beta_1^2 E_1 h_a (-a_0 + \alpha^2))) ; \\
c_{b9} &= \left\{ \beta_1 \left[-\alpha_{11} (-a_0 + \alpha_{11}^2 + \alpha_{12}^2) + \left(2 d_1 h_a \alpha_{11} \alpha_{12} \left(-\beta_2^2 E_2 \alpha_{12} (a_0 + \alpha_{11}^2 + \alpha_{12}^2) - \right. \right. \right. \\
&\quad \left. \left. \left. \beta_1 \beta_2^2 E_1 E_2 h_a^2 \alpha_{12} \left(a_0 (-3 \alpha_{11}^2 + \alpha_{12}^2) + (\alpha_{11}^2 + \alpha_{12}^2)^2 \right) \right) \right] \left(-3 \beta_1^2 E_1 (-2 a_0 \right. \right. \\
&\quad \left. \left. (\alpha_{11}^2 - \alpha_{12}^2) + (\alpha_{11}^2 + \alpha_{12}^2)^2 \right) + \beta_1^2 \beta_2 E_1 E_2 h_a^2 \left(-8 a_0^2 (\alpha_{11}^2 - \alpha_{12}^2) - 2 (\alpha_{11}^2 - \alpha_{12}^2) + \right. \right. \\
&\quad \left. \left. (\alpha_{11}^2 + \alpha_{12}^2)^2 + a_0 (7 \alpha_{11}^4 - 2 \alpha_{11}^2 \alpha_{12}^2 + 7 \alpha_{12}^4) \right) - 3 \beta_2^2 E_2 \left(2 a_0 (\alpha_{11}^2 - \alpha_{12}^2) + \right. \right. \\
&\quad \left. \left. (\alpha_{11}^2 + \alpha_{12}^2)^2 (-1 + d_1 h_a (\alpha_{11}^2 + \alpha_{12}^2)^2) \right) \right] \left. \right\} / \left\{ \beta_2 E_2 \left(9 \beta_2^2 d_1^2 (\alpha_{11}^2 + \alpha_{12}^2)^4 + \right. \right. \\
&\quad \left. \left. \beta_1^4 E_1^2 h_a^2 \left(a_0^2 - 2 a_0 (\alpha_{11}^2 - \alpha_{12}^2) + (\alpha_{11}^2 + \alpha_{12}^2)^2 \right) - 6 \beta_1^2 \beta_2 d_1 E_1 h_a \right. \right. \\
&\quad \left. \left. \left((-\alpha_{11}^2 + \alpha_{12}^2) (\alpha_{11}^2 + \alpha_{12}^2)^2 + a_0 (\alpha_{11}^4 - 6 \alpha_{11}^2 \alpha_{12}^2 + \alpha_{12}^4) \right) \right) \right\} + \\
&\quad \left\{ \beta_2 \alpha_{11} \left(-a_0 + \alpha_{11}^2 + \alpha_{12}^2 + \beta_1 E_1 h_a^2 \left(a_0 (\alpha_{11}^2 - 3 \alpha_{12}^2) - (\alpha_{11}^2 + \alpha_{12}^2)^2 \right) \right) \right. \\
&\quad \left. \left(9 \beta_2 d_1^2 (\alpha_{11}^2 + \alpha_{12}^2)^4 - 3 \beta_1^2 d_1 E_1 h_a \left((-\alpha_{11}^2 + \alpha_{12}^2) (\alpha_{11}^2 + \alpha_{12}^2)^2 + \right. \right. \right. \\
&\quad \left. \left. \left. a_0 (\alpha_{11}^4 - 6 \alpha_{11}^2 \alpha_{12}^2 + \alpha_{12}^4) \right) + \beta_1^2 \beta_2 E_1 E_2 h_a^2 \left((\alpha_{11}^2 + \alpha_{12}^2)^2 (1 + d_1 h_a \right. \right. \right. \\
&\quad \left. \left. \left. (\alpha_{11}^4 - 6 \alpha_{11}^2 \alpha_{12}^2 + \alpha_{12}^4) \right) + a_0^2 (1 + 4 d_1 h_a (\alpha_{11}^4 - 6 \alpha_{11}^2 \alpha_{12}^2 + \alpha_{12}^4)) - \right. \right. \\
&\quad \left. \left. a_0 (\alpha_{11}^2 - \alpha_{12}^2) (2 + d_1 h_a (5 \alpha_{11}^4 - 6 \alpha_{11}^2 \alpha_{12}^2 + 5 \alpha_{12}^4)) \right) - \right. \\
&\quad \left. 3 \beta_2^2 d_1 E_2 h_a \left((-\alpha_{11}^2 + \alpha_{12}^2) (\alpha_{11}^2 + \alpha_{12}^2)^2 (1 + d_1 h_a (\alpha_{11}^2 + \alpha_{12}^2)^2) + a_0 \right. \right. \\
&\quad \left. \left. (4 d_1 h_a \alpha_{11}^8 + 16 d_1 h_a \alpha_{11}^6 \alpha_{12}^2 + \alpha_{12}^4 + 4 d_1 h_a \alpha_{12}^8 + \right. \right. \\
&\quad \left. \left. \alpha_{11}^4 (1 + 24 d_1 h_a \alpha_{12}^4) + \alpha_{11}^2 (-6 \alpha_{12}^2 + 16 d_1 h_a \alpha_{12}^6) \right) \right) \right\} / \\
&\quad \left\{ 9 \beta_2^2 d_1^2 (\alpha_{11}^2 + \alpha_{12}^2)^4 + \beta_1^4 E_1^2 h_a^2 \left(a_0^2 - 2 a_0 (\alpha_{11}^2 - \alpha_{12}^2) + (\alpha_{11}^2 + \alpha_{12}^2)^2 \right) - \right. \\
&\quad \left. 6 \beta_1^2 \beta_2 d_1 E_1 h_a \left((-\alpha_{11}^2 + \alpha_{12}^2) (\alpha_{11}^2 + \alpha_{12}^2)^2 + a_0 (\alpha_{11}^4 - 6 \alpha_{11}^2 \alpha_{12}^2 + \alpha_{12}^4) \right) \right\} / \\
&\quad \left\{ 2 \beta_2 E_2 h_a \left(a_0^2 - 2 a_0 (\alpha_{11}^2 - \alpha_{12}^2) + (\alpha_{11}^2 + \alpha_{12}^2)^2 \right) \right\} ; \\
c_{b10} &= \left\{ \beta_1 \left(\alpha_{12} (a_0 + \alpha_{11}^2 + \alpha_{12}^2) + \left(2 \beta_2 d_1 h_a \alpha_{11}^2 \alpha_{12} \left(-a_0 + \alpha_{11}^2 + \alpha_{12}^2 + \beta_1 E_1 h_a^2 \right. \right. \right. \right. \\
&\quad \left. \left. \left. \left(a_0 (\alpha_{11}^2 - 3 \alpha_{12}^2) - (\alpha_{11}^2 + \alpha_{12}^2)^2 \right) \right) \right) \left(3 \beta_1^2 E_1 \left(-2 a_0 (\alpha_{11}^2 - \alpha_{12}^2) + (\alpha_{11}^2 + \alpha_{12}^2)^2 \right) + \right. \right. \\
&\quad \left. \left. \beta_1^2 \beta_2 E_1 E_2 h_a^2 \left(8 a_0^2 (\alpha_{11}^2 - \alpha_{12}^2) + 2 (\alpha_{11}^2 - \alpha_{12}^2) (\alpha_{11}^2 + \alpha_{12}^2)^2 + a_0 \right. \right. \right. \\
&\quad \left. \left. \left. (-7 \alpha_{11}^4 + 2 \alpha_{11}^2 \alpha_{12}^2 - 7 \alpha_{12}^4) \right) + 3 \beta_2^2 E_2 \left(2 a_0 (\alpha_{11}^2 - \alpha_{12}^2) + (\alpha_{11}^2 + \alpha_{12}^2)^2 \right) \right. \right. \\
&\quad \left. \left. \left. (-1 + d_1 h_a (\alpha_{11}^2 + \alpha_{12}^2)^2) \right) \right) \right\} / \left\{ 9 \beta_2^2 d_1^2 (\alpha_{11}^2 + \alpha_{12}^2)^4 + \beta_1^4 E_1^2 h_a^2 \left(a_0^2 - \right. \right. \\
&\quad \left. \left. 2 a_0 (\alpha_{11}^2 - \alpha_{12}^2) + (\alpha_{11}^2 + \alpha_{12}^2)^2 \right) - 6 \beta_1^2 \beta_2 d_1 E_1 h_a \left((-\alpha_{11}^2 + \alpha_{12}^2) (\alpha_{11}^2 + \alpha_{12}^2)^2 + \right. \right. \\
&\quad \left. \left. a_0 (\alpha_{11}^4 - 6 \alpha_{11}^2 \alpha_{12}^2 + \alpha_{12}^4) \right) \right\} + \left\{ \left(-\beta_2^2 E_2 \alpha_{12} (a_0 + \alpha_{11}^2 + \alpha_{12}^2) - \beta_1 \beta_2^2 E_1 E_2 h_a^2 \alpha_{12} \right. \right. \\
&\quad \left. \left. \left(a_0 (-3 \alpha_{11}^2 + \alpha_{12}^2) + (\alpha_{11}^2 + \alpha_{12}^2)^2 \right) \right) \left(9 \beta_2 d_1^2 (\alpha_{11}^2 + \alpha_{12}^2)^4 - 3 \beta_1^2 d_1 E_1 h_a \right. \right. \\
&\quad \left. \left. \left((-\alpha_{11}^2 + \alpha_{12}^2) (\alpha_{11}^2 + \alpha_{12}^2)^2 + a_0 (\alpha_{11}^4 - 6 \alpha_{11}^2 \alpha_{12}^2 + \alpha_{12}^4) \right) + \right. \right. \\
&\quad \left. \left. \beta_1^2 \beta_2 E_1 E_2 h_a^2 \left((\alpha_{11}^2 + \alpha_{12}^2)^2 (1 + d_1 h_a (\alpha_{11}^4 - 6 \alpha_{11}^2 \alpha_{12}^2 + \alpha_{12}^4)) + a_0^2 \right. \right. \right. \\
&\quad \left. \left. \left. (1 + 4 d_1 h_a (\alpha_{11}^4 - 6 \alpha_{11}^2 \alpha_{12}^2 + \alpha_{12}^4)) - a_0 (\alpha_{11}^2 - \alpha_{12}^2) \right. \right. \right. \\
&\quad \left. \left. \left. (2 + d_1 h_a (5 \alpha_{11}^4 - 6 \alpha_{11}^2 \alpha_{12}^2 + 5 \alpha_{12}^4)) \right) - 3 \beta_2^2 d_1 E_2 h_a \left((-\alpha_{11}^2 + \alpha_{12}^2) \right. \right. \right. \\
&\quad \left. \left. \left. (\alpha_{11}^2 + \alpha_{12}^2)^2 (1 + d_1 h_a (\alpha_{11}^2 + \alpha_{12}^2)^2) + a_0 (4 d_1 h_a \alpha_{11}^8 + 16 d_1 h_a \alpha_{11}^6 \alpha_{12}^2 + \right. \right. \right. \\
&\quad \left. \left. \left. \alpha_{12}^4 + 4 d_1 h_a \alpha_{12}^8 + \alpha_{11}^4 (1 + 24 d_1 h_a \alpha_{12}^4) + \alpha_{11}^2 (-6 \alpha_{12}^2 + 16 d_1 h_a \alpha_{12}^6) \right) \right) \right\} / \\
&\quad \left\{ \beta_2 E_2 \left(9 \beta_2^2 d_1^2 (\alpha_{11}^2 + \alpha_{12}^2)^4 + \beta_1^4 E_1^2 h_a^2 \left(a_0^2 - 2 a_0 (\alpha_{11}^2 - \alpha_{12}^2) + (\alpha_{11}^2 + \alpha_{12}^2)^2 \right) - \right. \right. \\
&\quad \left. \left. 6 \beta_1^2 \beta_2 d_1 E_1 h_a \left((-\alpha_{11}^2 + \alpha_{12}^2) (\alpha_{11}^2 + \alpha_{12}^2)^2 + a_0 (\alpha_{11}^4 - 6 \alpha_{11}^2 \alpha_{12}^2 + \alpha_{12}^4) \right) \right) \right\} / \\
&\quad \left\{ 2 \beta_2 E_2 h_a \left(a_0^2 - 2 a_0 (\alpha_{11}^2 - \alpha_{12}^2) + (\alpha_{11}^2 + \alpha_{12}^2)^2 \right) \right\} ; \tag{A.9}
\end{aligned}$$

where $c_{aai} = c_{aii} - 3(\beta_1 + \beta_2)h_a c_{i3}$, and $a_0 = \frac{1}{E_1 \beta_1 h_a^2} + \frac{1}{E_2 \beta_2 h_a^2}$.

The equations of longitudinal displacements ($z = \frac{h_1 + h_a}{2}$) for the upper adherend

and ($z = -\frac{h_2 + h_a}{2}$) for the lower adherend are expressed in the followings.

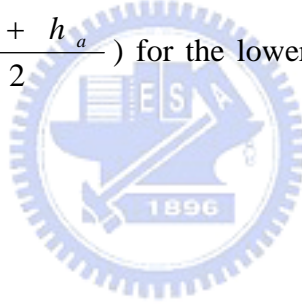
$$\begin{aligned}
u_i \left(\frac{h_1 + h_a}{2} \right) &= u_{ui0} + u_{u4}x + c_{i1}u_{u1} + c_{i2}u_{u5}x + c_{i3}(3u_{u2} + u_{u7}x^2) + u_{u10}(c_{i6}\overline{Sh} + c_{i7}\overline{Ch}) + \\
c_{i8}(-u_{b11}\overline{Ch_1}\overline{S} - u_{b12}\overline{Sh_1}\overline{C}) &+ c_{i9}(u_{b11}\overline{Ch_1}\overline{C} + u_{b12}\overline{Sh_1}\overline{S}) + \\
c_{i10}(u_{b12}\overline{Ch_1}\overline{C} - u_{b11}\overline{Sh_1}\overline{S}) &+ c_{i11}(u_{b12}\overline{Ch_1}\overline{S} + u_{b11}\overline{Sh_1}\overline{C})
\end{aligned} \tag{A.10}$$

$$\begin{aligned}
u_{ix} \left(-\frac{h_2 + h_a}{2} \right) &= u_{bi0} + u_{b4}x + c_{i1}u_{b1} + c_{i2}u_{b5}x + c_{i3}(3u_{b2} + u_{b7}x^2) + u_{b10}(c_{i6}\overline{Sh} + c_{i7}\overline{Ch}) + \\
c_{i8}(-u_{b12}\overline{Ch_1}\overline{S} - u_{b11}\overline{Sh_1}\overline{C}) &+ c_{i9}(u_{b12}\overline{Ch_1}\overline{C} + u_{b11}\overline{Sh_1}\overline{S}) + \\
c_{i10}(u_{b11}\overline{Ch_1}\overline{C} - u_{b12}\overline{Sh_1}\overline{S}) &+ c_{i11}(u_{b11}\overline{Ch_1}\overline{S} + u_{b12}\overline{Sh_1}\overline{C}),
\end{aligned} \tag{A.11}$$

The coefficients of the longitudinal displacement ($z = \frac{h_1 + h_a}{2}$) for the upper

adherend and ($z = -\frac{h_2 + h_a}{2}$) for the lower adherend are expressed in the

followings.



$$\begin{aligned}
u_{ui0} &= -\frac{C_{ai1}}{a_0}; \\
u_{u1} &= -\frac{\beta_1 h_a}{2}; \\
u_{u2} &= \frac{(\beta_1^2 E_1 - \beta_2^2 E_2)}{\beta_1 \beta_2 a_0^2 E_1 E_2 h_a}; \\
u_{u4} &= -\frac{C_{ai2}}{a_0}; \\
u_{u5} &= -\beta_1 h_a; \\
u_{u7} &= \left(\frac{3 \beta_1^2 E_1 - 3 \beta_2^2 E_2}{2 \beta_1 \beta_2 a_0 E_1 E_2 h_a} - \frac{3 \beta_1 h_a}{2} \right); \\
u_{u10} &= \frac{\beta_1 \alpha (\beta_1^2 E_1 (-1 + \beta_2 a_0 E_2 h_a^2) + \beta_2^2 E_2 (1 + d_1 h_a \alpha^4))}{2 \beta_2 E_2 (3 \beta_2 d_1 \alpha^4 + \beta_1^2 E_1 h_a (-a_0 + \alpha^2))}; \\
u_{u11} &= (\beta_1 (-3 \beta_1^2 \beta_2 d_1 E_1 \alpha_{12} (-3 \alpha_{11}^2 + \alpha_{12}^2) (\alpha_{11}^2 + \alpha_{12}^2) - \\
&\quad \beta_1^4 E_1^2 h_a (-1 + \beta_2 a_0 E_2 h_a^2) \alpha_{12} (a_0 + \alpha_{11}^2 + \alpha_{12}^2) + 3 \beta_2^3 d_1 E_2 \alpha_{12} (\alpha_{11}^2 + \alpha_{12}^2) \\
&\quad (d_1 h_a \alpha_{11}^6 + \alpha_{12}^2 + 3 d_1 h_a \alpha_{11}^4 \alpha_{12}^2 + d_1 h_a \alpha_{12}^6 + 3 \alpha_{11}^2 (-1 + d_1 h_a \alpha_{12}^4)) - \\
&\quad \beta_1^2 \beta_2^2 E_1 E_2 h_a \alpha_{12} (a_0 (1 + 2 d_1 h_a (7 \alpha_{11}^4 - 2 \alpha_{11}^2 \alpha_{12}^2 - \alpha_{12}^4)) - \\
&\quad (\alpha_{11}^2 + \alpha_{12}^2) (-1 + d_1 h_a (3 \alpha_{11}^4 + 2 \alpha_{11}^2 \alpha_{12}^2 - \alpha_{12}^4)))))) / \\
&\quad (2 \beta_2 E_2 (9 \beta_2^2 d_1^2 (\alpha_{11}^2 + \alpha_{12}^2)^4 + \beta_1^4 E_1^2 h_a^2 (a_0^2 - 2 a_0 (\alpha_{11}^2 - \alpha_{12}^2) + (\alpha_{11}^2 + \alpha_{12}^2)^2) \\
&\quad - 6 \beta_1^2 \beta_2 d_1 E_1 h_a (- (\alpha_{11}^2 - \alpha_{12}^2) (\alpha_{11}^2 + \alpha_{12}^2)^2 + a_0 (\alpha_{11}^4 - 6 \alpha_{11}^2 \alpha_{12}^2 + \alpha_{12}^4)))); \\
u_{u12} &= (\beta_1 (\beta_1^4 E_1^2 h_a (-1 + \beta_2 a_0 E_2 h_a^2) \alpha_{11} (-a_0 + \alpha_{11}^2 + \alpha_{12}^2) - \\
&\quad 3 \beta_1^2 \beta_2 d_1 E_1 (\alpha_{11}^2 + \alpha_{12}^2) (\alpha_{11}^3 - 3 \alpha_{11} \alpha_{12}^2) + 3 \beta_2^3 d_1 E_2 \alpha_{11} (\alpha_{11}^2 + \alpha_{12}^2) \\
&\quad (\alpha_{11}^2 + d_1 h_a \alpha_{11}^6 - 3 \alpha_{12}^2 + 3 d_1 h_a \alpha_{11}^4 \alpha_{12}^2 + 3 d_1 h_a \alpha_{11}^2 \alpha_{12}^4 + d_1 h_a \alpha_{12}^6) + \\
&\quad \beta_1^2 \beta_2^2 E_1 E_2 h_a \alpha_{11} (a_0 (-1 + 2 d_1 h_a (\alpha_{11}^4 + 2 \alpha_{11}^2 \alpha_{12}^2 - 7 \alpha_{12}^4)) + \\
&\quad (\alpha_{11}^2 + \alpha_{12}^2) (1 + d_1 h_a (\alpha_{11}^4 - 2 \alpha_{11}^2 \alpha_{12}^2 - 3 \alpha_{12}^4)))))) / \\
&\quad (2 \beta_2 E_2 (9 \beta_2^2 d_1^2 (\alpha_{11}^2 + \alpha_{12}^2)^4 + \beta_1^4 E_1^2 h_a^2 (a_0^2 - 2 a_0 (\alpha_{11}^2 - \alpha_{12}^2) + (\alpha_{11}^2 + \alpha_{12}^2)^2) - \\
&\quad - 6 \beta_1^2 \beta_2 d_1 E_1 h_a (- (\alpha_{11}^2 - \alpha_{12}^2) (\alpha_{11}^2 + \alpha_{12}^2)^2 + a_0 (\alpha_{11}^4 - 6 \alpha_{11}^2 \alpha_{12}^2 + \alpha_{12}^4)))); \tag{A.12}
\end{aligned}$$



$$\begin{aligned}
u_{bi0} &= -\frac{C_{aai1}}{a_0}; \\
u_{b1} &= \frac{\beta_2 h_a}{2}; \\
u_{b2} &= \frac{(\beta_1^2 E_1 - \beta_2^2 E_2)}{\beta_1 \beta_2 a_0^2 E_1 E_2 h_a}; \\
u_{b4} &= -\frac{C_{ai2}}{a_0}; \\
u_{b5} &= \beta_2 h_a; \\
u_{b7} &= \left(\frac{3 \beta_1^2 E_1 - 3 \beta_2^2 E_2}{2 \beta_1 \beta_2 a_0 E_1 E_2 h_a} + \frac{3 \beta_2 h_a}{2} \right); \\
u_{b10} &= (\beta_1 \alpha (\beta_1^2 E_1 (a_0 - \alpha^2) + \beta_2^2 E_2 (\alpha^2 + d_1 h_a \alpha^6 - a_0 (1 + 4 d_1 h_a \alpha^4)) + \\
&\quad \beta_1 \beta_2 a_0 E_1 h_a (-3 d_1 \alpha^4 + \beta_2 E_2 h_a (a_0 - \alpha^2 + 4 a_0 d_1 h_a \alpha^4 - d_1 h_a \alpha^6))) / \\
&\quad (2 \beta_2 E_2 (-a_0 + \alpha^2) (3 \beta_2 d_1 \alpha^4 + \beta_1^2 E_1 h_a (-a_0 + \alpha^2)));
\end{aligned}$$

Transverse displacement

The equation of transverse displacement for the lower adherend is

$$\begin{aligned}
 w_{ix} = & c_{i0} + c_{i1}x + c_{i2}x^2 + c_{i3}x^3 + c_{i4}x^4 + c_{i5}x^5 + c_{w7}(c_{i6}\overline{Ch} + c_{i7}\overline{Sh}) + \\
 & c_{i8}(c_{w9}\overline{Ch_1}\overline{C} - c_{w8}\overline{Sh_1}\overline{S}) + c_{i9}(c_{w9}\overline{Ch_1}\overline{S} + c_{w8}\overline{Sh_1}\overline{C}) + \\
 & c_{i10}(c_{w9}\overline{Sh_1}\overline{C} - c_{w8}\overline{Ch_1}\overline{S}) + c_{i11}(c_{w8}\overline{Ch_1}\overline{C} + c_{w9}\overline{Sh_1}\overline{S}).
 \end{aligned} \tag{A.15}$$

Their coefficients of transverse displacement for the lower adherend are shown in the followings.

$$\begin{aligned}
 c_{w7} = & (-\beta_1^2 \beta_2 a_0 E_1 E_2 h_a + \beta_1^2 \beta_2 E_1 E_2 h_a \alpha^2 + 3 \beta_1^2 d_1 E_1 \alpha^4 - 3 \beta_2^2 d_1 E_2 \alpha^4 - \\
 & 4 \beta_1^2 \beta_2 a_0 d_1 E_1 E_2 h_a^2 \alpha^4 + \beta_1^2 \beta_2 d_1 E_1 E_2 h_a^2 \alpha^6) / (\beta_1^2 \beta_2 E_1 E_2 h_a (-a_0 + \alpha^2)); \\
 c_{w8} = & (\beta_1^2 E_1 \{ 6 \beta_1^2 d_1 E_1 h_a \alpha_{11} \alpha_{12} \{ -2 a_0 (\alpha_{11}^2 - \alpha_{12}^2) + (\alpha_{11}^2 + \alpha_{12}^2)^2 \} + \\
 & 2 \beta_1^2 \beta_2 d_1 E_1 E_2 h_a^3 \alpha_{11} \alpha_{12} \{ 8 a_0^2 (\alpha_{11}^2 - \alpha_{12}^2) + 2 (\alpha_{11}^2 - \alpha_{12}^2) (\alpha_{11}^2 + \alpha_{12}^2)^2 + \\
 & a_0 (-7 \alpha_{11}^4 + 2 \alpha_{11}^2 \alpha_{12}^2 - 7 \alpha_{12}^4) \} + 6 \beta_2^2 d_1 E_2 h_a \alpha_{11} \alpha_{12} \\
 & \{ 2 a_0 (\alpha_{11}^2 - \alpha_{12}^2) + (\alpha_{11}^2 + \alpha_{12}^2)^2 (-1 + d_1 h_a (\alpha_{11}^2 + \alpha_{12}^2)^2) \} \} / \\
 & (\beta_2 E_2 \{ 9 \beta_2^2 d_1^2 (\alpha_{11}^2 + \alpha_{12}^2)^4 + \beta_1^4 E_1^2 h_a^2 \{ a_0^2 - 2 a_0 (\alpha_{11}^2 - \alpha_{12}^2) + (\alpha_{11}^2 + \alpha_{12}^2)^2 \} - \\
 & 6 \beta_1^2 \beta_2 d_1 E_1 h_a \{ -(\alpha_{11}^2 - \alpha_{12}^2) (\alpha_{11}^2 + \alpha_{12}^2)^2 + a_0 (\alpha_{11}^4 - 6 \alpha_{11}^2 \alpha_{12}^2 + \alpha_{12}^4) \} \}); \\
 c_{w9} = & (\beta_1^2 E_1 \{ 9 \beta_2 d_1^2 (\alpha_{11}^2 + \alpha_{12}^2)^4 - 3 \beta_1^2 d_1 E_1 h_a \{ -(\alpha_{11}^2 - \alpha_{12}^2) (\alpha_{11}^2 + \alpha_{12}^2)^2 + \\
 & a_0 (\alpha_{11}^4 - 6 \alpha_{11}^2 \alpha_{12}^2 + \alpha_{12}^4) \} + \beta_1^2 \beta_2 E_1 E_2 h_a^2 \{ (\alpha_{11}^2 + \alpha_{12}^2)^2 (1 + d_1 h_a \\
 & (\alpha_{11}^4 - 6 \alpha_{11}^2 \alpha_{12}^2 + \alpha_{12}^4)) + a_0^2 (1 + 4 d_1 h_a (\alpha_{11}^4 - 6 \alpha_{11}^2 \alpha_{12}^2 + \alpha_{12}^4)) - \\
 & a_0 (\alpha_{11}^2 - \alpha_{12}^2) (2 + d_1 h_a (5 \alpha_{11}^4 - 6 \alpha_{11}^2 \alpha_{12}^2 + 5 \alpha_{12}^4)) \} - \\
 & 3 \beta_2^2 d_1 E_2 h_a \{ -(\alpha_{11}^2 - \alpha_{12}^2) (\alpha_{11}^2 + \alpha_{12}^2)^2 (1 + d_1 h_a (\alpha_{11}^2 + \alpha_{12}^2)^2) + \\
 & a_0 (4 d_1 h_a \alpha_{11}^8 + 16 d_1 h_a \alpha_{11}^6 \alpha_{12}^2 + \alpha_{12}^4 + 4 d_1 h_a \alpha_{12}^8 + \\
 & \alpha_{11}^4 (1 + 24 d_1 h_a \alpha_{12}^4) + \alpha_{11}^2 (-6 \alpha_{12}^2 + 16 d_1 h_a \alpha_{12}^6) \} \}) / \\
 & (\beta_2 E_2 \{ 9 \beta_2^2 d_1^2 (\alpha_{11}^2 + \alpha_{12}^2)^4 + \beta_1^4 E_1^2 h_a^2 \{ a_0^2 - 2 a_0 (\alpha_{11}^2 - \alpha_{12}^2) + (\alpha_{11}^2 + \alpha_{12}^2)^2 \} - \\
 & 6 \beta_1^2 \beta_2 d_1 E_1 h_a \{ -(\alpha_{11}^2 - \alpha_{12}^2) (\alpha_{11}^2 + \alpha_{12}^2)^2 + a_0 (\alpha_{11}^4 - 6 \alpha_{11}^2 \alpha_{12}^2 + \alpha_{12}^4) \} \});
 \end{aligned} \tag{A.17}$$

Slope

The equations of the slope for the upper adherend and for the lower adherend are expressed in the followings.

$$\begin{aligned}
 \frac{dw_i}{dx} = & c_{i1} + 2c_{i2}x + 3c_{i3}x^2 + c_{i6}\alpha\overline{Ch} + c_{i7}\alpha\overline{Sh} + c_{i8}(-\alpha_{12}\overline{Ch_1}\overline{S} + \alpha_{11}\overline{Sh_1}\overline{C}) + \\
 & c_{i9}(\alpha_{12}\overline{Ch_1}\overline{C} + \alpha_{11}\overline{Sh_1}\overline{S}) + c_{i10}(\alpha_{11}\overline{Ch_1}\overline{C} - \alpha_{12}\overline{Sh_1}\overline{S}) + c_{i11}(\alpha_{11}\overline{Ch_1}\overline{S} + \alpha_{12}\overline{Sh_1}\overline{C})
 \end{aligned} \tag{A.18}$$

$$\begin{aligned} \frac{dw_{ix}}{dx} = & c_{i1} + 2c_{i2}x + 3c_{i3}x^2 + d_{b6}(c_{i6}\overline{Sh} + c_{i7}\overline{Ch}) + c_{i8}(-d_{b8}\overline{Ch_1S} + d_{b7}\overline{Sh_1C}) + \\ & c_{i9}(d_{b8}\overline{Ch_1C} + d_{b7}\overline{Sh_1S}) + c_{i10}(d_{b7}\overline{Ch_1C} - d_{b8}\overline{Sh_1S}) + c_{i11}(d_{b7}\overline{Ch_1S} + d_{b8}\overline{Sh_1C}) \end{aligned} \quad (\text{A.19})$$

Their coefficients of the slope for the lower adherend are obtained as shown.

$$\begin{aligned} d_{b6} = & (\beta_1^2 E_1 \alpha (3 d_1 \alpha^4 + \beta_2 E_2 h_a (\alpha^2 + d_1 h_a \alpha^6 - a_0 (1 + 4 d_1 h_a \alpha^4))) / \\ & (\beta_2 E_2 (3 \beta_2 d_1 \alpha^4 + \beta_1^2 E_1 h_a (-a_0 + \alpha^2))) ; \\ d_{b7} = & (\beta_1^2 E_1 (9 \beta_2 d_1^2 \alpha_{11} (\alpha_{11}^2 + \alpha_{12}^2)^4 - 3 \beta_1^2 d_1 E_1 h_a \alpha_{11} \\ & (- (\alpha_{11}^2 - 3 \alpha_{12}^2) (\alpha_{11}^2 + \alpha_{12}^2)^2 + a_0 (\alpha_{11}^4 - 10.0 \alpha_{11}^2 \alpha_{12}^2 + 5 \alpha_{12}^4)) - \\ & 3 \beta_2^2 d_1 E_2 h_a \alpha_{11} (\alpha_{11}^2 + \alpha_{12}^2) (a_0 (\alpha_{11}^2 + 4 d_1 h_a \alpha_{11}^6 - 3 \alpha_{12}^2 + 12 d_1 h_a \alpha_{11}^4 \alpha_{12}^2 + \\ & 12 d_1 h_a \alpha_{11}^2 \alpha_{12}^4 + 4 d_1 h_a \alpha_{12}^6) - (\alpha_{11}^2 + \alpha_{12}^2)^2 (1 + d_1 h_a (\alpha_{11}^4 - 2 \alpha_{11}^2 \alpha_{12}^2 - \\ & 3 \alpha_{12}^4))) + \beta_1^2 \beta_2 E_1 E_2 h_a^2 \alpha_{11} ((\alpha_{11}^2 + \alpha_{12}^2)^2 (1 + d_1 h_a (\alpha_{11}^4 - 10.0 \alpha_{11}^2 \alpha_{12}^2 + \\ & 5 \alpha_{12}^4)) + a_0^2 (1 + 4 d_1 h_a (\alpha_{11}^4 - 10.0 \alpha_{11}^2 \alpha_{12}^2 + 5 \alpha_{12}^4)) + a_0 (-5 d_1 h_a \alpha_{11}^6 + \\ & 25 d_1 h_a \alpha_{11}^4 \alpha_{12}^2 - \alpha_{11}^2 (2 + 15 d_1 h_a \alpha_{12}^4) + \alpha_{12}^2 (2 + 19 d_1 h_a \alpha_{12}^4))) / \\ & (\beta_2 E_2 (9 \beta_2^2 d_1^2 (\alpha_{11}^2 + \alpha_{12}^2)^4 + \beta_1^4 E_1^2 h_a^2 (a_0^2 - 2 a_0 (\alpha_{11}^2 - \alpha_{12}^2) + (\alpha_{11}^2 + \alpha_{12}^2)^2) - \\ & 6 \beta_1^2 \beta_2 d_1 E_1 h_a (- (\alpha_{11}^2 - \alpha_{12}^2) (\alpha_{11}^2 + \alpha_{12}^2)^2 + a_0 (\alpha_{11}^4 - 6 \alpha_{11}^2 \alpha_{12}^2 + \alpha_{12}^4))) ; \\ d_{b8} = & (\beta_1^2 E_1 (9 \beta_2 d_1^2 \alpha_{12} (\alpha_{11}^2 + \alpha_{12}^2)^4 - 3 \beta_1^2 d_1 E_1 h_a \alpha_{12} (- (3 \alpha_{11}^2 - \alpha_{12}^2) \\ & (\alpha_{11}^2 + \alpha_{12}^2)^2 + a_0 (5 \alpha_{11}^4 - 10.0 \alpha_{11}^2 \alpha_{12}^2 + \alpha_{12}^4)) - 3 \beta_2^2 d_1 E_2 h_a \alpha_{12} (\alpha_{11}^2 + \alpha_{12}^2) \\ & (- (\alpha_{11}^2 + \alpha_{12}^2)^2 (-1 + d_1 h_a (3 \alpha_{11}^4 + 2 \alpha_{11}^2 \alpha_{12}^2 - \alpha_{12}^4)) + a_0 (4 d_1 h_a \alpha_{11}^6 + \\ & \alpha_{12}^2 + 12 d_1 h_a \alpha_{11}^4 \alpha_{12}^2 + 4 d_1 h_a \alpha_{12}^6 + 3 \alpha_{11}^2 (-1 + 4 d_1 h_a \alpha_{12}^4))) + \\ & \beta_1^2 \beta_2 E_1 E_2 h_a^2 \alpha_{12} ((\alpha_{11}^2 + \alpha_{12}^2)^2 (1 + d_1 h_a (5 \alpha_{11}^4 - 10.0 \alpha_{11}^2 \alpha_{12}^2 + \alpha_{12}^4)) + \\ & a_0^2 (1 + 4 d_1 h_a (5 \alpha_{11}^4 - 10.0 \alpha_{11}^2 \alpha_{12}^2 + \alpha_{12}^4)) + a_0 (-19 d_1 h_a \alpha_{11}^6 + \\ & 15 d_1 h_a \alpha_{11}^4 \alpha_{12}^2 + \alpha_{12}^2 (2 + 5 d_1 h_a \alpha_{12}^4) - \alpha_{11}^2 (2 + 25 d_1 h_a \alpha_{12}^4))) / \\ & (\beta_2 E_2 (9 \beta_2^2 d_1^2 (\alpha_{11}^2 + \alpha_{12}^2)^4 + \beta_1^4 E_1^2 h_a^2 (a_0^2 - 2 a_0 (\alpha_{11}^2 - \alpha_{12}^2) + (\alpha_{11}^2 + \alpha_{12}^2)^2) - \\ & 6 \beta_1^2 \beta_2 d_1 E_1 h_a (- (\alpha_{11}^2 - \alpha_{12}^2) (\alpha_{11}^2 + \alpha_{12}^2)^2 + a_0 (\alpha_{11}^4 - 6 \alpha_{11}^2 \alpha_{12}^2 + \alpha_{12}^4))) ; \end{aligned} \quad (\text{A.20})$$

Appendix B

The equations of and their coefficients of peel stress, shear stress and shear force for the adhesive layer are shown as follows.

The equations of peel stress and shear stress for the adhesive layer are formulated as follows.

$$\begin{aligned} \bar{\sigma}_{ai} = & \frac{2cG_a}{P} (s_{a3}(c_{i6}\bar{Ch} + c_{i7}\bar{Sh}) + c_{i8}(s_{a5}\bar{Ch}_1\bar{C} - s_{a4}\bar{Sh}_1\bar{S}) + c_{i9}(s_{a5}\bar{Ch}_1\bar{S} + s_{a4}\bar{Sh}_1\bar{C}) + \\ & c_{i10}(-s_{a4}\bar{Ch}_1\bar{S} + s_{a5}\bar{Sh}_1\bar{C}) + c_{i11}(s_{a4}\bar{Ch}_1\bar{C} + s_{a5}\bar{Sh}_1\bar{S})) \end{aligned} \quad (\text{B.1})$$

$$\begin{aligned} \bar{\tau}_{ai} = & \frac{2cG_a}{P} (s_{s10} + s_{s8}(c_{i6}\bar{Sh} + c_{i7}\bar{Ch}) + c_{i8}(s_{s10}\bar{Sh}_1\bar{C} - s_{s9}\bar{Ch}_1\bar{S}) + \\ & c_{i9}(s_{s10}\bar{Ch}_1\bar{C} + s_{s9}\bar{Sh}_1\bar{S}) + c_{i10}(s_{s9}\bar{Ch}_1\bar{C} - s_{s10}\bar{Sh}_1\bar{S}) + c_{i11}(s_{s10}\bar{Ch}_1\bar{S} + s_{s9}\bar{Sh}_1\bar{C})) \end{aligned} \quad (\text{B.2})$$

Their coefficients are expressed below.

$$\begin{aligned} s_{a3} = & - \frac{d_1 E_0 \alpha^4 (-3 \beta_2^2 E_2 + \beta_1^2 E_1 (3 + \beta_2 E_2 h_a^2 (-4 a_0 + \alpha^2)))}{\beta_2 E_2 h_a (3 \beta_2 d_1 \alpha^4 + \beta_1^2 E_1 h_a (-a_0 + \alpha^2))}; \\ s_{a4} = & - \left(2 \beta_1^2 d_1 E_0 E_1 \alpha_{11} \alpha_{12} \left(3 \beta_1^2 E_1 (-2 a_0 (\alpha_{11}^2 - \alpha_{12}^2) + (\alpha_{11}^2 + \alpha_{12}^2)^2) + \right. \right. \\ & \beta_1^2 \beta_2 E_1 E_2 h_a^2 \left(8 a_0^2 (\alpha_{11}^2 - \alpha_{12}^2) + 2 (\alpha_{11}^2 - \alpha_{12}^2) (\alpha_{11}^2 + \alpha_{12}^2)^2 + \right. \\ & \left. \left. a_0 (-7 \alpha_{11}^4 + 2 \alpha_{11}^2 \alpha_{12}^2 - 7 \alpha_{12}^4) \right) + \right. \\ & \left. 3 \beta_2^2 E_2 \left(2 a_0 (\alpha_{11}^2 - \alpha_{12}^2) + (\alpha_{11}^2 + \alpha_{12}^2)^2 (-1 + d_1 h_a (\alpha_{11}^2 + \alpha_{12}^2)^2) \right) \right) / \\ & \left(\beta_2 E_2 \left(9 \beta_2^2 d_1^2 (\alpha_{11}^2 + \alpha_{12}^2)^4 + \beta_1^4 E_1^2 h_a^2 \left(a_0^2 - 2 a_0 (\alpha_{11}^2 - \alpha_{12}^2) + (\alpha_{11}^2 + \alpha_{12}^2)^2 \right) - \right. \right. \\ & \left. \left. 6 \beta_1^2 \beta_2 d_1 E_1 h_a \left((-\alpha_{11}^2 + \alpha_{12}^2) (\alpha_{11}^2 + \alpha_{12}^2)^2 + a_0 (\alpha_{11}^4 - 6 \alpha_{11}^2 \alpha_{12}^2 + \alpha_{12}^4) \right) \right) \right); \\ s_{a5} = & \frac{1}{h_a} \left(E_0 \left(1 - \left(\beta_1^2 E_1 \left(9 \beta_2 d_1^2 (\alpha_{11}^2 + \alpha_{12}^2)^4 - \right. \right. \right. \right. \\ & \left. \left. \left. 3 \beta_1^2 d_1 E_1 h_a \left((-\alpha_{11}^2 + \alpha_{12}^2) (\alpha_{11}^2 + \alpha_{12}^2)^2 + a_0 (\alpha_{11}^4 - 6 \alpha_{11}^2 \alpha_{12}^2 + \alpha_{12}^4) \right) + \right. \right. \right. \\ & \left. \left. \left. \beta_1^2 \beta_2 E_1 E_2 h_a^2 \left((\alpha_{11}^2 + \alpha_{12}^2)^2 (1 + d_1 h_a (\alpha_{11}^4 - 6 \alpha_{11}^2 \alpha_{12}^2 + \alpha_{12}^4)) + a_0^2 \right. \right. \right. \\ & \left. \left. \left. (1 + 4 d_1 h_a (\alpha_{11}^4 - 6 \alpha_{11}^2 \alpha_{12}^2 + \alpha_{12}^4)) - a_0 (\alpha_{11}^2 - \alpha_{12}^2) \right. \right. \right. \\ & \left. \left. \left. (2 + d_1 h_a (5 \alpha_{11}^4 - 6 \alpha_{11}^2 \alpha_{12}^2 + 5 \alpha_{12}^4)) \right) \right) - \right. \\ & \left. 3 \beta_2^2 d_1 E_2 h_a \left((-\alpha_{11}^2 + \alpha_{12}^2) (\alpha_{11}^2 + \alpha_{12}^2)^2 (1 + d_1 h_a (\alpha_{11}^2 + \alpha_{12}^2)^2) + a_0 \right. \right. \\ & \left. \left. (4 d_1 h_a \alpha_{11}^8 + 16 d_1 h_a \alpha_{11}^6 \alpha_{12}^2 + \alpha_{12}^4 + 4 d_1 h_a \alpha_{12}^8 + \right. \right. \\ & \left. \left. \left. \alpha_{11}^4 (1 + 24 d_1 h_a \alpha_{12}^4) + \alpha_{11}^2 (-6 \alpha_{12}^2 + 16 d_1 h_a \alpha_{12}^6) \right) \right) \right) / \\ & \left(\beta_2 E_2 \left(9 \beta_2^2 d_1^2 (\alpha_{11}^2 + \alpha_{12}^2)^4 + \beta_1^4 E_1^2 h_a^2 \left(a_0^2 - 2 a_0 (\alpha_{11}^2 - \alpha_{12}^2) + \right. \right. \right. \\ & \left. \left. \left. (\alpha_{11}^2 + \alpha_{12}^2)^2 \right) - 6 \beta_1^2 \beta_2 d_1 E_1 h_a \left((-\alpha_{11}^2 + \alpha_{12}^2) (\alpha_{11}^2 + \alpha_{12}^2)^2 + a_0 \right. \right. \right. \\ & \left. \left. \left. (\alpha_{11}^4 - 6 \alpha_{11}^2 \alpha_{12}^2 + \alpha_{12}^4) \right) \right) \right); \end{aligned}$$

$$\begin{aligned}
s_{s10} &= \frac{-C_{ai1} a_0 + C_{aai1} a_0}{a_0^2 h_a} ; \\
s_{s8} &= (\beta_1 \alpha^3 (3 \beta_2 d_1 E_2 \alpha^4 + \beta_1^2 E_1 E_2 h_a (-a_0 + \alpha^2) + \\
&\quad \beta_1 E_1 (3 d_1 \alpha^4 + \beta_2 E_2 h_a (-a_0 + \alpha^2 - 4 a_0 d_1 h_a \alpha^4 + d_1 h_a \alpha^6))) / \\
&\quad (2 E_2 (-a_0 + \alpha^2) (3 \beta_2 d_1 \alpha^4 + \beta_1^2 E_1 h_a (-a_0 + \alpha^2))) ; \\
s_{s9} &= \frac{1}{2 \beta_2 E_2 h_a} \left(\beta_1 \left((\alpha_{12} (-3 \beta_1^2 \beta_2 d_1 E_1 (-3 \alpha_{11}^2 + \alpha_{12}^2) (\alpha_{11}^2 + \alpha_{12}^2) + \right. \right. \\
&\quad 3 \beta_2^3 d_1 E_2 (\alpha_{11}^2 + \alpha_{12}^2) (4 d_1 h_a \alpha_{11}^6 + \alpha_{12}^2 + 12 d_1 h_a \alpha_{11}^4 \alpha_{12}^2 + 4 \\
&\quad d_1 h_a \alpha_{12}^6 + 3 \alpha_{11}^2 (-1 + 4 d_1 h_a \alpha_{12}^4)) + \\
&\quad \beta_1^4 E_1^2 h_a (a_0 (1 + \beta_2 E_2 h_a^2 (-3 \alpha_{11}^2 + \alpha_{12}^2)) + (\alpha_{11}^2 + \alpha_{12}^2) \\
&\quad (1 + \beta_2 E_2 h_a^2 (\alpha_{11}^2 + \alpha_{12}^2))) - \\
&\quad \beta_1^2 \beta_2^2 E_1 E_2 h_a (- (\alpha_{11}^2 + \alpha_{12}^2) (-1 + d_1 h_a (9 \alpha_{11}^4 + 2 \alpha_{11}^2 \alpha_{12}^2 - 7 \alpha_{12}^4)) + \\
&\quad a_0 (1 + 4 d_1 h_a (5 \alpha_{11}^4 - 10.0 \alpha_{11}^2 \alpha_{12}^2 + \alpha_{12}^4))) \Big) / \\
&\quad \left(9 \beta_2^2 d_1^2 (\alpha_{11}^2 + \alpha_{12}^2)^4 + \beta_1^4 E_1^2 h_a^2 (a_0^2 - 2 a_0 (\alpha_{11}^2 - \alpha_{12}^2) + (\alpha_{11}^2 + \alpha_{12}^2)^2) - \right. \\
&\quad 6 \beta_1^2 \beta_2 d_1 E_1 h_a \left((-\alpha_{11}^2 + \alpha_{12}^2) (\alpha_{11}^2 + \alpha_{12}^2)^2 + a_0 (\alpha_{11}^4 - 6 \alpha_{11}^2 \alpha_{12}^2 + \alpha_{12}^4) \right) \Big) - \\
&\quad \left(\alpha_{12} (a_0 + \alpha_{11}^2 + \alpha_{12}^2) + \left(2 \beta_2 d_1 h_a \alpha_{11}^2 \alpha_{12} (-a_0 + \alpha_{11}^2 + \alpha_{12}^2 + \beta_1 E_1 h_a^2 \right. \right. \\
&\quad \left. \left. (a_0 (\alpha_{11}^2 - 3 \alpha_{12}^2) - (\alpha_{11}^2 + \alpha_{12}^2)^2) \right) \right) \left(3 \beta_1^2 E_1 (-2 a_0 (\alpha_{11}^2 - \alpha_{12}^2) + (\alpha_{11}^2 + \alpha_{12}^2)^2) + \right. \\
&\quad \left. \beta_1^2 \beta_2 E_1 E_2 h_a^2 (8 a_0^2 (\alpha_{11}^2 - \alpha_{12}^2) + 2 (\alpha_{11}^2 - \alpha_{12}^2) (\alpha_{11}^2 + \alpha_{12}^2)^2 + \right. \\
&\quad \left. a_0 (-7 \alpha_{11}^4 + 2 \alpha_{11}^2 \alpha_{12}^2 - 7 \alpha_{12}^4) \right) + 3 \beta_2^2 E_2 \\
&\quad \left. \left(2 a_0 (\alpha_{11}^2 - \alpha_{12}^2) + (\alpha_{11}^2 + \alpha_{12}^2)^2 (-1 + d_1 h_a (\alpha_{11}^2 + \alpha_{12}^2)^2) \right) \right) / \\
&\quad \left(9 \beta_2^2 d_1^2 (\alpha_{11}^2 + \alpha_{12}^2)^4 + \beta_1^4 E_1^2 h_a^2 (a_0^2 - 2 a_0 (\alpha_{11}^2 - \alpha_{12}^2) + (\alpha_{11}^2 + \alpha_{12}^2)^2) - \right. \\
&\quad 6 \beta_1^2 \beta_2 d_1 E_1 h_a \left((-\alpha_{11}^2 + \alpha_{12}^2) (\alpha_{11}^2 + \alpha_{12}^2)^2 + \right. \\
&\quad \left. a_0 (\alpha_{11}^4 - 6 \alpha_{11}^2 \alpha_{12}^2 + \alpha_{12}^4) \right) \Big) + \left((-\beta_2^2 E_2 \alpha_{12} (a_0 + \alpha_{11}^2 + \alpha_{12}^2) - \beta_1 \beta_2^2 E_1 E_2 h_a^2 \alpha_{12} \right. \\
&\quad \left. (a_0 (-3 \alpha_{11}^2 + \alpha_{12}^2) + (\alpha_{11}^2 + \alpha_{12}^2)^2) \right) \left(9 \beta_2 d_1^2 (\alpha_{11}^2 + \alpha_{12}^2)^4 - 3 \beta_1^2 d_1 E_1 h_a \right. \\
&\quad \left. \left((-\alpha_{11}^2 + \alpha_{12}^2) (\alpha_{11}^2 + \alpha_{12}^2)^2 + a_0 (\alpha_{11}^4 - 6 \alpha_{11}^2 \alpha_{12}^2 + \alpha_{12}^4) \right) + \beta_1^2 \right. \\
&\quad \left. \beta_2 E_1 E_2 h_a^2 \left((\alpha_{11}^2 + \alpha_{12}^2)^2 (1 + d_1 h_a (\alpha_{11}^4 - 6 \alpha_{11}^2 \alpha_{12}^2 + \alpha_{12}^4)) + \right. \right. \\
&\quad \left. \left. a_0^2 (1 + 4 d_1 h_a (\alpha_{11}^4 - 6 \alpha_{11}^2 \alpha_{12}^2 + \alpha_{12}^4)) - \right. \right. \\
&\quad \left. \left. a_0 (\alpha_{11}^2 - \alpha_{12}^2) (2 + d_1 h_a (5 \alpha_{11}^4 - 6 \alpha_{11}^2 \alpha_{12}^2 + 5 \alpha_{12}^4)) \right) \right) - 3 \\
&\quad \left. \beta_2^2 d_1 E_2 h_a \left((-\alpha_{11}^2 + \alpha_{12}^2) (\alpha_{11}^2 + \alpha_{12}^2)^2 (1 + d_1 h_a (\alpha_{11}^2 + \alpha_{12}^2)^2) + \right. \right. \\
&\quad \left. \left. a_0 (4 d_1 h_a \alpha_{11}^8 + 16 d_1 h_a \alpha_{11}^6 \alpha_{12}^2 + \alpha_{12}^4 + 4 d_1 h_a \alpha_{12}^8 + \right. \right. \\
&\quad \left. \left. \alpha_{11}^4 (1 + 24 d_1 h_a \alpha_{12}^4) + \alpha_{11}^2 (-6 \alpha_{12}^2 + 16 d_1 h_a \alpha_{12}^6) \right) \right) \Big) / \\
&\quad \left(\beta_2 E_2 \left(9 \beta_2^2 d_1^2 (\alpha_{11}^2 + \alpha_{12}^2)^4 + \beta_1^4 E_1^2 h_a^2 \right. \right. \\
&\quad \left. \left. (a_0^2 - 2 a_0 (\alpha_{11}^2 - \alpha_{12}^2) + (\alpha_{11}^2 + \alpha_{12}^2)^2) - 6 \beta_1^2 \beta_2 d_1 E_1 h_a \right. \right. \\
&\quad \left. \left. \left((-\alpha_{11}^2 + \alpha_{12}^2) (\alpha_{11}^2 + \alpha_{12}^2)^2 + a_0 (\alpha_{11}^4 - 6 \alpha_{11}^2 \alpha_{12}^2 + \alpha_{12}^4) \right) \right) \right) / \\
&\quad \left(h_a (a_0^2 - 2 a_0 (\alpha_{11}^2 - \alpha_{12}^2) + (\alpha_{11}^2 + \alpha_{12}^2)^2) \right) ;
\end{aligned} \tag{B.3}$$

$$\begin{aligned}
s_{s10} = & \frac{+}{2 \beta_2 E_2 h_a} \left(\beta_1 \left((-3 \beta_1^2 \beta_2 d_1 E_1 (\alpha_{11}^2 + \alpha_{12}^2) (\alpha_{11}^3 - 3 \alpha_{11} \alpha_{12}^2) + \right. \right. \\
& 3 \beta_2^3 d_1 E_2 \alpha_{11} (\alpha_{11}^2 + \alpha_{12}^2) (\alpha_{11}^2 + 4 d_1 h_a \alpha_{11}^6 - 3 \alpha_{12}^2 + 12 d_1 h_a \alpha_{11}^4 \alpha_{12}^2 + \\
& 12 d_1 h_a \alpha_{11}^2 \alpha_{12}^4 + 4 d_1 h_a \alpha_{12}^6) + \beta_1^4 E_1^2 h_a \alpha_{11} (a_0 (1 - \beta_2 E_2 h_a^2 (\alpha_{11}^2 - 3 \alpha_{12}^2)) + \\
& (\alpha_{11}^2 + \alpha_{12}^2) (-1 + \beta_2 E_2 h_a^2 (\alpha_{11}^2 + \alpha_{12}^2))) + \\
& \beta_1^2 \beta_2^2 E_1 E_2 h_a \alpha_{11} ((\alpha_{11}^2 + \alpha_{12}^2) (1 + d_1 h_a (7 \alpha_{11}^4 - 2 \alpha_{11}^2 \alpha_{12}^2 - 9 \alpha_{12}^4)) - \\
& a_0 (1 + 4 d_1 h_a (\alpha_{11}^4 - 10.0 \alpha_{11}^2 \alpha_{12}^2 + 5 \alpha_{12}^4))) \Big) / \\
& \left(9 \beta_2^2 d_1^2 (\alpha_{11}^2 + \alpha_{12}^2)^4 + \beta_1^4 E_1^2 h_a^2 (a_0^2 - 2 a_0 (\alpha_{11}^2 - \alpha_{12}^2) + (\alpha_{11}^2 + \alpha_{12}^2)^2) - \right. \\
& 6 \beta_1^2 \beta_2 d_1 E_1 h_a \left((-\alpha_{11}^2 + \alpha_{12}^2) (\alpha_{11}^2 + \alpha_{12}^2)^2 + a_0 (\alpha_{11}^4 - 6 \alpha_{11}^2 \alpha_{12}^2 + \alpha_{12}^4) \right) \Big) - \\
& \left(\alpha_{11} (a_0 - \alpha_{11}^2 - \alpha_{12}^2 + (2 d_1 h_a \alpha_{12} (-\beta_2^2 E_2 \alpha_{12} (a_0 + \alpha_{11}^2 + \alpha_{12}^2) - \beta_1 \beta_2^2 E_1 E_2 h_a^2 \alpha_{12} \right. \\
& (a_0 (-3 \alpha_{11}^2 + \alpha_{12}^2) + (\alpha_{11}^2 + \alpha_{12}^2)^2)) (-3 \beta_1^2 E_1 (-2 a_0 (\alpha_{11}^2 - \alpha_{12}^2) + (\alpha_{11}^2 + \alpha_{12}^2)^2) \\
& \beta_1^2 \beta_2 E_1 E_2 h_a^2 (-8 a_0^2 (\alpha_{11}^2 - \alpha_{12}^2) - 2 (\alpha_{11}^2 - \alpha_{12}^2) (\alpha_{11}^2 + \alpha_{12}^2)^2 + \\
& a_0 (7 \alpha_{11}^4 - 2 \alpha_{11}^2 \alpha_{12}^2 + 7 \alpha_{12}^4)) - 3 \beta_2^2 E_2 (2 a_0 (\alpha_{11}^2 - \alpha_{12}^2) + (\alpha_{11}^2 + \alpha_{12}^2)^2 \\
& (-1 + d_1 h_a (\alpha_{11}^2 + \alpha_{12}^2)^2)) \Big) \Big) / \left(\beta_2 E_2 (9 \beta_2^2 d_1^2 (\alpha_{11}^2 + \alpha_{12}^2)^4 + \beta_1^4 E_1^2 h_a^2 \right. \\
& (a_0^2 - 2 a_0 (\alpha_{11}^2 - \alpha_{12}^2) + (\alpha_{11}^2 + \alpha_{12}^2)^2) - 6 \beta_1^2 \beta_2 d_1 E_1 h_a \\
& \left. \left((-\alpha_{11}^2 + \alpha_{12}^2) (\alpha_{11}^2 + \alpha_{12}^2)^2 + a_0 (\alpha_{11}^4 - 6 \alpha_{11}^2 \alpha_{12}^2 + \alpha_{12}^4) \right) \right) \Big) + \\
& \left(\beta_2 (-a_0 + \alpha_{11}^2 + \alpha_{12}^2 + \beta_1 E_1 h_a^2 (a_0 (\alpha_{11}^2 - 3 \alpha_{12}^2) - (\alpha_{11}^2 + \alpha_{12}^2)^2)) \right. \\
& \left. \left(9 \beta_2 d_1^2 (\alpha_{11}^2 + \alpha_{12}^2)^4 - 3 \beta_1^2 d_1 E_1 h_a \right. \right. \\
& \left. \left. \left((-\alpha_{11}^2 + \alpha_{12}^2) (\alpha_{11}^2 + \alpha_{12}^2)^2 + a_0 (\alpha_{11}^4 - 6 \alpha_{11}^2 \alpha_{12}^2 + \alpha_{12}^4) \right) \right) + \right. \\
& \left. \beta_1^2 \beta_2 E_1 E_2 h_a^2 \left((\alpha_{11}^2 + \alpha_{12}^2)^2 (1 + d_1 h_a (\alpha_{11}^4 - 6 \alpha_{11}^2 \alpha_{12}^2 + \alpha_{12}^4)) + \right. \right. \\
& \left. \left. a_0^2 (1 + 4 d_1 h_a (\alpha_{11}^4 - 6 \alpha_{11}^2 \alpha_{12}^2 + \alpha_{12}^4)) - \right. \right. \\
& \left. \left. a_0 (\alpha_{11}^2 - \alpha_{12}^2) (2 + d_1 h_a (5 \alpha_{11}^4 - 6 \alpha_{11}^2 \alpha_{12}^2 + 5 \alpha_{12}^4)) \right) \right) - \\
& 3 \beta_2^2 d_1 E_2 h_a \left((-\alpha_{11}^2 + \alpha_{12}^2) (\alpha_{11}^2 + \alpha_{12}^2)^2 \left(1 + d_1 h_a (\alpha_{11}^2 + \alpha_{12}^2)^2 \right) + \right. \\
& \left. a_0 (4 d_1 h_a \alpha_{11}^8 + 16 d_1 h_a \alpha_{11}^6 \alpha_{12}^2 + \alpha_{12}^4 + 4 d_1 h_a \alpha_{12}^8 + \right. \\
& \left. \left. \alpha_{11}^4 (1 + 24 d_1 h_a \alpha_{12}^4) + \alpha_{11}^2 (-6 \alpha_{12}^2 + 16 d_1 h_a \alpha_{12}^6) \right) \right) \Big) \Big) / \\
& \left(9 \beta_2^2 d_1^2 (\alpha_{11}^2 + \alpha_{12}^2)^4 + \beta_1^4 E_1^2 h_a^2 (a_0^2 - 2 a_0 (\alpha_{11}^2 - \alpha_{12}^2) + (\alpha_{11}^2 + \alpha_{12}^2)^2) - \right. \\
& \left. 6 \beta_1^2 \beta_2 d_1 E_1 h_a \left((-\alpha_{11}^2 + \alpha_{12}^2) (\alpha_{11}^2 + \alpha_{12}^2)^2 + a_0 (\alpha_{11}^4 - 6 \alpha_{11}^2 \alpha_{12}^2 + \alpha_{12}^4) \right) \right) \Big) \Big) / \\
& \left. \left(h_a (a_0^2 - 2 a_0 (\alpha_{11}^2 - \alpha_{12}^2) + (\alpha_{11}^2 + \alpha_{12}^2)^2) \right) \right); \tag{B.4}
\end{aligned}$$

The equations of shear force for the adhesive layer are expressed in the followings.

$$\begin{aligned}
\bar{Q}_a = & \frac{\tau_a h_a}{P} = \frac{G_a}{P} (f_{a10} + f_{a8} (c_{i6} \bar{S} h + c_{i7} \bar{C} h) + c_{i8} (-f_{a10} \bar{C} h_1 \bar{S} + f_{a9} \bar{S} h_1 \bar{C}) + \\
& c_{i9} (f_{a10} \bar{C} h_1 \bar{C} + f_{a9} \bar{S} h_1 \bar{S}) + c_{i10} (f_{a9} \bar{C} h_1 \bar{C} - f_{a10} \bar{S} h_1 \bar{S}) + c_{i11} (f_{a9} \bar{C} h_1 \bar{S} + f_{a10} \bar{S} h_1 \bar{C})) \tag{B.5}
\end{aligned}$$

where

$$f_{a10} = s_{s10} h_a, \tag{B.6}$$

$$f_{a8} = s_{s8} h_a, \tag{B.7}$$

$$f_{a9} = s_{s9} h_a, \tag{B.8}$$

$$f_{a10} = s_{s10} h_a. \tag{B.9}$$

Appendix C

The coefficients of moment and of shear force for the upper adherend, the adhesive layer and the lower adherend are shown as follows.

The equations of the moment for the upper adherend and for lower adherend are expressed in the followings.

$$\begin{aligned} \overline{M}_i = \frac{G_a}{2Pc} & (c_{i2}m_{u0} + 3c_{i3}m_{u0}x + m_{u5}(c_{i6}\overline{Ch} + c_{i7}\overline{Sh}) + c_{i8}(m_{u7}\overline{Ch}_1\overline{C} - m_{u6}\overline{Sh}_1\overline{S}) + \\ & c_{i9}(m_{u7}\overline{Ch}_1\overline{S} + m_{u6}\overline{Sh}_1\overline{C}) + c_{i10}(-m_{u6}\overline{Ch}_1\overline{S} + m_{u7}\overline{Sh}_1\overline{C}) + c_{i11}(m_{u6}\overline{Ch}_1\overline{C} + m_{u7}\overline{Sh}_1\overline{S})) \end{aligned} \quad (C.1)$$

$$\begin{aligned} \overline{M}_{ix} = \frac{G_a}{2Pc} & (c_{i2}m_{b0} + 3c_{i3}m_{b0}x + m_{b5}(c_{i6}\overline{Ch} + c_{i7}\overline{Sh}) + c_{i8}(m_{b7}\overline{Ch}_1\overline{C} - m_{b6}\overline{Sh}_1\overline{S}) + \\ & c_{i9}(m_{b7}\overline{Ch}_1\overline{S} + m_{b6}\overline{Sh}_1\overline{C}) + c_{i10}(-m_{b6}\overline{Ch}_1\overline{S} + m_{b7}\overline{Sh}_1\overline{C}) + c_{i11}(m_{b6}\overline{Ch}_1\overline{C} + m_{b7}\overline{Sh}_1\overline{S})) \end{aligned} \quad (C.2)$$

Their coefficients are

$$\begin{aligned} m_{u0} &= \frac{1}{6} \beta_1^3 E_1 h_a^3; \\ m_{u5} &= \frac{1}{12} \beta_1^3 E_1 h_a^3 \alpha^2; \\ m_{u6} &= \frac{1}{6} \beta_1^3 E_1 h_a^3 \alpha_{11} \alpha_{12}; \\ m_{u7} &= \frac{1}{12} \beta_1^3 E_1 h_a^3 (\alpha_{11}^2 - \alpha_{12}^2); \\ m_{b0} &= \frac{1}{6} \beta_2^3 E_2 h_a^3; \\ m_{b5} &= (\beta_1^2 \beta_2^2 E_1 E_2 h_a^3 \alpha^2 (3 d_1 \alpha^4 + \beta_2 E_2 h_a (\alpha^2 + d_1 h_a \alpha^6 - a_0 (1 + 4 d_1 h_a \alpha^4))) / \\ & (12 E_2 (3 \beta_2 d_1 \alpha^4 + \beta_1^2 E_1 h_a (-a_0 + \alpha^2)))); \end{aligned} \quad (C.3)$$

$$\begin{aligned}
m_{b6} = & \left(\beta_1^2 \beta_2^2 E_1 E_2 h_a^3 \left(18 \beta_2 d_1^2 \alpha_{11} \alpha_{12} (\alpha_{11}^2 + \alpha_{12}^2)^4 - 6 \beta_1^2 d_1 E_1 h_a \alpha_{11} \alpha_{12} \right. \right. \\
& \left. \left. (-2 (\alpha_{11}^2 - \alpha_{12}^2) (\alpha_{11}^2 + \alpha_{12}^2)^2 + a_0 (3 \alpha_{11}^4 - 10.0 \alpha_{11}^2 \alpha_{12}^2 + 3 \alpha_{12}^4)) \right) - \right. \\
& 6 \beta_2^2 d_1 E_2 h_a \alpha_{11} \alpha_{12} (\alpha_{11}^2 + \alpha_{12}^2)^2 \left(-2 d_1 h_a (\alpha_{11}^2 - \alpha_{12}^2) (\alpha_{11}^2 + \alpha_{12}^2)^2 + \right. \\
& \left. a_0 (-1 + 4 d_1 h_a (\alpha_{11}^2 + \alpha_{12}^2)^2) \right) + 2 \beta_1^2 \beta_2 E_1 E_2 h_a^2 \alpha_{11} \alpha_{12} \\
& \left((\alpha_{11}^2 + \alpha_{12}^2)^2 (1 + d_1 h_a (3 \alpha_{11}^4 - 10.0 \alpha_{11}^2 \alpha_{12}^2 + 3 \alpha_{12}^4)) + \right. \\
& \left. a_0^2 (1 + 4 d_1 h_a (3 \alpha_{11}^4 - 10.0 \alpha_{11}^2 \alpha_{12}^2 + 3 \alpha_{12}^4)) - \right. \\
& \left. 2 a_0 (\alpha_{11}^2 - \alpha_{12}^2) (1 + 2 d_1 h_a (3 \alpha_{11}^4 - 2 \alpha_{11}^2 \alpha_{12}^2 + 3 \alpha_{12}^4)) \right) \Big) / \\
& \left(12 E_2 \left(9 \beta_2^2 d_1^2 (\alpha_{11}^2 + \alpha_{12}^2)^4 + \beta_1^4 E_1^2 h_a^2 (a_0^2 - 2 a_0 (\alpha_{11}^2 - \alpha_{12}^2) + (\alpha_{11}^2 + \alpha_{12}^2)^2) - \right. \right. \\
& \left. \left. 6 \beta_1^2 \beta_2 d_1 E_1 h_a (- (\alpha_{11}^2 - \alpha_{12}^2) (\alpha_{11}^2 + \alpha_{12}^2)^2 + a_0 (\alpha_{11}^4 - 6 \alpha_{11}^2 \alpha_{12}^2 + \alpha_{12}^4)) \right) \right); \\
m_{b7} = & \left(\beta_1^2 \beta_2^2 E_1 E_2 h_a^3 \left(9 \beta_2 d_1^2 (\alpha_{11}^2 - \alpha_{12}^2) (\alpha_{11}^2 + \alpha_{12}^2)^4 - 3 \beta_1^2 d_1 E_1 h_a (- (\alpha_{11}^2 + \alpha_{12}^2)^2 \right. \right. \\
& \left. \left. (\alpha_{11}^4 - 6 \alpha_{11}^2 \alpha_{12}^2 + \alpha_{12}^4) + a_0 (\alpha_{11}^6 - 15 \alpha_{11}^4 \alpha_{12}^2 + 15 \alpha_{11}^2 \alpha_{12}^4 - \alpha_{12}^6) \right) + \right. \\
& 3 \beta_2^2 d_1 E_2 h_a (\alpha_{11}^2 + \alpha_{12}^2)^2 \left(-a_0 (\alpha_{11}^2 - \alpha_{12}^2) (1 + 4 d_1 h_a (\alpha_{11}^2 + \alpha_{12}^2)^2) + \right. \\
& \left. (\alpha_{11}^2 + \alpha_{12}^2)^2 (1 + d_1 h_a (\alpha_{11}^4 - 6 \alpha_{11}^2 \alpha_{12}^2 + \alpha_{12}^4)) \right) + \\
& \beta_1^2 \beta_2 E_1 E_2 h_a^2 \left((\alpha_{11}^2 - \alpha_{12}^2) (\alpha_{11}^2 + \alpha_{12}^2)^2 (1 + d_1 h_a (\alpha_{11}^4 - 14 \alpha_{11}^2 \alpha_{12}^2 + \alpha_{12}^4)) + \right. \\
& \left. a_0^2 (\alpha_{11}^2 - \alpha_{12}^2) (1 + 4 d_1 h_a (\alpha_{11}^4 - 14 \alpha_{11}^2 \alpha_{12}^2 + \alpha_{12}^4)) - \right. \\
& \left. a_0 (5 d_1 h_a \alpha_{11}^8 - 44 d_1 h_a \alpha_{11}^6 \alpha_{12}^2 + \alpha_{12}^4 (2 + 5 d_1 h_a \alpha_{12}^4) + \right. \\
& \left. \alpha_{11}^4 (2 + 30.0 d_1 h_a \alpha_{12}^4) - 4 \alpha_{11}^2 (\alpha_{12}^2 + 11 d_1 h_a \alpha_{12}^6)) \right) \Big) / \\
& \left(12 E_2 \left(9 \beta_2^2 d_1^2 (\alpha_{11}^2 + \alpha_{12}^2)^4 + \beta_1^4 E_1^2 h_a^2 (a_0^2 - 2 a_0 (\alpha_{11}^2 - \alpha_{12}^2) + (\alpha_{11}^2 + \alpha_{12}^2)^2) - \right. \right. \\
& \left. \left. 6 \beta_1^2 \beta_2 d_1 E_1 h_a (- (\alpha_{11}^2 - \alpha_{12}^2) (\alpha_{11}^2 + \alpha_{12}^2)^2 + a_0 (\alpha_{11}^4 - 6 \alpha_{11}^2 \alpha_{12}^2 + \alpha_{12}^4)) \right) \right); \tag{C.4}
\end{aligned}$$

The equations of longitudinal force for the upper adherend and for the lower adherend are expressed in the followings.

$$\begin{aligned}
\bar{N}_i = & \frac{G_a}{P} (n_{u0} + c_{i2} n_{u1} + c_{i3} n_{u3} x + n_{u7} (c_{i6} \bar{Ch} + c_{i7} \bar{Sh}) + c_{i8} (n_{u9} \bar{Ch}_1 \bar{C} - n_{u8} \bar{Sh}_1 \bar{S}) + \\
& c_{i9} (n_{u9} \bar{Ch}_1 \bar{S} + n_{u8} \bar{Sh}_1 \bar{C}) + c_{i10} (-n_{u8} \bar{Ch}_1 \bar{S} + n_{u9} \bar{Sh}_1 \bar{C}) + c_{i11} (n_{u8} \bar{Ch}_1 \bar{C} + n_{u9} \bar{Sh}_1 \bar{S})) \tag{C.5}
\end{aligned}$$

$$\begin{aligned}
\bar{N}_{ix} = & \frac{G_a}{P} (n_{b0} + c_{i2} n_{b1} + c_{i3} n_{b3} x + n_{b7} (c_{i6} \bar{Ch} + c_{i7} \bar{Sh}) + c_{i8} (n_{b9} \bar{Ch}_1 \bar{C} - n_{b8} \bar{Sh}_1 \bar{S}) + \\
& c_{i9} (n_{b9} \bar{Ch}_1 \bar{S} + n_{b8} \bar{Sh}_1 \bar{C}) + c_{i10} (-n_{b8} \bar{Ch}_1 \bar{S} + n_{b9} \bar{Sh}_1 \bar{C}) + c_{i11} (n_{b8} \bar{Ch}_1 \bar{C} + n_{b9} \bar{Sh}_1 \bar{S})) \tag{C.6}
\end{aligned}$$

Their coefficients are obtained as shown.

$$\begin{aligned}
n_{ui0} &= -\frac{c_{ai2} \beta_1 E_1 h_a}{a_0}; \\
n_{u1} &= -\beta_1^2 E_1 h_a^2; \\
n_{u3} &= -\frac{3 E_1 (\beta_2^2 E_2 + \beta_1^2 E_1 (-1 + \beta_2 a_0 E_2 h_a^2))}{\beta_2 a_0 E_1 E_2}; \\
n_{u7} &= (\beta_1^2 E_1 h_a \alpha^2 (\beta_1^2 E_1 (-1 + \beta_2 a_0 E_2 h_a^2) + \beta_2^2 E_2 (1 + d_1 h_a \alpha^4))) / \\
&\quad (2 \beta_2 E_2 (3 \beta_2 d_1 \alpha^4 + \beta_1^2 E_1 h_a (-a_0 + \alpha^2))); \\
n_{u8} &= (\beta_1^2 E_1 h_a (-2 \beta_1^4 a_0 E_1^2 h_a (-1 + \beta_2 a_0 E_2 h_a^2) \alpha_{11} \alpha_{12} + 6 \beta_1^2 \beta_2 d_1 E_1 \alpha_{11} \alpha_{12} \\
&\quad (\alpha_{11}^2 + \alpha_{12}^2)^2 + 6 \beta_2^3 d_1 E_2 \alpha_{11} \alpha_{12} (\alpha_{11}^2 + \alpha_{12}^2)^2 (-1 + d_1 h_a (\alpha_{11}^2 + \alpha_{12}^2)^2) - \\
&\quad 2 \beta_1^2 \beta_2^2 E_1 E_2 h_a \alpha_{11} \alpha_{12} (-2 d_1 h_a (\alpha_{11}^2 - \alpha_{12}^2) (\alpha_{11}^2 + \alpha_{12}^2)^2 + \\
&\quad a_0 (1 + 2 d_1 h_a (3 \alpha_{11}^4 - 2 \alpha_{11}^2 \alpha_{12}^2 + 3 \alpha_{12}^4)))) / \\
&\quad (2 \beta_2 E_2 (9 \beta_2^2 d_1^2 (\alpha_{11}^2 + \alpha_{12}^2)^4 + \beta_1^4 E_1^2 h_a^2 (a_0^2 - 2 a_0 (\alpha_{11}^2 - \alpha_{12}^2) + (\alpha_{11}^2 + \alpha_{12}^2)^2) - \\
&\quad 6 \beta_1^2 \beta_2 d_1 E_1 h_a (- (\alpha_{11}^2 - \alpha_{12}^2) (\alpha_{11}^2 + \alpha_{12}^2)^2 + a_0 (\alpha_{11}^4 - 6 \alpha_{11}^2 \alpha_{12}^2 + \alpha_{12}^4))))); \\
n_{u9} &= (\beta_1^2 E_1 h_a (-3 \beta_1^2 \beta_2 d_1 E_1 (\alpha_{11}^2 - \alpha_{12}^2) (\alpha_{11}^2 + \alpha_{12}^2)^2 - \\
&\quad \beta_1^4 E_1^2 h_a (-1 + \beta_2 a_0 E_2 h_a^2) (a_0 (\alpha_{11}^2 - \alpha_{12}^2) - (\alpha_{11}^2 + \alpha_{12}^2)^2) + \\
&\quad 3 \beta_2^3 d_1 E_2 (\alpha_{11}^2 - \alpha_{12}^2) (\alpha_{11}^2 + \alpha_{12}^2)^2 (1 + d_1 h_a (\alpha_{11}^2 + \alpha_{12}^2)^2) + \\
&\quad \beta_1^2 \beta_2^2 E_1 E_2 h_a ((\alpha_{11}^2 + \alpha_{12}^2)^2 (1 + d_1 h_a (\alpha_{11}^4 - 6 \alpha_{11}^2 \alpha_{12}^2 + \alpha_{12}^4)) + \\
&\quad a_0 (\alpha_{11}^2 - \alpha_{12}^2) (-1 + 2 d_1 h_a (\alpha_{11}^4 + 10.0 \alpha_{11}^2 \alpha_{12}^2 + \alpha_{12}^4)))) / \\
&\quad (2 \beta_2 E_2 (9 \beta_2^2 d_1^2 (\alpha_{11}^2 + \alpha_{12}^2)^4 + \beta_1^4 E_1^2 h_a^2 (a_0^2 - 2 a_0 (\alpha_{11}^2 - \alpha_{12}^2) + (\alpha_{11}^2 + \alpha_{12}^2)^2) - \\
&\quad 6 \beta_1^2 \beta_2 d_1 E_1 h_a (- (\alpha_{11}^2 - \alpha_{12}^2) (\alpha_{11}^2 + \alpha_{12}^2)^2 + a_0 (\alpha_{11}^4 - 6 \alpha_{11}^2 \alpha_{12}^2 + \alpha_{12}^4))))); \\
n_{bi0} &= -\frac{c_{ai2} \beta_2 E_2 h_a}{a_0}; \\
n_{b1} &= \beta_2^2 E_2 h_a^2; \\
n_{b2} &= \frac{3 E_2 (\beta_1^2 E_1 - \beta_2^2 E_2 + \beta_1 \beta_2^2 a_0 E_1 E_2 h_a^2)}{\beta_1 a_0 E_1 E_2}; \\
n_{b7} &= (\beta_1 E_2 h_a \alpha^2 (\beta_1^2 E_1 (a_0 - \alpha^2) + \beta_2^2 E_2 (\alpha^2 + d_1 h_a \alpha^6 - a_0 (1 + 4 d_1 h_a \alpha^4)) + \\
&\quad \beta_1 \beta_2 a_0 E_1 h_a (-3 d_1 \alpha^4 + \beta_2 E_2 h_a (a_0 - \alpha^2 + 4 a_0 d_1 h_a \alpha^4 - d_1 h_a \alpha^6)))) / \\
&\quad (2 E_2 (-a_0 + \alpha^2) (3 \beta_2 d_1 \alpha^4 + \beta_1^2 E_1 h_a (-a_0 + \alpha^2)));
\end{aligned} \tag{C.7}$$

$$\begin{aligned}
n_{b8} &= (\beta_1 E_2 h_a (18 \beta_1 \beta_2^2 a_0^2 d_1^2 E_1 h_a \alpha_{11} \alpha_{12} (\alpha_{11}^2 + \alpha_{12}^2)^4 + \\
&\quad 2 \beta_1^4 a_0 E_1^2 h_a \alpha_{11} \alpha_{12} (a_0^2 - 2 a_0 (\alpha_{11}^2 - \alpha_{12}^2) + (\alpha_{11}^2 + \alpha_{12}^2)^2) + \\
&\quad 6 \beta_1^2 \beta_2 d_1 E_1 \alpha_{11} \alpha_{12} (\alpha_{11}^2 + \alpha_{12}^2)^2 (a_0^2 - 2 a_0 (\alpha_{11}^2 - \alpha_{12}^2) + (\alpha_{11}^2 + \alpha_{12}^2)^2) - \\
&\quad 6 \beta_1^3 \beta_2 a_0 d_1 E_1^2 h_a^2 \alpha_{11} \alpha_{12} (-4 a_0 (\alpha_{11}^2 - \alpha_{12}^2) (\alpha_{11}^2 + \alpha_{12}^2)^2 + (\alpha_{11}^2 + \alpha_{12}^2)^4 + \\
&\quad a_0^2 (3 \alpha_{11}^4 - 10 \alpha_{11}^2 \alpha_{12}^2 + 3 \alpha_{12}^4)) + 6 \beta_2^3 d_1 E_2 \alpha_{11} \alpha_{12} (\alpha_{11}^2 + \alpha_{12}^2)^2 \\
&\quad (-2 a_0 (\alpha_{11}^2 - \alpha_{12}^2) (-1 + d_1 h_a (\alpha_{11}^2 + \alpha_{12}^2)^2) + (\alpha_{11}^2 + \alpha_{12}^2)^2 (-1 + d_1 h_a \\
&\quad (\alpha_{11}^2 + \alpha_{12}^2)^2) + a_0^2 (-1 + 4 d_1 h_a (\alpha_{11}^2 + \alpha_{12}^2)^2)) - 6 \beta_1 \beta_2^3 a_0 d_1 E_1 E_2 h_a^2 \alpha_{11} \alpha_{12} \\
&\quad (\alpha_{11}^2 + \alpha_{12}^2)^2 (-2 a_0 (\alpha_{11}^2 - \alpha_{12}^2) (-1 + d_1 h_a (\alpha_{11}^2 + \alpha_{12}^2)^2) + \\
&\quad (\alpha_{11}^2 + \alpha_{12}^2)^2 (-1 + d_1 h_a (\alpha_{11}^2 + \alpha_{12}^2)^2) + a_0^2 (-1 + 4 d_1 h_a (\alpha_{11}^2 + \alpha_{12}^2)^2)) - \\
&\quad 2 \beta_1^2 \beta_2^2 E_1 E_2 h_a \alpha_{11} \alpha_{12} (-2 d_1 h_a (\alpha_{11}^2 - \alpha_{12}^2) (\alpha_{11}^2 + \alpha_{12}^2)^4 + \\
&\quad a_0^3 (1 + 4 d_1 h_a (3 \alpha_{11}^4 - 10 \alpha_{11}^2 \alpha_{12}^2 + 3 \alpha_{12}^4)) + \\
&\quad a_0 (\alpha_{11}^2 + \alpha_{12}^2)^2 (1 + 2 d_1 h_a (5 \alpha_{11}^4 - 6 \alpha_{11}^2 \alpha_{12}^2 + 5 \alpha_{12}^4)) - \\
&\quad 2 a_0^2 (\alpha_{11}^2 - \alpha_{12}^2) (1 + 2 d_1 h_a (5 \alpha_{11}^4 + 2 \alpha_{11}^2 \alpha_{12}^2 + 5 \alpha_{12}^4))) + \\
&\quad 2 \beta_1^3 \beta_2^2 a_0 E_1^2 E_2 h_a^3 \alpha_{11} \alpha_{12} (-2 d_1 h_a (\alpha_{11}^2 - \alpha_{12}^2) (\alpha_{11}^2 + \alpha_{12}^2)^4 + \\
&\quad a_0^3 (1 + 4 d_1 h_a (3 \alpha_{11}^4 - 10 \alpha_{11}^2 \alpha_{12}^2 + 3 \alpha_{12}^4)) + \\
&\quad a_0 (\alpha_{11}^2 + \alpha_{12}^2)^2 (1 + 2 d_1 h_a (5 \alpha_{11}^4 - 6 \alpha_{11}^2 \alpha_{12}^2 + 5 \alpha_{12}^4)) - \\
&\quad 2 a_0^2 (\alpha_{11}^2 - \alpha_{12}^2) (1 + 2 d_1 h_a (5 \alpha_{11}^4 + 2 \alpha_{11}^2 \alpha_{12}^2 + 5 \alpha_{12}^4)))) / \\
&\quad (2 E_2 (a_0^2 - 2 a_0 (\alpha_{11}^2 - \alpha_{12}^2) + (\alpha_{11}^2 + \alpha_{12}^2)^2) \\
&\quad (9 \beta_2^2 d_1^2 (\alpha_{11}^2 + \alpha_{12}^2)^4 + \beta_1^4 E_1^2 h_a^2 (a_0^2 - 2 a_0 (\alpha_{11}^2 - \alpha_{12}^2) + (\alpha_{11}^2 + \alpha_{12}^2)^2) - \\
&\quad 6 \beta_1^2 \beta_2 d_1 E_1 h_a (- (\alpha_{11}^2 - \alpha_{12}^2) (\alpha_{11}^2 + \alpha_{12}^2)^2 + a_0 (\alpha_{11}^4 - 6 \alpha_{11}^2 \alpha_{12}^2 + \alpha_{12}^4)))));
\end{aligned} \tag{C.8}$$

$$\begin{aligned}
n_{b9} = & \left(\beta_1 E_2 h_a \left[-3 \beta_1^2 \beta_2 d_1 E_1 (\alpha_{11}^2 - \alpha_{12}^2) (\alpha_{11}^2 + \alpha_{12}^2)^2 (a_0^2 - 2 a_0 (\alpha_{11}^2 - \alpha_{12}^2) + \right. \right. \\
& (\alpha_{11}^2 + \alpha_{12}^2)^2) + \beta_1^4 E_1^2 h_a \left(a_0 (\alpha_{11}^2 - \alpha_{12}^2) - (\alpha_{11}^2 + \alpha_{12}^2)^2 \right) \\
& \left. \left(a_0^2 - 2 a_0 (\alpha_{11}^2 - \alpha_{12}^2) + (\alpha_{11}^2 + \alpha_{12}^2)^2 \right) - 9 \beta_1 \beta_2^2 a_0 d_1^2 E_1 h_a (\alpha_{11}^2 + \alpha_{12}^2)^4 \right. \\
& \left. \left(a_0 (-\alpha_{11}^2 + \alpha_{12}^2) + (\alpha_{11}^2 + \alpha_{12}^2)^2 \right) - 3 \beta_1^3 \beta_2 a_0 d_1 E_1^2 h_a^2 \right. \\
& \left. \left((\alpha_{11}^2 - \alpha_{12}^2) (\alpha_{11}^2 + \alpha_{12}^2)^4 - 2 a_0 (\alpha_{11}^2 + \alpha_{12}^2)^2 (\alpha_{11}^4 - 6 \alpha_{11}^2 \alpha_{12}^2 + \alpha_{12}^4) + \right. \right. \\
& \left. \left. a_0^2 (\alpha_{11}^6 - 15 \alpha_{11}^4 \alpha_{12}^2 + 15 \alpha_{11}^2 \alpha_{12}^4 - \alpha_{12}^6) \right) + 3 \beta_2^3 d_1 E_2 (\alpha_{11}^2 + \alpha_{12}^2)^2 \right. \\
& \left. \left((\alpha_{11}^2 - \alpha_{12}^2) (\alpha_{11}^2 + \alpha_{12}^2)^2 (1 + d_1 h_a (\alpha_{11}^2 + \alpha_{12}^2)^2) + a_0^2 (\alpha_{11}^2 - \alpha_{12}^2) (1 + \right. \right. \\
& \left. \left. 4 d_1 h_a (\alpha_{11}^2 + \alpha_{12}^2)^2) - a_0 (5 d_1 h_a \alpha_{11}^8 + 12 d_1 h_a \alpha_{11}^6 \alpha_{12}^2 + 4 \alpha_{11}^2 \alpha_{12}^2 \right. \right. \\
& \left. \left. (-1 + 3 d_1 h_a \alpha_{12}^4) + \alpha_{12}^4 (2 + 5 d_1 h_a \alpha_{12}^4) + 2 \alpha_{11}^4 (1 + 7 d_1 h_a \alpha_{12}^4) \right) \right) - \\
& \left. 3 \beta_1 \beta_2^3 a_0 d_1 E_1 E_2 h_a^2 (\alpha_{11}^2 + \alpha_{12}^2)^2 \left((\alpha_{11}^2 - \alpha_{12}^2) (\alpha_{11}^2 + \alpha_{12}^2)^2 \right. \right. \\
& \left. \left. (1 + d_1 h_a (\alpha_{11}^2 + \alpha_{12}^2)^2) + a_0^2 (\alpha_{11}^2 - \alpha_{12}^2) (1 + 4 d_1 h_a (\alpha_{11}^2 + \alpha_{12}^2)^2) - \right. \right. \\
& \left. \left. a_0 (5 d_1 h_a \alpha_{11}^8 + 12 d_1 h_a \alpha_{11}^6 \alpha_{12}^2 + 4 \alpha_{11}^2 \alpha_{12}^2 (-1 + 3 d_1 h_a \alpha_{12}^4) + \right. \right. \\
& \left. \left. \alpha_{12}^4 (2 + 5 d_1 h_a \alpha_{12}^4) + 2 \alpha_{11}^4 (1 + 7 d_1 h_a \alpha_{12}^4) \right) \right) - \\
& \left. \beta_1^2 \beta_2^2 E_1 E_2 h_a \left(a_0^3 (\alpha_{11}^2 - \alpha_{12}^2) (1 + 4 d_1 h_a (\alpha_{11}^4 - 14 \alpha_{11}^2 \alpha_{12}^2 + \alpha_{12}^4)) - \right. \right. \\
& \left. \left. (\alpha_{11}^2 + \alpha_{12}^2)^4 (1 + d_1 h_a (\alpha_{11}^4 - 6 \alpha_{11}^2 \alpha_{12}^2 + \alpha_{12}^4)) + \right. \right. \\
& \left. \left. a_0 (\alpha_{11}^2 - \alpha_{12}^2) (\alpha_{11}^2 + \alpha_{12}^2)^2 (3 + 2 d_1 h_a (3 \alpha_{11}^4 - 10.0 \alpha_{11}^2 \alpha_{12}^2 + 3 \alpha_{12}^4)) + \right. \right. \\
& \left. \left. a_0^2 (-9 d_1 h_a \alpha_{11}^8 + 60.0 d_1 h_a \alpha_{11}^6 \alpha_{12}^2 + \alpha_{11}^4 (-3 + 10.0 d_1 h_a \alpha_{12}^4) + \right. \right. \\
& \left. \left. 2 \alpha_{11}^2 (\alpha_{12}^2 + 30.0 d_1 h_a \alpha_{12}^6) - 3 (\alpha_{12}^4 + 3 d_1 h_a \alpha_{12}^8) \right) \right) + \\
& \left. \beta_1^3 \beta_2^2 a_0 E_1^2 E_2 h_a^3 \left(a_0^3 (\alpha_{11}^2 - \alpha_{12}^2) (1 + 4 d_1 h_a (\alpha_{11}^4 - 14 \alpha_{11}^2 \alpha_{12}^2 + \alpha_{12}^4)) - \right. \right. \\
& \left. \left. (\alpha_{11}^2 + \alpha_{12}^2)^4 (1 + d_1 h_a (\alpha_{11}^4 - 6 \alpha_{11}^2 \alpha_{12}^2 + \alpha_{12}^4)) + \right. \right. \\
& \left. \left. a_0 (\alpha_{11}^2 - \alpha_{12}^2) (\alpha_{11}^2 + \alpha_{12}^2)^2 (3 + 2 d_1 h_a (3 \alpha_{11}^4 - 10.0 \alpha_{11}^2 \alpha_{12}^2 + 3 \alpha_{12}^4)) + \right. \right. \\
& \left. \left. a_0^2 (-9 d_1 h_a \alpha_{11}^8 + 60.0 d_1 h_a \alpha_{11}^6 \alpha_{12}^2 + \alpha_{11}^4 (-3 + 10.0 d_1 h_a \alpha_{12}^4) + \right. \right. \\
& \left. \left. 2 \alpha_{11}^2 (\alpha_{12}^2 + 30.0 d_1 h_a \alpha_{12}^6) - 3 (\alpha_{12}^4 + 3 d_1 h_a \alpha_{12}^8) \right) \right) \right) \Big/ \\
& \left. \left(2 E_2 (a_0^2 - 2 a_0 (\alpha_{11}^2 - \alpha_{12}^2) + (\alpha_{11}^2 + \alpha_{12}^2)^2) \right. \right. \\
& \left. \left. \left(9 \beta_2^2 d_1^2 (\alpha_{11}^2 + \alpha_{12}^2)^4 + \beta_1^4 E_1^2 h_a^2 (a_0^2 - 2 a_0 (\alpha_{11}^2 - \alpha_{12}^2) + (\alpha_{11}^2 + \alpha_{12}^2)^2) - \right. \right. \right. \\
& \left. \left. \left. 6 \beta_1^2 \beta_2 d_1 E_1 h_a \left(-(\alpha_{11}^2 - \alpha_{12}^2) (\alpha_{11}^2 + \alpha_{12}^2)^2 + a_0 (\alpha_{11}^4 - 6 \alpha_{11}^2 \alpha_{12}^2 + \alpha_{12}^4) \right) \right) \right) \right); \quad (C.9)
\end{aligned}$$



The equations of shear force for the upper adherend and for the lower adherend are expressed in the followings.

$$\begin{aligned}
\bar{Q}_i = & \frac{G_a}{P} (f_{u10} + c_{i3} f_{u1} + f_{u8} (c_{i6} \bar{Sh} + c_{i7} \bar{Ch}) + c_{i8} (-f_{u10} \bar{Ch}_1 \bar{S} + f_{u9} \bar{Sh}_1 \bar{C}) + \\
& c_{i9} (f_{u10} \bar{Ch}_1 \bar{C} + f_{u9} \bar{Sh}_1 \bar{S}) + c_{i10} (f_{u9} \bar{Ch}_1 \bar{C} - f_{u10} \bar{Sh}_1 \bar{S}) + c_{i11} (f_{u9} \bar{Ch}_1 \bar{S} + f_{u10} \bar{Sh}_1 \bar{C})) \quad (C.10)
\end{aligned}$$

$$\begin{aligned}
\bar{Q}_{ix} = & \frac{G_a}{P} (f_{b10} + c_{i3} f_{b1} + f_{b8} (c_{i6} \bar{Sh} + c_{i7} \bar{Ch}) + c_{i8} (-f_{b10} \bar{Ch}_1 \bar{S} + f_{b9} \bar{Sh}_1 \bar{C}) + \\
& c_{i9} (f_{b10} \bar{Ch}_1 \bar{C} + f_{b9} \bar{Sh}_1 \bar{S}) + c_{i10} (f_{b9} \bar{Ch}_1 \bar{C} - f_{b10} \bar{Sh}_1 \bar{S}) + c_{i11} (f_{b9} \bar{Ch}_1 \bar{S} + f_{b10} \bar{Sh}_1 \bar{C})) \quad (C.11)
\end{aligned}$$

Their coefficients are formulated as shown.

$$\begin{aligned}
f_{ui0} &= -\frac{\beta_1 (C_{ai1} a_0 - C_{aai1} a_0)}{2 a_0^2}; \\
f_{u1} &= -\frac{1}{2} \beta_1^3 E_1 h_a^3; \\
f_{u8} &= \frac{1}{12} \beta_1^2 h_a \alpha^3 (-\beta_1 E_1 h_a^2 + (3 (3 \beta_2 d_1 E_2 \alpha^4 + \beta_1^2 E_1 E_2 h_a (-a_0 + \alpha^2) + \\
&\quad \beta_1 E_1 (3 d_1 \alpha^4 + \beta_2 E_2 h_a (-a_0 + \alpha^2 - 4 a_0 d_1 h_a \alpha^4 + d_1 h_a \alpha^6))) / \\
&\quad (E_2 (-a_0 + \alpha^2) (3 \beta_2 d_1 \alpha^4 + \beta_1^2 E_1 h_a (-a_0 + \alpha^2))))); \\
f_{u9} &= \frac{1}{12} \beta_1^2 \left(2 \beta_1 E_1 h_a^3 \alpha_{11} \alpha_{12}^2 - \beta_1 E_1 h_a^3 \alpha_{11} (\alpha_{11}^2 - \alpha_{12}^2) + \frac{1}{\beta_2 E_2} \left(3 \right. \right. \\
&\quad \left. \left((-3 \beta_1^2 \beta_2 d_1 E_1 (\alpha_{11}^2 + \alpha_{12}^2) (\alpha_{11}^3 - 3 \alpha_{11} \alpha_{12}^2) + 3 \beta_2^3 d_1 E_2 \alpha_{11} (\alpha_{11}^2 + \alpha_{12}^2) \right. \right. \\
&\quad \left. \left. (\alpha_{11}^2 + 4 d_1 h_a \alpha_{11}^6 - 3 \alpha_{12}^2 + 12 d_1 h_a \alpha_{11}^4 \alpha_{12}^2 + 12 d_1 h_a \alpha_{11}^2 \alpha_{12}^4 + 4 d_1 h_a \alpha_{12}^6) + \right. \right. \\
&\quad \left. \left. \beta_1^4 E_1^2 h_a \alpha_{11} (a_0 (1 - \beta_2 E_2 h_a^2 (\alpha_{11}^2 - 3 \alpha_{12}^2)) + (\alpha_{11}^2 + \alpha_{12}^2) (-1 + \beta_2 E_2 h_a^2 \right. \right. \\
&\quad \left. \left. (\alpha_{11}^2 + \alpha_{12}^2))) + \beta_1^2 \beta_2^2 E_1 E_2 h_a \alpha_{11} ((\alpha_{11}^2 + \alpha_{12}^2) (1 + d_1 h_a \right. \right. \\
&\quad \left. \left. (7 \alpha_{11}^4 - 2 \alpha_{11}^2 \alpha_{12}^2 - 9 \alpha_{12}^4)) - a_0 (1 + 4 d_1 h_a (\alpha_{11}^4 - 10.0 \alpha_{11}^2 \alpha_{12}^2 + 5 \alpha_{12}^4))) \right) / \right. \\
&\quad \left. (9 \beta_2^2 d_1^2 (\alpha_{11}^2 + \alpha_{12}^2)^4 + \beta_1^4 E_1^2 h_a^2 (a_0^2 - 2 a_0 (\alpha_{11}^2 - \alpha_{12}^2) + (\alpha_{11}^2 + \alpha_{12}^2)^2) - \right. \\
&\quad \left. 6 \beta_1^2 \beta_2 d_1 E_1 h_a ((-\alpha_{11}^2 + \alpha_{12}^2) (\alpha_{11}^2 + \alpha_{12}^2)^2 + a_0 (\alpha_{11}^4 - 6 \alpha_{11}^2 \alpha_{12}^2 + \alpha_{12}^4)) \right) - \\
&\quad \left. (\alpha_{11} (a_0 - \alpha_{11}^2 - \alpha_{12}^2) + (2 d_1 h_a \alpha_{12} (-\beta_2^2 E_2 \alpha_{12} (a_0 + \alpha_{11}^2 + \alpha_{12}^2) - \right. \\
&\quad \left. \beta_1 \beta_2^2 E_1 E_2 h_a^2 \alpha_{12} (a_0 (-3 \alpha_{11}^2 + \alpha_{12}^2) + (\alpha_{11}^2 + \alpha_{12}^2)^2))) \right) \\
&\quad \left. (-3 \beta_1^2 E_1 (-2 a_0 (\alpha_{11}^2 - \alpha_{12}^2) + (\alpha_{11}^2 + \alpha_{12}^2)^2) + \right. \\
&\quad \left. \beta_1^2 \beta_2 E_1 E_2 h_a^2 (-8 a_0^2 (\alpha_{11}^2 - \alpha_{12}^2) - 2 (\alpha_{11}^2 - \alpha_{12}^2) (\alpha_{11}^2 + \alpha_{12}^2)^2 + \right. \\
&\quad \left. a_0 (7 \alpha_{11}^4 - 2 \alpha_{11}^2 \alpha_{12}^2 + 7 \alpha_{12}^4)) - 3 \beta_2^2 E_2 (2 a_0 (\alpha_{11}^2 - \alpha_{12}^2) + (\alpha_{11}^2 + \alpha_{12}^2)^2 \right. \\
&\quad \left. (-1 + d_1 h_a (\alpha_{11}^2 + \alpha_{12}^2)^2)) \right) \left. \right) / \left(\beta_2 E_2 (9 \beta_2^2 d_1^2 (\alpha_{11}^2 + \alpha_{12}^2)^4 + \beta_1^4 E_1^2 h_a^2 \right. \\
&\quad \left. (a_0^2 - 2 a_0 (\alpha_{11}^2 - \alpha_{12}^2) + (\alpha_{11}^2 + \alpha_{12}^2)^2) - 6 \beta_1^2 \beta_2 d_1 E_1 h_a ((-\alpha_{11}^2 + \alpha_{12}^2) \right. \\
&\quad \left. (\alpha_{11}^2 + \alpha_{12}^2)^2 + a_0 (\alpha_{11}^4 - 6 \alpha_{11}^2 \alpha_{12}^2 + \alpha_{12}^4)) \right) + (\beta_2 (-a_0 + \alpha_{11}^2 + \alpha_{12}^2 + \beta_1 E_1 h_a^2 \\
&\quad (a_0 (\alpha_{11}^2 - 3 \alpha_{12}^2) - (\alpha_{11}^2 + \alpha_{12}^2)^2)) (9 \beta_2 d_1^2 (\alpha_{11}^2 + \alpha_{12}^2)^4 - 3 \beta_1^2 d_1 E_1 h_a \\
&\quad ((-\alpha_{11}^2 + \alpha_{12}^2) (\alpha_{11}^2 + \alpha_{12}^2)^2 + a_0 (\alpha_{11}^4 - 6 \alpha_{11}^2 \alpha_{12}^2 + \alpha_{12}^4)) + \\
&\quad \beta_1^2 \beta_2 E_1 E_2 h_a^2 ((\alpha_{11}^2 + \alpha_{12}^2)^2 (1 + d_1 h_a (\alpha_{11}^4 - 6 \alpha_{11}^2 \alpha_{12}^2 + \alpha_{12}^4)) + \\
&\quad a_0^2 (1 + 4 d_1 h_a (\alpha_{11}^4 - 6 \alpha_{11}^2 \alpha_{12}^2 + \alpha_{12}^4)) - a_0 (\alpha_{11}^2 - \alpha_{12}^2) (2 + d_1 h_a \\
&\quad (5 \alpha_{11}^4 - 6 \alpha_{11}^2 \alpha_{12}^2 + 5 \alpha_{12}^4))) - 3 \beta_2^2 d_1 E_2 h_a ((-\alpha_{11}^2 + \alpha_{12}^2) (\alpha_{11}^2 + \alpha_{12}^2)^2 \\
&\quad (1 + d_1 h_a (\alpha_{11}^2 + \alpha_{12}^2)^2) + a_0 (4 d_1 h_a \alpha_{11}^8 + 16 d_1 h_a \alpha_{11}^6 \alpha_{12}^2 + \alpha_{12}^4 + 4 d_1 h_a \alpha_{12}^8 + \\
&\quad \alpha_{11}^4 (1 + 24 d_1 h_a \alpha_{12}^4) + \alpha_{11}^2 (-6 \alpha_{12}^2 + 16 d_1 h_a \alpha_{12}^6))) \left. \right) \left. \right) / \\
&\quad \left. (9 \beta_2^2 d_1^2 (\alpha_{11}^2 + \alpha_{12}^2)^4 + \beta_1^4 E_1^2 h_a^2 (a_0^2 - 2 a_0 (\alpha_{11}^2 - \alpha_{12}^2) + (\alpha_{11}^2 + \alpha_{12}^2)^2) - \right. \\
&\quad \left. 6 \beta_1^2 \beta_2 d_1 E_1 h_a ((-\alpha_{11}^2 + \alpha_{12}^2) (\alpha_{11}^2 + \alpha_{12}^2)^2 + a_0 (\alpha_{11}^4 - 6 \alpha_{11}^2 \alpha_{12}^2 + \alpha_{12}^4))) \left. \right) \right) / \\
&\quad \left. (h_a (a_0^2 - 2 a_0 (\alpha_{11}^2 - \alpha_{12}^2) + (\alpha_{11}^2 + \alpha_{12}^2)^2)) \right);
\end{aligned} \tag{C.12}$$

$$\begin{aligned}
f_{u10} = & \frac{1}{12} \beta_1^2 \left(-2 \beta_1 E_1 h_a^3 \alpha_{11}^2 \alpha_{12} + \beta_1 E_1 h_a^3 \alpha_{12} (-\alpha_{11}^2 + \alpha_{12}^2) + \frac{1}{\beta_2 E_2} \left(3 \right. \right. \\
& \left. \left. \left((\alpha_{12} (-3 \beta_1^2 \beta_2 d_1 E_1 (-3 \alpha_{11}^2 + \alpha_{12}^2) (\alpha_{11}^2 + \alpha_{12}^2) + 3 \beta_2^3 d_1 E_2 (\alpha_{11}^2 + \alpha_{12}^2) \right. \right. \right. \\
& \left. \left. \left. (4 d_1 h_a \alpha_{11}^6 + \alpha_{12}^2 + 12 d_1 h_a \alpha_{11}^4 \alpha_{12}^2 + 4 d_1 h_a \alpha_{12}^6 + 3 \alpha_{11}^2 (-1 + 4 d_1 h_a \alpha_{12}^4) \right) + \right. \right. \\
& \left. \left. \beta_1^4 E_1^2 h_a (a_0 (1 + \beta_2 E_2 h_a^2 (-3 \alpha_{11}^2 + \alpha_{12}^2)) + (\alpha_{11}^2 + \alpha_{12}^2) (1 + \beta_2 E_2 h_a^2 \right. \right. \\
& \left. \left. (\alpha_{11}^2 + \alpha_{12}^2))) - \beta_1^2 \beta_2^2 E_1 E_2 h_a (- (\alpha_{11}^2 + \alpha_{12}^2) (-1 + d_1 h_a (9 \alpha_{11}^4 + 2 \alpha_{11}^2 \alpha_{12}^2 \right. \right. \\
& \left. \left. - 7 \alpha_{12}^4)) + a_0 (1 + 4 d_1 h_a (5 \alpha_{11}^4 - 10.0 \alpha_{11}^2 \alpha_{12}^2 + \alpha_{12}^4))) \right) \right) / \\
& \left(9 \beta_2^2 d_1^2 (\alpha_{11}^2 + \alpha_{12}^2)^4 + \beta_1^4 E_1^2 h_a^2 (a_0^2 - 2 a_0 (\alpha_{11}^2 - \alpha_{12}^2) + (\alpha_{11}^2 + \alpha_{12}^2)^2) - \right. \\
& \left. 6 \beta_1^2 \beta_2 d_1 E_1 h_a \left((-\alpha_{11}^2 + \alpha_{12}^2) (\alpha_{11}^2 + \alpha_{12}^2)^2 + a_0 (\alpha_{11}^4 - 6 \alpha_{11}^2 \alpha_{12}^2 + \alpha_{12}^4) \right) \right) - \\
& \left(\alpha_{12} (a_0 + \alpha_{11}^2 + \alpha_{12}^2) + \left(2 \beta_2 d_1 h_a \alpha_{11}^2 \alpha_{12} \left(-a_0 + \alpha_{11}^2 + \alpha_{12}^2 + \beta_1 E_1 h_a^2 \right. \right. \right. \\
& \left. \left. \left. \left(a_0 (\alpha_{11}^2 - 3 \alpha_{12}^2) - (\alpha_{11}^2 + \alpha_{12}^2)^2 \right) \right) \left(3 \beta_1^2 E_1 \left(-2 a_0 (\alpha_{11}^2 - \alpha_{12}^2) + (\alpha_{11}^2 + \alpha_{12}^2)^2 \right) + \right. \right. \\
& \left. \left. \beta_1^2 \beta_2 E_1 E_2 h_a^2 \left(8 a_0^2 (\alpha_{11}^2 - \alpha_{12}^2) + 2 (\alpha_{11}^2 - \alpha_{12}^2) (\alpha_{11}^2 + \alpha_{12}^2)^2 + \right. \right. \right. \\
& \left. \left. \left. a_0 (-7 \alpha_{11}^4 + 2 \alpha_{11}^2 \alpha_{12}^2 - 7 \alpha_{12}^4) \right) + 3 \beta_2^2 E_2 \left(2 a_0 (\alpha_{11}^2 - \alpha_{12}^2) + (\alpha_{11}^2 + \alpha_{12}^2)^2 \right. \right. \\
& \left. \left. \left. (-1 + d_1 h_a (\alpha_{11}^2 + \alpha_{12}^2)^2) \right) \right) \right) / \left(9 \beta_2^2 d_1^2 (\alpha_{11}^2 + \alpha_{12}^2)^4 + \beta_1^4 E_1^2 h_a^2 \right. \\
& \left. \left(a_0^2 - 2 a_0 (\alpha_{11}^2 - \alpha_{12}^2) + (\alpha_{11}^2 + \alpha_{12}^2)^2 \right) - 6 \beta_1^2 \beta_2 d_1 E_1 h_a \right. \\
& \left. \left((-\alpha_{11}^2 + \alpha_{12}^2) (\alpha_{11}^2 + \alpha_{12}^2)^2 + a_0 (\alpha_{11}^4 - 6 \alpha_{11}^2 \alpha_{12}^2 + \alpha_{12}^4) \right) \right) + \\
& \left(\left(-\beta_2^2 E_2 \alpha_{12} (a_0 + \alpha_{11}^2 + \alpha_{12}^2) - \beta_1 \beta_2^2 E_1 E_2 h_a^2 \alpha_{12} \right. \right. \\
& \left. \left. \left(a_0 (-3 \alpha_{11}^2 + \alpha_{12}^2) + (\alpha_{11}^2 + \alpha_{12}^2)^2 \right) \right) \left(9 \beta_2 d_1^2 (\alpha_{11}^2 + \alpha_{12}^2)^4 - 3 \beta_1^2 d_1 E_1 h_a \right. \right. \\
& \left. \left. \left((-\alpha_{11}^2 + \alpha_{12}^2) (\alpha_{11}^2 + \alpha_{12}^2)^2 + a_0 (\alpha_{11}^4 - 6 \alpha_{11}^2 \alpha_{12}^2 + \alpha_{12}^4) \right) + \right. \right. \\
& \left. \left. \beta_1^2 \beta_2 E_1 E_2 h_a^2 \left((\alpha_{11}^2 + \alpha_{12}^2)^2 (1 + d_1 h_a (\alpha_{11}^4 - 6 \alpha_{11}^2 \alpha_{12}^2 + \alpha_{12}^4)) + \right. \right. \right. \\
& \left. \left. \left. a_0^2 (1 + 4 d_1 h_a (\alpha_{11}^4 - 6 \alpha_{11}^2 \alpha_{12}^2 + \alpha_{12}^4)) - \right. \right. \right. \\
& \left. \left. \left. a_0 (\alpha_{11}^2 - \alpha_{12}^2) (2 + d_1 h_a (5 \alpha_{11}^4 - 6 \alpha_{11}^2 \alpha_{12}^2 + 5 \alpha_{12}^4)) \right) \right) - \right. \\
& \left. 3 \beta_2^2 d_1 E_2 h_a \left((-\alpha_{11}^2 + \alpha_{12}^2) (\alpha_{11}^2 + \alpha_{12}^2)^2 (1 + d_1 h_a (\alpha_{11}^2 + \alpha_{12}^2)^2) + \right. \right. \\
& \left. \left. a_0 (4 d_1 h_a \alpha_{11}^8 + 16 d_1 h_a \alpha_{11}^6 \alpha_{12}^2 + \alpha_{12}^4 + 4 d_1 h_a \alpha_{12}^8 + \right. \right. \\
& \left. \left. \alpha_{11}^4 (1 + 24 d_1 h_a \alpha_{12}^4) + \alpha_{11}^2 (-6 \alpha_{12}^2 + 16 d_1 h_a \alpha_{12}^6) \right) \right) \right) / \\
& \left(\beta_2 E_2 \left(9 \beta_2^2 d_1^2 (\alpha_{11}^2 + \alpha_{12}^2)^4 + \beta_1^4 E_1^2 h_a^2 (a_0^2 - 2 a_0 (\alpha_{11}^2 - \alpha_{12}^2) + \right. \right. \\
& \left. \left. (\alpha_{11}^2 + \alpha_{12}^2)^2) - 6 \beta_1^2 \beta_2 d_1 E_1 h_a \left((-\alpha_{11}^2 + \alpha_{12}^2) (\alpha_{11}^2 + \alpha_{12}^2)^2 + a_0 (\alpha_{11}^4 - \right. \right. \right. \\
& \left. \left. \left. 6 \alpha_{11}^2 \alpha_{12}^2 + \alpha_{12}^4) \right) \right) \right) \right) / \left(h_a (a_0^2 - 2 a_0 (\alpha_{11}^2 - \alpha_{12}^2) + (\alpha_{11}^2 + \alpha_{12}^2)^2) \right) \Big); \tag{C.13}
\end{aligned}$$

$$f_{b10} = -\frac{\beta_2 (c_{ai1} a_0 - c_{aai1} a_0)}{2 a_0^2};$$

$$f_{b1} = -\frac{1}{2} \beta_2^3 E_2 h_a^3;$$

$$\begin{aligned}
f_{b8} = & (\beta_1 \beta_2 h_a \alpha^3 (9 \beta_2 d_1 E_2 \alpha^4 - 3 \beta_1^2 E_1 E_2 h_a (a_0 - \alpha^2) - \beta_1 E_1 (3 + \beta_2 E_2 h_a^2 (a_0 - \alpha^2)) \\
& (-3 d_1 \alpha^4 + \beta_2 E_2 h_a (a_0 + 4 a_0 d_1 h_a \alpha^4 - \alpha^2 (1 + d_1 h_a \alpha^4)))) / \\
& (12 E_2 (-a_0 + \alpha^2) (3 \beta_2 d_1 \alpha^4 + \beta_1^2 E_1 h_a (-a_0 + \alpha^2)));
\end{aligned}$$

$$\begin{aligned}
f_{b9} = & \frac{1}{12 E_2} \left\{ \beta_1 \left(\left(2 \beta_1 \beta_2^2 E_1 E_2 h_a^3 \alpha_{11} \alpha_{12}^2 \left(9 \beta_2 d_1^2 (\alpha_{11}^2 + \alpha_{12}^2)^4 - 3 \beta_1^2 d_1 E_1 h_a \right. \right. \right. \right. \\
& \left. \left. \left. \left(-2 (\alpha_{11}^2 - \alpha_{12}^2) (\alpha_{11}^2 + \alpha_{12}^2)^2 + a_0 (3 \alpha_{11}^4 - 10.0 \alpha_{11}^2 \alpha_{12}^2 + 3 \alpha_{12}^4) \right) - \right. \right. \\
& \left. \left. 3 \beta_2^2 d_1 E_2 h_a (\alpha_{11}^2 + \alpha_{12}^2)^2 \left(-2 d_1 h_a (\alpha_{11}^2 - \alpha_{12}^2) (\alpha_{11}^2 + \alpha_{12}^2)^2 + a_0 (-1 + \right. \right. \right. \\
& \left. \left. \left. 4 d_1 h_a (\alpha_{11}^2 + \alpha_{12}^2)^2 \right) \right) + \beta_1^2 \beta_2 E_1 E_2 h_a^2 \left((\alpha_{11}^2 + \alpha_{12}^2)^2 (1 + d_1 h_a (3 \alpha_{11}^4 - \right. \right. \\
& \left. \left. 10.0 \alpha_{11}^2 \alpha_{12}^2 + 3 \alpha_{12}^4) \right) + a_0^2 (1 + 4 d_1 h_a (3 \alpha_{11}^4 - 10.0 \alpha_{11}^2 \alpha_{12}^2 + 3 \alpha_{12}^4)) - \right. \\
& \left. \left. 2 a_0 (\alpha_{11}^2 - \alpha_{12}^2) (1 + 2 d_1 h_a (3 \alpha_{11}^4 - 2 \alpha_{11}^2 \alpha_{12}^2 + 3 \alpha_{12}^4)) \right) \right) \right) \Big/ \\
& \left(9 \beta_2^2 d_1^2 (\alpha_{11}^2 + \alpha_{12}^2)^4 + \beta_1^4 E_1^2 h_a^2 \left(a_0^2 - 2 a_0 (\alpha_{11}^2 - \alpha_{12}^2) + (\alpha_{11}^2 + \alpha_{12}^2)^2 \right) - \right. \\
& \left. 6 \beta_1^2 \beta_2 d_1 E_1 h_a \left((-\alpha_{11}^2 + \alpha_{12}^2) (\alpha_{11}^2 + \alpha_{12}^2)^2 + a_0 (\alpha_{11}^4 - 6 \alpha_{11}^2 \alpha_{12}^2 + \alpha_{12}^4) \right) \right) - \\
& \left(\beta_1 \beta_2^2 E_1 E_2 h_a^3 \alpha_{11} \left(9 \beta_2 d_1^2 (\alpha_{11}^2 - \alpha_{12}^2) (\alpha_{11}^2 + \alpha_{12}^2)^4 - 3 \beta_1^2 d_1 E_1 h_a \right. \right. \\
& \left. \left. \left(-(\alpha_{11}^2 + \alpha_{12}^2)^2 (\alpha_{11}^4 - 6 \alpha_{11}^2 \alpha_{12}^2 + \alpha_{12}^4) + a_0 (\alpha_{11}^6 - 15 \alpha_{11}^4 \alpha_{12}^2 + \right. \right. \right. \\
& \left. \left. \left. 15 \alpha_{11}^2 \alpha_{12}^4 - \alpha_{12}^6) \right) + 3 \beta_2^2 d_1 E_2 h_a (\alpha_{11}^2 + \alpha_{12}^2)^2 \left(-a_0 (\alpha_{11}^2 - \alpha_{12}^2) \right. \right. \\
& \left. \left. \left(1 + 4 d_1 h_a (\alpha_{11}^2 + \alpha_{12}^2)^2 \right) + (\alpha_{11}^2 + \alpha_{12}^2)^2 (1 + d_1 h_a (\alpha_{11}^4 - 6 \alpha_{11}^2 \alpha_{12}^2 + \alpha_{12}^4)) \right) \right) + \\
& \left. \beta_1^2 \beta_2 E_1 E_2 h_a^2 \left((\alpha_{11}^2 - \alpha_{12}^2) (\alpha_{11}^2 + \alpha_{12}^2)^2 (1 + d_1 h_a (\alpha_{11}^4 - 14 \alpha_{11}^2 \alpha_{12}^2 + \alpha_{12}^4)) + \right. \right. \\
& \left. \left. a_0^2 (\alpha_{11}^2 - \alpha_{12}^2) (1 + 4 d_1 h_a (\alpha_{11}^4 - 14 \alpha_{11}^2 \alpha_{12}^2 + \alpha_{12}^4)) - \right. \right. \\
& \left. \left. a_0 (5 d_1 h_a \alpha_{11}^8 - 44 d_1 h_a \alpha_{11}^6 \alpha_{12}^2 + \alpha_{12}^4 (2 + 5 d_1 h_a \alpha_{12}^4) + \right. \right. \\
& \left. \left. \alpha_{11}^4 (2 + 30.0 d_1 h_a \alpha_{12}^4) - 4 \alpha_{11}^2 (\alpha_{12}^2 + 11 d_1 h_a \alpha_{12}^6) \right) \right) \Big/ \\
& \left(9 \beta_2^2 d_1^2 (\alpha_{11}^2 + \alpha_{12}^2)^4 + \beta_1^4 E_1^2 h_a^2 \left(a_0^2 - 2 a_0 (\alpha_{11}^2 - \alpha_{12}^2) + (\alpha_{11}^2 + \alpha_{12}^2)^2 \right) - \right. \\
& \left. 6 \beta_1^2 \beta_2 d_1 E_1 h_a \left((-\alpha_{11}^2 + \alpha_{12}^2) (\alpha_{11}^2 + \alpha_{12}^2)^2 + a_0 (\alpha_{11}^4 - 6 \alpha_{11}^2 \alpha_{12}^2 + \alpha_{12}^4) \right) \right) + \\
& 3 \left((-3 \beta_1^2 \beta_2 d_1 E_1 (\alpha_{11}^2 + \alpha_{12}^2) (\alpha_{11}^3 - 3 \alpha_{11} \alpha_{12}^2) + 3 \beta_2^3 d_1 E_2 \alpha_{11} (\alpha_{11}^2 + \alpha_{12}^2) \right. \\
& \left. (\alpha_{11}^2 + 4 d_1 h_a \alpha_{11}^6 - 3 \alpha_{12}^2 + 12 d_1 h_a \alpha_{11}^4 \alpha_{12}^2 + 12 d_1 h_a \alpha_{11}^2 \alpha_{12}^4 + 4 d_1 h_a \alpha_{12}^6) + \right. \\
& \left. \beta_1^4 E_1^2 h_a \alpha_{11} (a_0 (1 - \beta_2 E_2 h_a^2 (\alpha_{11}^2 - 3 \alpha_{12}^2)) + (\alpha_{11}^2 + \alpha_{12}^2) (-1 + \beta_2 E_2 h_a^2 \right. \\
& \left. (\alpha_{11}^2 + \alpha_{12}^2))) + \beta_1^2 \beta_2^2 E_1 E_2 h_a \alpha_{11} ((\alpha_{11}^2 + \alpha_{12}^2) (1 + d_1 h_a (7 \alpha_{11}^4 - \right. \\
& \left. 2 \alpha_{11}^2 \alpha_{12}^2 - 9 \alpha_{12}^4)) - a_0 (1 + 4 d_1 h_a (\alpha_{11}^4 - 10.0 \alpha_{11}^2 \alpha_{12}^2 + 5 \alpha_{12}^4))) \right) \Big/ \\
& \left(9 \beta_2^2 d_1^2 (\alpha_{11}^2 + \alpha_{12}^2)^4 + \beta_1^4 E_1^2 h_a^2 \left(a_0^2 - 2 a_0 (\alpha_{11}^2 - \alpha_{12}^2) + (\alpha_{11}^2 + \alpha_{12}^2)^2 \right) - \right. \\
& \left. 6 \beta_1^2 \beta_2 d_1 E_1 h_a \left((-\alpha_{11}^2 + \alpha_{12}^2) (\alpha_{11}^2 + \alpha_{12}^2)^2 + a_0 (\alpha_{11}^4 - 6 \alpha_{11}^2 \alpha_{12}^2 + \alpha_{12}^4) \right) \right) - \\
& \left(\alpha_{11} (a_0 - \alpha_{11}^2 - \alpha_{12}^2 + (2 d_1 h_a \alpha_{12} (-\beta_2^2 E_2 \alpha_{12} (a_0 + \alpha_{11}^2 + \alpha_{12}^2) - \right. \\
& \left. \beta_1 \beta_2^2 E_1 E_2 h_a^2 \alpha_{12} (a_0 (-3 \alpha_{11}^2 + \alpha_{12}^2) + (\alpha_{11}^2 + \alpha_{12}^2)^2)) \right) \\
& \left. (-3 \beta_1^2 E_1 (-2 a_0 (\alpha_{11}^2 - \alpha_{12}^2) + (\alpha_{11}^2 + \alpha_{12}^2)^2) + \beta_1^2 \beta_2 E_1 E_2 h_a^2 \right. \\
& \left. (-8 a_0^2 (\alpha_{11}^2 - \alpha_{12}^2) - 2 (\alpha_{11}^2 - \alpha_{12}^2) (\alpha_{11}^2 + \alpha_{12}^2)^2 + a_0 (7 \alpha_{11}^4 - 2 \alpha_{11}^2 \alpha_{12}^2 + \right. \\
& \left. 7 \alpha_{12}^4)) - 3 \beta_2^2 E_2 (2 a_0 (\alpha_{11}^2 - \alpha_{12}^2) + (\alpha_{11}^2 + \alpha_{12}^2)^2 (-1 + d_1 h_a (\alpha_{11}^2 + \right. \\
& \left. \alpha_{12}^2)^2) \right) \Big/ \left(\beta_2 E_2 (9 \beta_2^2 d_1^2 (\alpha_{11}^2 + \alpha_{12}^2)^4 + \beta_1^4 E_1^2 h_a^2 \right. \\
& \left. (a_0^2 - 2 a_0 (\alpha_{11}^2 - \alpha_{12}^2) + (\alpha_{11}^2 + \alpha_{12}^2)^2) - 6 \beta_1^2 \beta_2 d_1 E_1 h_a \left((-\alpha_{11}^2 + \alpha_{12}^2) \right. \right. \\
& \left. \left. (\alpha_{11}^2 + \alpha_{12}^2)^2 + a_0 (\alpha_{11}^4 - 6 \alpha_{11}^2 \alpha_{12}^2 + \alpha_{12}^4) \right) \right) + \left(\beta_2 (-a_0 + \alpha_{11}^2 + \alpha_{12}^2 + \right. \\
& \left. \beta_1 E_1 h_a^2 (a_0 (\alpha_{11}^2 - 3 \alpha_{12}^2) - (\alpha_{11}^2 + \alpha_{12}^2)^2) \right) (9 \beta_2 d_1^2 (\alpha_{11}^2 + \alpha_{12}^2)^4 - 3 \beta_1^2 d_1 E_1 h_a \\
& \left. \left((-\alpha_{11}^2 + \alpha_{12}^2) (\alpha_{11}^2 + \alpha_{12}^2)^2 + a_0 (\alpha_{11}^4 - 6 \alpha_{11}^2 \alpha_{12}^2 + \alpha_{12}^4) \right) + \right. \\
& \left. \beta_1^2 \beta_2 E_1 E_2 h_a^2 \left((\alpha_{11}^2 + \alpha_{12}^2)^2 (1 + d_1 h_a (\alpha_{11}^4 - 6 \alpha_{11}^2 \alpha_{12}^2 + \alpha_{12}^4)) + \right. \right. \\
& \left. \left. a_0^2 (1 + 4 d_1 h_a (\alpha_{11}^4 - 6 \alpha_{11}^2 \alpha_{12}^2 + \alpha_{12}^4)) - a_0 (\alpha_{11}^2 - \alpha_{12}^2) (2 + d_1 h_a (5 \alpha_{11}^4 - \right. \right. \\
& \left. \left. 6 \alpha_{11}^2 \alpha_{12}^2 + 5 \alpha_{12}^4)) \right) - 3 \beta_2^2 d_1 E_2 h_a \left((-\alpha_{11}^2 + \alpha_{12}^2) (\alpha_{11}^2 + \alpha_{12}^2)^2 \right. \\
& \left. \left(1 + d_1 h_a (\alpha_{11}^2 + \alpha_{12}^2)^2 \right) + a_0 (4 d_1 h_a \alpha_{11}^8 + 16 d_1 h_a \alpha_{11}^6 \alpha_{12}^2 + \alpha_{12}^4 + 4 d_1 h_a \alpha_{12}^8 + \right. \\
& \left. \alpha_{11}^4 (1 + 24 d_1 h_a \alpha_{12}^4) + \alpha_{11}^2 (-6 \alpha_{12}^2 + 16 d_1 h_a \alpha_{12}^6) \right) \Big/ \\
& \left(9 \beta_2^2 d_1^2 (\alpha_{11}^2 + \alpha_{12}^2)^4 + \beta_1^4 E_1^2 h_a^2 \left(a_0^2 - 2 a_0 (\alpha_{11}^2 - \alpha_{12}^2) + (\alpha_{11}^2 + \alpha_{12}^2)^2 \right) - \right. \\
& \left. 6 \beta_1^2 \beta_2 d_1 E_1 h_a \left((-\alpha_{11}^2 + \alpha_{12}^2) (\alpha_{11}^2 + \alpha_{12}^2)^2 + a_0 (\alpha_{11}^4 - 6 \alpha_{11}^2 \alpha_{12}^2 + \alpha_{12}^4) \right) \right) \Big/ \\
& \left(h_a (a_0^2 - 2 a_0 (\alpha_{11}^2 - \alpha_{12}^2) + (\alpha_{11}^2 + \alpha_{12}^2)^2) \right) \Big);
\end{aligned} \tag{C.14}$$

$$\begin{aligned}
f_{b10} = & \frac{1}{12 E_2} \left(\beta_1 \left(- \left(2 \beta_1 \beta_2^2 E_1 E_2 h_a^3 \alpha_{11}^2 \alpha_{12} \left(9 \beta_2 d_1^2 (\alpha_{11}^2 + \alpha_{12}^2)^4 - 3 \beta_1^2 d_1 E_1 h_a \right. \right. \right. \right. \\
& \left. \left. \left. \left. \left(-2 (\alpha_{11}^2 - \alpha_{12}^2) (\alpha_{11}^2 + \alpha_{12}^2)^2 + a_0 (3 \alpha_{11}^4 - 10.0 \alpha_{11}^2 \alpha_{12}^2 + 3 \alpha_{12}^4) \right) - \right. \right. \right. \\
& \left. \left. \left. 3 \beta_2^2 d_1 E_2 h_a (\alpha_{11}^2 + \alpha_{12}^2)^2 \left(-2 d_1 h_a (\alpha_{11}^2 - \alpha_{12}^2) (\alpha_{11}^2 + \alpha_{12}^2)^2 + a_0 (-1 + \right. \right. \right. \\
& \left. \left. \left. 4 d_1 h_a (\alpha_{11}^2 + \alpha_{12}^2)^2 \right) \right) + \beta_1^2 \beta_2 E_1 E_2 h_a^2 \left((\alpha_{11}^2 + \alpha_{12}^2)^2 (1 + d_1 h_a (3 \alpha_{11}^4 - \right. \right. \\
& \left. \left. 10.0 \alpha_{11}^2 \alpha_{12}^2 + 3 \alpha_{12}^4)) + a_0^2 (1 + 4 d_1 h_a (3 \alpha_{11}^4 - 10.0 \alpha_{11}^2 \alpha_{12}^2 + 3 \alpha_{12}^4)) - 2 a_0 \right. \right. \\
& \left. \left. (\alpha_{11}^2 - \alpha_{12}^2) (1 + 2 d_1 h_a (3 \alpha_{11}^4 - 2 \alpha_{11}^2 \alpha_{12}^2 + 3 \alpha_{12}^4)) \right) \right) \Big/ \\
& \left(9 \beta_2^2 d_1^2 (\alpha_{11}^2 + \alpha_{12}^2)^4 + \beta_1^4 E_1^2 h_a^2 \left(a_0^2 - 2 a_0 (\alpha_{11}^2 - \alpha_{12}^2) + (\alpha_{11}^2 + \alpha_{12}^2)^2 \right) - \right. \\
& \left. 6 \beta_1^2 \beta_2 d_1 E_1 h_a \left((-\alpha_{11}^2 + \alpha_{12}^2) (\alpha_{11}^2 + \alpha_{12}^2)^2 + a_0 (\alpha_{11}^4 - 6 \alpha_{11}^2 \alpha_{12}^2 + \alpha_{12}^4) \right) \right) + \\
& \left(\beta_1 \beta_2^2 E_1 E_2 h_a^3 \alpha_{12} \left(-9 \beta_2 d_1^2 (\alpha_{11}^2 - \alpha_{12}^2) (\alpha_{11}^2 + \alpha_{12}^2)^4 - \right. \right. \\
& \left. \left. 3 \beta_1^2 d_1 E_1 h_a \left((\alpha_{11}^2 + \alpha_{12}^2)^2 (\alpha_{11}^4 - 6 \alpha_{11}^2 \alpha_{12}^2 + \alpha_{12}^4) + \right. \right. \right. \\
& \left. \left. \left. a_0 (-\alpha_{11}^6 + 15 \alpha_{11}^4 \alpha_{12}^2 - 15 \alpha_{11}^2 \alpha_{12}^4 + \alpha_{12}^6) \right) - 3 \beta_2^2 d_1 E_2 h_a (\alpha_{11}^2 + \alpha_{12}^2)^2 \right. \right. \\
& \left. \left. (-a_0 (\alpha_{11}^2 - \alpha_{12}^2) (1 + 4 d_1 h_a (\alpha_{11}^2 + \alpha_{12}^2)^2) + \right. \right. \\
& \left. \left. (\alpha_{11}^2 + \alpha_{12}^2)^2 (1 + d_1 h_a (\alpha_{11}^4 - 6 \alpha_{11}^2 \alpha_{12}^2 + \alpha_{12}^4)) \right) + \beta_1^2 \beta_2 E_1 E_2 h_a^2 \right. \\
& \left. \left((-\alpha_{11}^2 + \alpha_{12}^2) (\alpha_{11}^2 + \alpha_{12}^2)^2 (1 + d_1 h_a (\alpha_{11}^4 - 14 \alpha_{11}^2 \alpha_{12}^2 + \alpha_{12}^4)) - \right. \right. \\
& \left. \left. a_0^2 (\alpha_{11}^2 - \alpha_{12}^2) (1 + 4 d_1 h_a (\alpha_{11}^4 - 14 \alpha_{11}^2 \alpha_{12}^2 + \alpha_{12}^4)) + \right. \right. \\
& \left. \left. a_0 (5 d_1 h_a \alpha_{11}^8 - 44 d_1 h_a \alpha_{11}^6 \alpha_{12}^2 + \alpha_{12}^4 (2 + 5 d_1 h_a \alpha_{12}^4) + \right. \right. \\
& \left. \left. \alpha_{11}^4 (2 + 30.0 d_1 h_a \alpha_{12}^4) - 4 \alpha_{11}^2 (\alpha_{12}^2 + 11 d_1 h_a \alpha_{12}^6) \right) \right) \Big/ \\
& \left(9 \beta_2^2 d_1^2 (\alpha_{11}^2 + \alpha_{12}^2)^4 + \beta_1^4 E_1^2 h_a^2 \left(a_0^2 - 2 a_0 (\alpha_{11}^2 - \alpha_{12}^2) + (\alpha_{11}^2 + \alpha_{12}^2)^2 \right) - \right. \\
& \left. 6 \beta_1^2 \beta_2 d_1 E_1 h_a \left((-\alpha_{11}^2 + \alpha_{12}^2) (\alpha_{11}^2 + \alpha_{12}^2)^2 + a_0 (\alpha_{11}^4 - 6 \alpha_{11}^2 \alpha_{12}^2 + \alpha_{12}^4) \right) \right) + \\
& 3 \left((\alpha_{12} (-3 \beta_1^2 \beta_2 d_1 E_1 (-3 \alpha_{11}^2 + \alpha_{12}^2) (\alpha_{11}^2 + \alpha_{12}^2) + \right. \\
& \left. 3 \beta_2^3 d_1 E_2 (\alpha_{11}^2 + \alpha_{12}^2) (4 d_1 h_a \alpha_{11}^6 + \alpha_{12}^2 + 12 d_1 h_a \alpha_{11}^4 \alpha_{12}^2 + \right. \\
& \left. 4 d_1 h_a \alpha_{12}^6 + 3 \alpha_{11}^2 (-1 + 4 d_1 h_a \alpha_{12}^4)) + \right. \\
& \left. \beta_1^4 E_1^2 h_a (a_0 (1 + \beta_2 E_2 h_a^2 (-3 \alpha_{11}^2 + \alpha_{12}^2)) + \right. \\
& \left. (\alpha_{11}^2 + \alpha_{12}^2) (1 + \beta_2 E_2 h_a^2 (\alpha_{11}^2 + \alpha_{12}^2))) - \right. \\
& \left. \beta_1^2 \beta_2^2 E_1 E_2 h_a (- (\alpha_{11}^2 + \alpha_{12}^2) (-1 + d_1 h_a (9 \alpha_{11}^4 + 2 \alpha_{11}^2 \alpha_{12}^2 - 7 \alpha_{12}^4)) + \right. \\
& \left. a_0 (1 + 4 d_1 h_a (5 \alpha_{11}^4 - 10.0 \alpha_{11}^2 \alpha_{12}^2 + \alpha_{12}^4))) \right) \Big/ \\
& \left(9 \beta_2^2 d_1^2 (\alpha_{11}^2 + \alpha_{12}^2)^4 + \beta_1^4 E_1^2 h_a^2 \left(a_0^2 - 2 a_0 (\alpha_{11}^2 - 2 d_1 E_1 h_a \right. \right. \\
& \left. \left. (- (\alpha_{11}^2 + \alpha_{12}^2) (\alpha_{11}^2 + \alpha_{12}^2)^2 + a_0 (\alpha_{11}^4 - 6 \alpha_{11}^2 \alpha_{12}^2 + \alpha_{12}^4)) + \beta_1^2 \beta_2 E_1 E_2 h_a^2 \right. \right. \\
& \left. \left. ((\alpha_{11}^2 + \alpha_{12}^2)^2 (1 + d_1 h_a (\alpha_{11}^4 - 6 \alpha_{11}^2 \alpha_{12}^2 + \alpha_{12}^4)) + a_0^2 (1 + 4 d_1 h_a \right. \right. \\
& \left. \left. (\alpha_{11}^4 - 6 \alpha_{11}^2 \alpha_{12}^2 + \alpha_{12}^4)) - a_0 (\alpha_{11}^2 - \alpha_{12}^2) (2 + d_1 h_a (5 \alpha_{11}^4 - 6 \alpha_{11}^2 \alpha_{12}^2 + \right. \right. \\
& \left. \left. 5 \alpha_{12}^4)) \right) - 3 \beta_2^2 d_1 E_2 h_a \left((-\alpha_{11}^2 + \alpha_{12}^2) (\alpha_{11}^2 + \alpha_{12}^2)^2 (1 + d_1 h_a (\alpha_{11}^2 + \alpha_{12}^2)^2) + \right. \\
& \left. a_0 (4 d_1 h_a \alpha_{11}^8 + 16 d_1 h_a \alpha_{11}^6 \alpha_{12}^2 + \alpha_{12}^4 + 4 d_1 h_a \alpha_{12}^8 + \right. \\
& \left. \alpha_{11}^4 (1 + 24 d_1 h_a \alpha_{12}^4) + \alpha_{11}^2 (-6 \alpha_{12}^2 + 16 d_1 h_a \alpha_{12}^6) \right) \Big/ \\
& \left(\beta_2 E_2 \left[9 \beta_2^2 d_1^2 (\alpha_{11}^2 + \alpha_{12}^2)^4 + \beta_1^4 E_1^2 h_a^2 6 \beta_1^2 \beta_2 d_1 E_1 h_a \left((-\alpha_{11}^2 + \alpha_{12}^2) \right. \right. \right. \\
& \left. \left. (\alpha_{11}^2 + \alpha_{12}^2)^2 + a_0 (\alpha_{11}^4 - 6 \alpha_{11}^2 \alpha_{12}^2 + \alpha_{12}^4) \right) \right] \Big/ \\
& \left. \left(h_a \left(a_0^2 - 2 a_0 (\alpha_{11}^2 - \alpha_{12}^2) + (\alpha_{11}^2 + \alpha_{12}^2)^2 \right) \right) \right) ; \tag{C.15}
\end{aligned}$$

Appendix D

The [A], [B], [C] matrix of conditions are shown as follows.

	1c	2c	3c	4c	5c	6c	7c	8c	9c	10c	11c	12c	13c	14c	15c	16c
$\frac{-1}{E_2 \rho_2 \lambda_0}$	0	-1 ₁	1	0	0	0	0	0	0	0	0	0	0	0	0	0
$\frac{-1}{E_2 \rho_2 \lambda_0}$	0	0	1	0	0	0	0	0	0	0	0	0	0	0	0	0
0	c	-1	0	1	-c	c ²	-c ³	0	0	0	0	0	0	0	0	0
0	-1	0	0	0	1	-2c	3c ²	0	0	0	0	0	0	0	0	0
0	0	0	0	0	0	m ₅₀	-3m ₆₀ c	0	0	0	0	0	0	0	0	0
$\frac{0}{E_2 \rho_2 \lambda_0}$	0	0	-1	0	u ₅₁	-m ₅₅ c	3u ₅₂ +u ₅₇ c ² - $\frac{3(O_1+O_2)\lambda_0}{n_0}$	$\frac{-1}{n_0}$	0	0	0	0	0	0	0	0
0	0	0	0	0	0	0	$\frac{f_{51}-\frac{3(O_1+O_2)\lambda_0}{2n_0}}{n_0}$	0	0	0	0	0	0	0	0	0
-1	0	0	0	0	0	m ₅₁	-m ₅₃ c	0	0	$\frac{-O_2 E_2 \lambda_0}{n_0}$	m ₅₇ \overline{CH}_4	m ₅₇ \overline{CH}_4	m ₅₇ $\overline{C}_2 \overline{CH}_4 - m_{58} \overline{C}_2 \overline{SH}_4$	m ₅₇ $\overline{C}_2 \overline{CH}_4 - m_{58} \overline{C}_2 \overline{SH}_4$	m ₅₇ $\overline{C}_2 \overline{CH}_4 - m_{58} \overline{C}_2 \overline{SH}_4$	m ₅₇ $\overline{C}_2 \overline{CH}_4 - m_{58} \overline{C}_2 \overline{SH}_4$
0	0	0	0	0	0	m ₅₀	-3m ₅₀ c	0	0	0	m ₅₇ \overline{CH}_4	m ₅₇ \overline{CH}_4	m ₅₇ $\overline{C}_2 \overline{CH}_4 - m_{58} \overline{C}_2 \overline{SH}_4$	m ₅₇ $\overline{C}_2 \overline{CH}_4 - m_{58} \overline{C}_2 \overline{SH}_4$	m ₅₇ $\overline{C}_2 \overline{CH}_4 - m_{58} \overline{C}_2 \overline{SH}_4$	m ₅₇ $\overline{C}_2 \overline{CH}_4 - m_{58} \overline{C}_2 \overline{SH}_4$
0	0	0	0	0	0	m ₅₁	-m ₅₃ c	0	0	$\frac{-O_1 E_2 \lambda_0}{n_0}$	m ₅₇ \overline{CH}_4	m ₅₇ \overline{CH}_4	m ₅₇ $\overline{C}_2 \overline{CH}_4 - m_{58} \overline{C}_2 \overline{SH}_4$	m ₅₇ $\overline{C}_2 \overline{CH}_4 - m_{58} \overline{C}_2 \overline{SH}_4$	m ₅₇ $\overline{C}_2 \overline{CH}_4 - m_{58} \overline{C}_2 \overline{SH}_4$	m ₅₇ $\overline{C}_2 \overline{CH}_4 - m_{58} \overline{C}_2 \overline{SH}_4$
0	0	0	0	-1	d	-d ²	d ³	0	0	0	0	0	0	0	0	0
0	0	0	0	0	0	u ₅₅ d	-3u ₅₂ -u ₅₇ d ²	$\frac{1}{n_0}$	0	$\frac{-1}{n_0}$	u ₅₁₀ \overline{SH}_4	u ₅₁₀ \overline{CH}_4	u ₅₁₁ $\overline{CH}_4 \overline{S}_4 + u_{512} \overline{C}_4 \overline{SH}_4$	u ₅₁₁ $\overline{CH}_4 \overline{S}_4 + u_{512} \overline{C}_4 \overline{SH}_4$	u ₅₁₁ $\overline{CH}_4 \overline{S}_4 + u_{512} \overline{C}_4 \overline{SH}_4$	u ₅₁₂ $\overline{CH}_4 \overline{S}_4 + u_{511} \overline{C}_4 \overline{SH}_4$
0	0	0	0	0	-1	2d	-3d ²	0	0	0	$\alpha \overline{SH}_4$	$-\alpha \overline{CH}_4$	$-\alpha_{12} \overline{CH}_4 \overline{S}_4 + \alpha_{11} \overline{C}_4 \overline{SH}_4$	$-\alpha_{12} \overline{CH}_4 \overline{S}_4 + \alpha_{11} \overline{C}_4 \overline{SH}_4$	$-\alpha_{11} \overline{C}_4 \overline{CH}_4 + \alpha_{12} \overline{S}_4 \overline{SH}_4$	$\alpha_{11} \overline{CH}_4 \overline{S}_4 + \alpha_{12} \overline{C}_4 \overline{SH}_4$
0	0	0	0	0	0	-m ₅₀	3m ₅₀ d	0	0	0	-m ₅₅ \overline{CH}_4	-m ₅₅ \overline{CH}_4	-m ₅₇ $\overline{C}_2 \overline{CH}_4 \overline{S}_4 + m_{56} \overline{S}_4 \overline{SH}_4$	-m ₅₇ $\overline{C}_2 \overline{CH}_4 \overline{S}_4 + m_{56} \overline{S}_4 \overline{SH}_4$	-m ₅₇ $\overline{C}_2 \overline{CH}_4 \overline{S}_4 + m_{56} \overline{S}_4 \overline{SH}_4$	-m ₅₇ $\overline{C}_2 \overline{CH}_4 \overline{S}_4 + m_{56} \overline{S}_4 \overline{SH}_4$
0	0	0	0	0	0	0	0	0	0	0	-f ₅₈ \overline{SH}_4	-f ₅₈ \overline{CH}_4	f ₅₁₀ $\overline{CH}_4 \overline{S}_4 - f_{59} \overline{C}_4 \overline{SH}_4$	f ₅₁₀ $\overline{CH}_4 \overline{S}_4 - f_{59} \overline{C}_4 \overline{SH}_4$	f ₅₁₀ $\overline{CH}_4 \overline{S}_4 - f_{59} \overline{C}_4 \overline{SH}_4$	f ₅₁₀ $\overline{CH}_4 \overline{S}_4 - f_{59} \overline{C}_4 \overline{SH}_4$
0	0	0	0	0	0	0	0	0	0	0	-f ₅₈ \overline{SH}_4	-f ₅₈ \overline{CH}_4	f ₅₁₀ $\overline{CH}_4 \overline{S}_4 - f_{59} \overline{C}_4 \overline{SH}_4$	f ₅₁₀ $\overline{CH}_4 \overline{S}_4 - f_{59} \overline{C}_4 \overline{SH}_4$	f ₅₁₀ $\overline{CH}_4 \overline{S}_4 - f_{59} \overline{C}_4 \overline{SH}_4$	f ₅₁₀ $\overline{CH}_4 \overline{S}_4 - f_{59} \overline{C}_4 \overline{SH}_4$
0	0	0	0	0	0	0	0	0	0	0	0	0	0	0	0	0
0	0	0	0	0	0	0	0	0	0	0	0	0	0	0	0	0
0	0	0	0	0	0	0	0	0	0	0	0	0	0	0	0	0
0	0	0	0	0	0	0	0	0	0	0	0	0	0	0	0	0
0	0	0	0	0	0	0	0	0	0	0	0	0	0	0	0	0
0	0	0	0	0	0	0	0	0	0	0	0	0	0	0	0	0
0	0	0	0	0	0	0	0	0	0	0	0	0	0	0	0	0
$\frac{-1}{E_2 \rho_2 \lambda_0}$	0	0	0	0	0	0	0	0	0	0	0	0	0	0	0	0
$\frac{-1}{E_2 \rho_2 \lambda_0}$	0	0	0	0	0	0	0	0	0	0	0	0	0	0	0	0

(D.1)

	17c	18c	19c	20c	21c	22c	23c	24c	25c	26c	27c	28c	29c	30c	31c
0	0	0	0	0	0	0	0	0	0	0	0	0	0	0	1r
0	0	0	0	0	0	0	0	0	0	0	0	0	0	0	2r
0	0	0	0	0	0	0	0	0	0	0	0	0	0	0	3r
0	0	0	0	0	0	0	0	0	0	0	0	0	0	0	4r
0	0	0	0	0	0	0	0	0	0	0	0	0	0	0	5r
0	0	0	0	0	0	0	0	0	0	0	0	0	0	0	6r
0	0	0	0	0	0	0	0	0	0	0	0	0	0	0	7r
0	0	0	0	0	0	0	0	0	0	0	0	0	0	0	8r
0	0	0	0	0	0	0	0	0	0	0	0	0	0	0	9r
1	-d	d ²	-d ³	-d ³	0	0	0	0	0	0	0	0	0	0	10r
0	u _{A1}	-u _{S5} d	3 u _{S2} + u _{S1} d ²	3 u _{S2} + u _{S1} d ²	0	0	0	0	0	0	0	0	0	0	11r
0	1	-2 d	3 d ²	3 d ²	0	0	0	0	0	0	0	0	0	0	13r
0	0	m _{S0}	-3 m _{S0} d	-3 m _{S0} d	0	0	0	0	0	0	0	0	0	0	14r
0	0	0	0	0	0	0	0	0	0	0	0	0	0	0	15r
0	0	m _{A1} + m _{S1}	-(m _{S5} + m _{S3}) d	-(m _{S5} + m _{S3}) d	0	0	0	0	0	0	0	0	0	0	16r
0	0	0	0	0	0	0	0	0	0	0	0	0	0	0	17r
0	0	0	0	0	0	0	0	0	0	0	0	0	0	0	18r
0	1	-2 d	3 d ²	3 d ²	0	0	0	0	0	0	0	0	0	0	19r
0	u _{S1}	-u _{S5} d	3 u _{S2} + u _{S1} d ²	3 u _{S2} + u _{S1} d ²	0	0	0	0	0	0	0	0	0	0	20r
1	-d	d ²	-d ³	-d ³	0	0	0	0	0	0	0	0	0	0	21r
0	0	m _{A1}	m _{S3} c	m _{S3} c	0	0	0	0	0	0	0	0	0	0	22r
0	0	m _{S0}	3 m _{S0} c	3 m _{S0} c	0	0	0	0	0	0	0	0	0	0	23r
0	0	m _{S1}	m _{S3} c	m _{S3} c	0	0	0	0	0	0	0	0	0	0	24r
0	0	0	0	0	0	0	0	0	0	0	0	0	0	0	25r
0	0	0	0	0	0	0	0	0	0	0	0	0	0	0	26r
0	0	0	0	0	0	0	0	0	0	0	0	0	0	0	27r
0	0	0	0	0	0	0	0	0	0	0	0	0	0	0	28r
1	c	c ²	c ³	c ³	0	0	0	0	0	0	0	0	0	0	29r
0	0	0	0	0	0	0	0	0	0	0	0	0	0	0	30r
0	0	0	0	0	0	0	0	0	0	0	0	0	0	0	31r

(D.2)

$$[B] = \begin{bmatrix} \frac{4 \bar{F}_L L_1^3}{B_2 h_2^3 \alpha_2^3} \\ 0 \\ \frac{2c^3 \bar{F}_L}{B_2 h_2^3 \alpha_2^3} - \frac{6c^2 \bar{F}_L L_1}{B_2 h_2^3 \alpha_2^3} \\ - \frac{6c^2 \bar{F}_L}{B_2 h_2^3 \alpha_2^3} + \frac{12c \bar{F}_L L_1}{B_2 h_2^3 \alpha_2^3} \\ - \frac{6c^3 \bar{F}_L}{B_2 h_2^3 \alpha_2^3} \\ c \bar{F}_L - \bar{F}_L L_1 \\ 0 \\ \bar{F}_L \\ 0 \\ 0 \\ 0 \\ 0 \\ 0 \\ 0 \\ 0 \\ 0 \\ 0 \\ 0 \\ 0 \\ 0 \\ 0 \\ 0 \\ 0 \\ 0 \\ 0 \\ -\bar{P} + \bar{F}_L \\ \bar{F}_L \\ 0 \\ 0 \\ 0 \\ 0 \\ -c \left(-\bar{P} + \bar{F}_L \right) + \left(-\bar{P} + \bar{F}_L \right) L_2 \\ - \frac{6c^2 \left(\bar{P} - \bar{F}_L \right)}{B_2 h_2^3 \alpha_2^3} + \frac{12c \left(\bar{P} - \bar{F}_L \right) L_1}{B_2 h_2^3 \alpha_2^3} \\ \frac{2c^3 \left(\bar{P} - \bar{F}_L \right)}{B_2 h_2^3 \alpha_2^3} - \frac{6c^2 \left(\bar{P} - \bar{F}_L \right) L_1}{B_2 h_2^3 \alpha_2^3} \\ 0 \\ \frac{4 \left(\bar{P} - \bar{F}_L \right) L_1^3}{B_2 h_2^3 \alpha_2^3} \\ 0 \end{bmatrix} \quad (D.3)$$

$$[C] = \begin{bmatrix} \bar{N}_L \\ C_{311} \\ C_{312} \\ C_{313} \\ C_{320} \\ C_{321} \\ C_{322} \\ C_{323} \\ C_{321} \\ C_{322} \\ C_{322} \\ C_{326} \\ C_{327} \\ C_{328} \\ C_{329} \\ C_{320} \\ C_{321} \\ C_{321} \\ C_{330} \\ C_{331} \\ C_{332} \\ C_{332} \\ C_{337} \\ C_{338} \\ C_{339} \\ C_{320} \\ C_{311} \\ C_{41} \\ C_{42} \\ C_{43} \end{bmatrix} \quad (D.4)$$

where

$$\begin{aligned} \bar{Sh}_c &= \sinh(\alpha c), & \bar{Sh}_d &= \sinh(\alpha d), & \bar{Ch}_c &= \cosh(\alpha c), & \bar{Ch}_d &= \cosh(\alpha d), \\ \bar{Sh}_{1c} &= \sinh(\alpha_{11} c), & \bar{Sh}_{1d} &= \sinh(\alpha_{11} d), & \bar{Ch}_{1c} &= \cosh(\alpha_{11} c), & \bar{Ch}_{1d} &= \cosh(\alpha_{11} d) \\ \bar{S}_c &= \sin(\alpha_{12} c), & \bar{S}_d &= \sinh(\alpha_{12} d), & \bar{C}_c &= \cos(\alpha_{12} c) & \text{and} & \bar{C}_d &= \cos(\alpha_{12} d). \end{aligned}$$

$$\text{Then, } f_{ub10} = f_{a10} + f_{u10} + f_{b10}, \quad f_{ub9} = f_{a9} + f_{u9} + f_{b9}, \quad f_{ub8} = f_{a8} + f_{u8} + f_{b8},$$

$$n_{ub7} = n_{u7} + n_{b7}, \quad n_{ub8} = n_{u8} + n_{b8}, \quad n_{ub9} = n_{u9} + n_{b9}, \quad \bar{F}_L = F_L / G_a \quad \text{and}$$

$$\bar{N}_L = N_L / G_a$$

VITA

姓名：鄭桐華

E-mail: chength@nfu.edu.tw

經歷

國立中央大學 機械系 畢業

民國 69 年 9 月至民國 73 年 6 月 (1980/9 ~ 1984/6)

國立中央大學 機械系 碩士 畢業

民國 74 年 9 月至民國 75 年 6 月 (1984/9 ~ 1986/6)

雲林工業專科學校 講師

民國 77 年 8 月至民國 88 年 8 月 (1988/8 ~ 1999/8)

國立虎尾技術學院 講師

民國 88 年 8 月至民國 93 年 8 月 (1999/8 ~ 2004/8)

國立虎尾科技大學 講師

民國 93 年 8 月至今 (2004/8~2006/12)

國立交通大學機械系博士班

民國 90 年 9 月至民國 95 年 12 月 (2001/9 ~ 2006/12)

